Effect of varying operating conditions on cathode surface roughness using guar as a smoothing agent in copper electrowinning

by

Nhlamulo Mkhawana

Thesis presented in partial fulfilment
of the requirements for the Degree

of

MASTER OF ENGINEERING
(EXTRACTIVE METALLURGICAL ENGINEERING)

in the Faculty of Engineering
at Stellenbosch University

Supervisor
Dr Margreth Tadie

Co-Supervisor
Prof. Christie Dorfling

December 2021

DECLARATION

By submitting this thesis electronically, I declare that the entirety of the work contained therein is my own, original work, that I am the sole author thereof (save to the extent explicitly otherwise stated), that reproduction and publication thereof by Stellenbosch University will not infringe any third party rights and that I have not previously in its entirety or in part submitted it for obtaining any qualification.

Date: December 2021

PLAGIARISM DECLARATION

1. Plagiarism is the use of ideas, material, and other intellectual property of another's work and to present is as my own.

2. I agree that plagiarism is a punishable offence because it constitutes theft.

3. I also understand that direct translations are plagiarism.

4. Accordingly, all quotations and contributions from any source whatsoever (including the internet) have been cited fully. I understand that the reproduction of text without quotation marks (even when the source is cited) is plagiarism.

5. I declare that the work contained in this assignment, except where otherwise stated, is my original work and that I have not previously (in its entirety or in part) submitted it for grading in this module/assignment or another module/assignment.

Initials and surname: N.T Mkhawana

Date: December 2021

ABSTRACT

Organic additives play a very important role in copper electrowinning to facilitate the production of cathode deposits with improved morphology. Guar has been used as the standard organic additive in copper electrowinning (EW) because of its compatibility with solvent extraction (SX) stage, as well as its ability to eliminate dendrite growth on the cathode surface. Dendrite formation produces an undesirable rough cathode surface, and a loss in current efficiency can be expected due to short circuits resulting from dendrite growth. In tankhouses, guar is dosed continuously since its performance reduces as it degrades by hydrolysis under acidic conditions. This project investigated the interaction of guar dosage with other electrowinning operating parameters and their effect on current efficiency and deposit quality.

A bench scale electrowinning cell was used to conduct 24-hour electrowinning experiments by employing a mixed level factorial experimental design to investigate the interaction of guar dosage (2, 10 and 18 mg/l) with copper (35 and 45 g/l), sulphuric acid (150 and 180 g/l) and current density (180 and 300 A/m^2) at a temperature of 40^{o}C and their effect on the measured responses (current efficiency and cathode deposit quality). The electrolyte used was free of impurities with the addition of 25 mg/l chloride to act as de-polarizer and grain refiner in the copper deposition process. The mean surface deviation (S_a) value, which is a measure of surface roughness, was calculated for each copper plate produced. Acid digestion tests using aqua regia were conducted for 24 hours to investigate the chemical composition for all the copper plates. The amount of sulphur in the dissolved copper plates was analysed using the ICP analysis technique. A statistical analysis was performed to analyse the deposited surface roughness, current efficiency, and sulphur content.

The electrowinning results showed an improvement in the elimination of dendrites, producing a smoother copper deposit in the presence of guar than a deposit achieved in the absence of guar in the electrolyte. The calculated S_a values and interaction plots shows that the individual and interactive effects of the operating parameters on the surface roughness in the presence of guar are dependent on the experimental conditions. The copper deposit achieved at 300 A/m^2 current density, 45 g/l initial copper concentration, 180 g/l sulphuric acid concentration and 18 mg/l guar concentration had the lowest calculated S_a value (30.95 µm) and arguably the smoothest, brightest of all the deposits. Current density was observed to be the most influential parameter affecting the roughness of copper deposits while guar has an insignificant effect as predicted by statistical analysis. The interaction plots suggest that higher guar concentrations (10 mg/l or 18 mg/l) are more effective in reducing surface roughness than 2 mg/l guar concentration.

Current efficiency (CE) values calculated for each experiment were high (98-99%) and varied by less than 1%. The little variance shows that varying guar concentrations had a minor impact on the CE for various operating conditions. Current density is the only influential parameter affecting current efficiency as predicted by statistical analysis. The chemical composition results show that the sulphur content in copper deposits increases at high guar concentrations and low current density. It was suggested that sulphate ions may be the source of sulphur entrapped in copper deposits. Statistical analysis of sulphur on each copper plate produced shows that current density and guar concentration significantly influences the amount of sulphur content.

This study provides an industrially informed baseline against which new organic additives can be compared. Based on electrowinning experiments and statistical analysis results, it can be concluded that the adjustment of operating parameters in conjunction with an effective smoothing agent can reduce short-circuiting in copper electrowinning.

OPSOMMING

Organiese bymiddels speel ’n baie belangrike rol in koperelektroherwinning om die produksie van katodeneersettings met verbeterde morfologie te fasiliteer. Guar is gebruik as die standaard organiese bymiddel in koperelektroherwinning vanweë guar se versoenbaarheid met die oplosmiddelekstraksie (SX) stadium, sowel as guar se vermoë om dendriete se groei op die katode-oppervlak te elimineer. Dendrietformasie produseer ’n ongewenste growwe katode-oppervlak en ’n verlies aan stroomdoeltreffendheid kan verwag word as gevolg van kortsluitings wat volg uit dendrietgroei. In tenkhuise word guar aanhoudend gedoseer aangesien sy doeltreffendheid verlaag soos dit degradeer deur hidrolise onder suur kondisies. Hierdie projek het die interaksie van guar dosering met ander koperelektroherwinning bedryfsparameters en hul effek op stroomdoeltreffendheid en katodeneerslagkwaliteit ondersoek.

’n Banktoetsskaalelektroherwinningsel is gebruik om 24-uur elektroherwinningeksperimente uit te voer deur ’n gemengde vlak faktoriaal eksperimentele ontwerp te gebruik om die interaksie van guardosis (2, 10 en 18 mg/l) met koper (35 en 45 g/l), swaelsuur (150 en 180 g/l) en stroomdigtheid (180 en 300 A/m^2) te ondersoek by ’n temperatuur van 40°C, en hul effek op die gemete response (stroomdoeltreffendheid en katodeneerslagkwaliteit). Die elektroliet wat gebruik is, het geen onsuiwerhede gehad nie, met die byvoeging van 25 mg/l chloried om as de-polariseerder en graanraffineerder op te tree in die koperneerslagproses. Die gemiddelde oppervlakafwyking (S_a)-waarde, wat ’n mate van oppervlakgrofheid is, is bereken vir elke koperplaat wat geproduseer is. Suurverteringtoetse wat koningswater gebruik het, is vir 24 uur uitgevoer om die chemiese samestelling vir al die koperplate te ondersoek. Die hoeveelheid swael in die opgeloste koperplate is geanaliseer deur die ICP-analisetegniek te gebruik. ’n Statistiese analise is uitgevoer om die neerslagoppervlakgrofheid, stroomdoeltreffendheid, en swaelinhoud te analiseer.

Die elektroherwinningresultate het ’n verbetering in die eliminasie van dendriete getoon wat ’n gladder koperneerslag in die teenwoordigheid van guar produseer, teenoor dié geproduseer in die afwesigheid van guar in die elektroliet. Die berekende S_a-waardes en interaksieplotte wys dat die individuele en interaktiewe effek van die bedryfsparameters op die oppervlakgrofheid in die teenwoordigheid van guar afhanklik is van die eksperimentele kondisies. Die koperneerslag bereik by 300 A/m^2 stroomdigtheid, 45 g/l aanvanklike koperkonsentrasie, 180 g/l swaelsuurkonsentrasie en 18 mg/l guarkonsentrasie het die laagste berekende S_a-waarde (30.95 µm) en is besmoontlik die gladste, helderste van al die neerslae. Stroomdigtheid is waargeneem om die mees invloedryke parameter te wees wat die grofheid van koperneerslae affekteer terwyl guar ’n onbeduidende effek gehad het, soos voorspel deur statistiese analise. Die interaksieplotte stel voor dat hoër guarkonsentrasies (10 mg/l of 18 mg/l) meer effektief is in die vermindering van oppervlakgrofheid as 2 mg/l guarkonsentrasie.

Stroomdoeltreffendheid (CE)-waardes bereken vir elke eksperiment was hoog (98 – 99%) en het met minder as 1% gevarieer. Die bietjie variansie het gewys dat verskeidenheid guarkonsentrasies minimale impak op die CE vir verskeie bedryfskondisies het. Stroomdigtheid is die enigste invloedryke parameter wat stroomdoeltreffendheid affekteer soos voorspel deur statistiese analise. Die chemiese samestelling se resultate toon dat die swaelinhoud in koperneerslae verhoog by hoër guarkonsentrasies en lae stroomdigtheid. Dit is voorgestel dat sulfaatione moontlik die bron is van swael wat vassit in koperneerslae. Statistiese analise van swael op elke koperplaat geproduseer, het getoon dat stroomdigtheid en guarkonsentrasie beduidende invloed het op die swaelinhoud.

Hierdie studie verskaf ’n industriële ingeligte basislyn waarteen nuwe organiese bymiddels opgeweeg kan word. Gebaseer op elektroherwinningeksperimente en statistiese resultate kan dit beslis word dat

die verstelling van bedryfsparameters in samewerking met ’n doeltreffende gladmakingsbymiddel kortsluiting in koperelektroherwinning kan verminder.

ACKNOWLEDGEMENTS

I would like to express my gratitude to the following people:

- My supervisors, Dr Margreth Tadie and Prof. Christie Dorfling for their support and providing technical advice to guide me in shaping this project. I am very grateful of your time and mentoring.
- The South African Minerals to Metals Research Institute (SAMMRI) for funding the research project and providing support from an industry perspective.
- The support staff from department of Process Engineering at Stellenbosch University for their assistance in the workshop, analytical facilities, and administration.
- My parents, siblings and friends for their support and words of encouragement to keep me going throughout my research journey.

TABLE OF CONTENTS

LIST OF FIGURES

LIST OF TABLES

NOMENCLATURE

Category	Symbol	Description	Unit
Numerical Symbols	A	Area	m^2
	C_{bulk}	Bulk concentration	mol/m^3
	C_i	Concentration of species i	mol/dm^3
	D	Diffusion coefficient	m^2/s
	e	Electron charge	Coulomb
	E_o	Standard electrode potential	V
	E_{cell}	Applied cell voltage	V
	E_{equ}	Equilibrium potential	V
	F	Faradays constant	C/mol
	ΔG	Gibbs free energy	J/mol
	ΔG_{crit}	Critical Gibbs free energy	J/mol
	i	Current density	A/m^2
	i_L	Limiting current density	A/m^2
	i_o	Exchange current density	A/m^2
	I	Current	A
	J	Flux	$mol/ (cm^2.s)$
	K	Boltzmann constant	J/K
	M	Mass	g
	M	Molar mass	g/mol
	N	Number of electros in reaction	
	Q	Charge	Coulomb
	R	Gas constant	J/(mol.K)
	R_a	Arithmetic mean height of a line	µm
	S_a	Mean surface deviation	µm
	T	Time	s, min, or h
	T	Temperature	^oC or K

	V	Volume	L
	z	Charge number of ion	
Greek symbols	α_a	Anodic charge transfer coefficient	
	α_c	Cathodic charge transfer coefficient	
	δ	Diffusion layer thickness	m
	η	Overpotential	V
	σ	Surface tension	N/cm^2
Acronyms	ANOVA	Analysis of variance	
	CAF	Central Analytical Facilities	
	CE	Current Efficiency	%
	DLC	Diffusion Limited Current	A
	E.C	Energy Consumption	kWh/t
	EW	Electrowinning	
	HPLC	High Performance Liquid Chromatography	
	ICP	Inductively Coupled Plasma	
	IHP	Inner Helmholtz Plane	
	OHP	Outer Helmholtz Plane	
	PCB	Printed circuit board	

1. INTRODUCTION

1.1. BACKGROUND

The recovery of high purity copper in the mining industry from ore bodies includes electrowinning or electrorefining as the final steps depending on whether the copper mined is processed through the hydrometallurgical or pyrometallurgical process. The energy required to produce one tonne of copper during electrowinning is about 2000 kWh whereas for electrorefining is 300-400 kWh (Davenport et al., 2002). Even though high energy is required during electrowinning operations, copper production through the hydrometallurgical route has seen an increase from 3% in 1980 to 20% in 2005 (Moats and Free, 2007). The reason for growth in hydrometallurgy includes lower capital investments and energy consumption as well as reduced environmental impacts compared to pyrometallurgy which involves high energy consumption processes such as smelting.

There are approximately 75 hydrometallurgical copper processing plants globally that each produce more than 10000 tonnes per annum through leaching and solvent extraction coupled with electrowinning (Robinson et al., 2013). Therefore, copper recovered via electrowinning significantly contributes to the global copper commodity supply. Electrowinning is the primary economical purification method for recovering high-quality copper metal. Two electrodes (cathode and anode) are inserted in a solution containing copper ions and electric current is passed through them allowing deposition of solid copper on the cathode through the reduction reaction. Simultaneously, water undergoes an oxidation reaction at the anode producing hydrogen ions and oxygen bubbles. The copper metal is electrodeposited on cathode blanks made from stainless steel and the anodes are usually made from lead-based alloys.

To ensure that the copper electrowinning process remains as efficient and effective as possible in terms of energy and cost it is important to control the key performance indicators (current efficiency, copper deposit quality and specific energy consumption). The amount of copper produced must meet the industry demand while ensuring that less energy is consumed, and high-quality copper cathode is produced. The quality is measured by the purity and smoothness of the copper deposit produced. An increase in energy consumption and decrease in the amount and quality of copper produced during the electrowinning process can result if there is electrical resistance or disruption in the EW cell like loose electrode busbar contacts and short-circuits between the electrodes (Shukla, 2013). The uniformity of current distribution in the EW cell affects the industrial copper electrowinning operation performance. The problem of high energy consumption and short-circuits associated with the operation of the electrowinning process at high current density may be reduced by changing the busbar electrode design or proper adjustment of the process operating parameters such as current density, copper concentration, electrolyte temperature and concentration of additives. Research to reduce the short-circuiting in the electrowinning cell is ongoing. The growth of dendrites on the cathode surface until it reaches the anode is one of the causes of short-circuiting in the EW cell. Thus, organic smoothing agents are dosed to control the morphology and growth of copper deposits in copper electrowinning.

1.2. PROBLEM STATEMENT

Over the past decades, efforts have been made to operate tankhouses at increased current densities since the coupling of solvent extraction with the electrowinning plant. Tankhouses can be operated at

relatively high current densities allowing a high rate of copper production, however, increased current densities lead to the formation of dendrites/nodules at the cathode surface. If the dendrite grows from the cathode until it reaches the anode it will cause short-circuiting in the EW cell. Short circuits in the electrowinning cell cause current maldistribution which results in high specific energy consumption, loss in copper production and a detrimental effect on the quality of copper cathode.

The detrimental effects of current maldistribution on the quality of copper cathode can be reduced by dosing an organic smoothing agent to eliminate the formation of dendrites, facilitating the production of smoother, denser, and brighter copper cathodes. Guar gum has been used as the standard smoothing agent in copper electrowinning since the introduction of solvent extraction as the interface between leaching and electrowinning plants, since it does not have problems associated with the formation of crud in solvent extraction. It has been a concern within the industry that additives other than guar may affect the components of the organic solvent extractant (LIX® 984, ACORGA ® M5640 and kerosene type diluent) (Fabian et al., 2003). Guar is dosed continuously in tankhouses since its performance reduces as it degrades by hydrolysis under acidic conditions. However, a recent trend on the shift from the use of usage of guar to low-cost polyacrylamides and modified polysaccharides (HydroStar) in copper electrowinning has been observed (Robinson et al., 2013).

With the recently observed trend of replacing guar with alternative organic additives it is important to have a benchmark which can be used as a reference for the performance of organic additives in copper electrowinning. Therefore, since guar has been used as the smoothing agent for over 40 years with success its performance in copper electrowinning can be used as a benchmark for the newer organic additives. Even though guar has been widely used in copper electrowinning there is little information available in the published literature related to the performance of guar at varying concentrations with other parameters to control localized growth (dendrites) during the copper electrodeposition process. Therefore, this study was undertaken to understand and quantify the interactive effects of varying operating conditions on guar requirements as well as their implications on the electrowinning performance (current efficiency and copper cathode quality).

1.3. RESEARCH AIM AND OBJECTIVES

The aim of this project is to understand the performance of guar at varying concentrations with other parameters to enable improved control of guar addition during copper electrowinning. To achieve the aim of this project the following objectives were set:

1. Conduct bench-scale copper electrowinning experiments according to a factorial design where cathode deposits can be obtained to investigate the interaction of guar dosage with other electrowinning parameters and their effect on electrowinning performance (surface roughness and current efficiency).
2. Analyze and compare the morphology of the copper deposits obtained from the various experimental conditions.
3. Investigate the quality of the copper plates in terms of chemical composition to infer the grade of copper cathodes produced at the different experimental conditions.

1.4. RESEARCH QUESTIONS

To accomplish the objectives listed in Section 1.3 the following questions will be addressed:

1. What is the relationship between cathode morphology and operating parameters during the electrowinning process?
2. Does varying experimental conditions affect the current efficiency in the electrodeposition process?
3. How does varying experimental conditions affect the chemical composition of copper deposit in the electrowinning process.

1.5. RESEARCH APPROACH AND SCOPE

The scope of understanding the effect of varying operating conditions on guar requirements in copper electrowinning developed in this research was based on investigating possible interactions between operating parameters and their effect on the key performance indicators of quality of copper cathode and current efficiency. The performance indicator for the specific energy consumption fell beyond the scope of this research. Impurities were also not included in the electrolyte to allow for determining the performance of guar at different concentrations without interferences.

The experimental approach to complete the objectives of this research was divided into bench-scale electrowinning experiments, 3D scanning tests for copper deposit morphology determination and acid digestion tests. Bench scale copper electrowinning experimental work allowed for analysis of copper deposit quality and current efficiency achieved over varying electrolyte composition. The electrolyte composition was determined by using a mixed level factorial design of experiments with four operating factors which include copper concentration, sulphuric acid concentration, current density, and guar concentration. A mixed level design was used since it allowed for the study of several factors with more levels to provide enough comparable data to determine the main and interactive effects of the operating factors on the key performance indicators. The cathode deposit quality was determined in terms of cathode morphology (dendrites) and chemical composition (grade of copper).

Each of the copper plates produced from electrowinning experiments was scanned using a hand-held Artec-Spider surface scanner to provide data on the cathode morphology. The high-quality 3D-Volumetric data on each plate was analysed on Volume Graphics VGStudioMax 3.1 software to estimate a mean surface deviation which is a surface roughness factor. To determine the chemical composition on the copper cathodes an approach for conducting acid digestion tests to dissolve the copper plates was allowed. ICP analysis was used to determine the content of sulphur in the dissolved copper plates and the data generated from statistical analysis would be used to determine the influence of each operating factor on the sulphur content. Finally, current efficiencies of each copper plate after electrowinning experiments were calculated based on the actual mass of copper plated and allowed for their comparison at various operating conditions in the presence of guar.

1.6. THESIS STRUCTURE

Chapter 1: This chapter gives an introduction to the research project, which includes a brief background of copper production worldwide using hydrometallurgical and pyrometallurgical processes, problem statement, the aim and objectives of the research, project scope and research approach to fulfil the objectives of the current study.

Chapter 2: This chapter provides a review of the most relevant and recent literature including an overview of copper electrowinning process principles and electrodepositions fundamentals. The relevant literature on dendrite formation and growth, the use of organic additives in copper electrowinning, physicochemical properties of guar, surface roughness characterization technique, acid digestion theory are also provided in this chapter as well as the recent literature regarding the effect of some important operating parameters in copper electrowinning.

Chapter 3: The experiments conducted to achieve the objectives of this project which include bench-scale copper electrowinning experiments, 3D scanning tests, and acid digestion tests are described in this chapter. An outline on the materials, methodology and equipment's used to conduct the experimental work is also included in this chapter as well as the experimental design used to conduct the bench-scale electrowinning experiments. Thereafter, details on sample analysis methods which includes, surface scanning, visual analysis, ICP analysis and statistical analysis is provided.

Chapter 4: This chapter presents the results and discussion of the bench-scale copper electrowinning tests, 3D scanning tests for morphology determination and acid digestion tests.

Chapter 5: The conclusions which summarizes the important findings of this research are outlined in this chapter as well as the recommendations for future research.

Chapter 6: The list of references used for this research study is provided in this chapter.

Chapter 7: This chapter is the appendices which provide supporting results, experimental procedure, sample calculations, and guar degradation evaluation.

2. LITERATURE REVIEW

2.1 PROCESS OVERVIEW

2.1.1 Electrometallurgy

Electrometallurgy is a method in extractive metallurgy used for extracting high purity metals through the application of electrical energy by electrolysis. The two commonly used electrometallurgical processes used as the last stage in copper metal production are electrowinning and electrorefining which correspond to the hydrometallurgical or pyrometallurgical operations, respectively. Whether the production of copper is through hydrometallurgical or pyrometallurgical processes is dependent on the type of copper hosting orebody.

The pyrometallurgical process is usually used to extract copper hosted in sulphide ores and the process entails comminution, flotation, smelting and electrorefining, while copper contained in oxide ores is extracted through the hydrometallurgical process (Davenport et al., 2002). The steps involved in the hydrometallurgical process usually include comminution, leaching, solvent extraction, and the electrowinning stage (Schlesinger et al., 2011). The hydrometallurgical processing of copper was developed after the pyrometallurgical processing route and it is a more environmentally friendly process since its sulphur dioxide emissions are lower compared to pyrometallurgy (Murray et al., 2016).

2.1.2 Copper hydrometallurgical process

The extraction of copper bearing ores from underground, open-pit, or solution mining is the initial stage to produce copper metal. In a typical hydrometallurgical process, the extraction of high-purity copper from its ore involves the stages represented by the flow diagram in Figure 2.1. Firstly, the oxide ore is crushed and ground in the comminution stage to liberate the copper minerals. After this stage, the copper minerals with a reduced size undergo acid leaching. In the leaching process, copper is dissolved in tanks or hill size heaps using sulphuric acid as a lixiviant to produce a copper sulphate solution rich in cupric ions. The pregnant leach solution which usually contains 1 g/l to 6 g/l copper, 0.5 g/l to 5 g/l sulphuric acid and some impurities is then sent to the solvent extraction stage to reduce impurities and produce high concentration copper electrolyte (Davenport et al., 2002).

Copper is selectively extracted from the pregnant leach solution into an organic phase during the SX stage when the pregnant leach solution is contacted with an immiscible organic phase which contains a copper-selective extractant. After phase separation, the raffinate is recycled to the leaching process and the copper bearing organic phase enters the stripping stage. In the stripping stage copper is released into a high acid solution known as the electrolyte which usually contains about 45 g/l Cu (Schlesinger et al., 2011). The stripped organic is recycled to the SX stage, and the pregnant electrolyte is sent to the electrowinning process. In the electrowinning process, electric current is applied to the electrolytic cell where copper metal is deposited on the cathode, and the copper depleted solution (spent electrolyte) is recycled into the stripping stage.

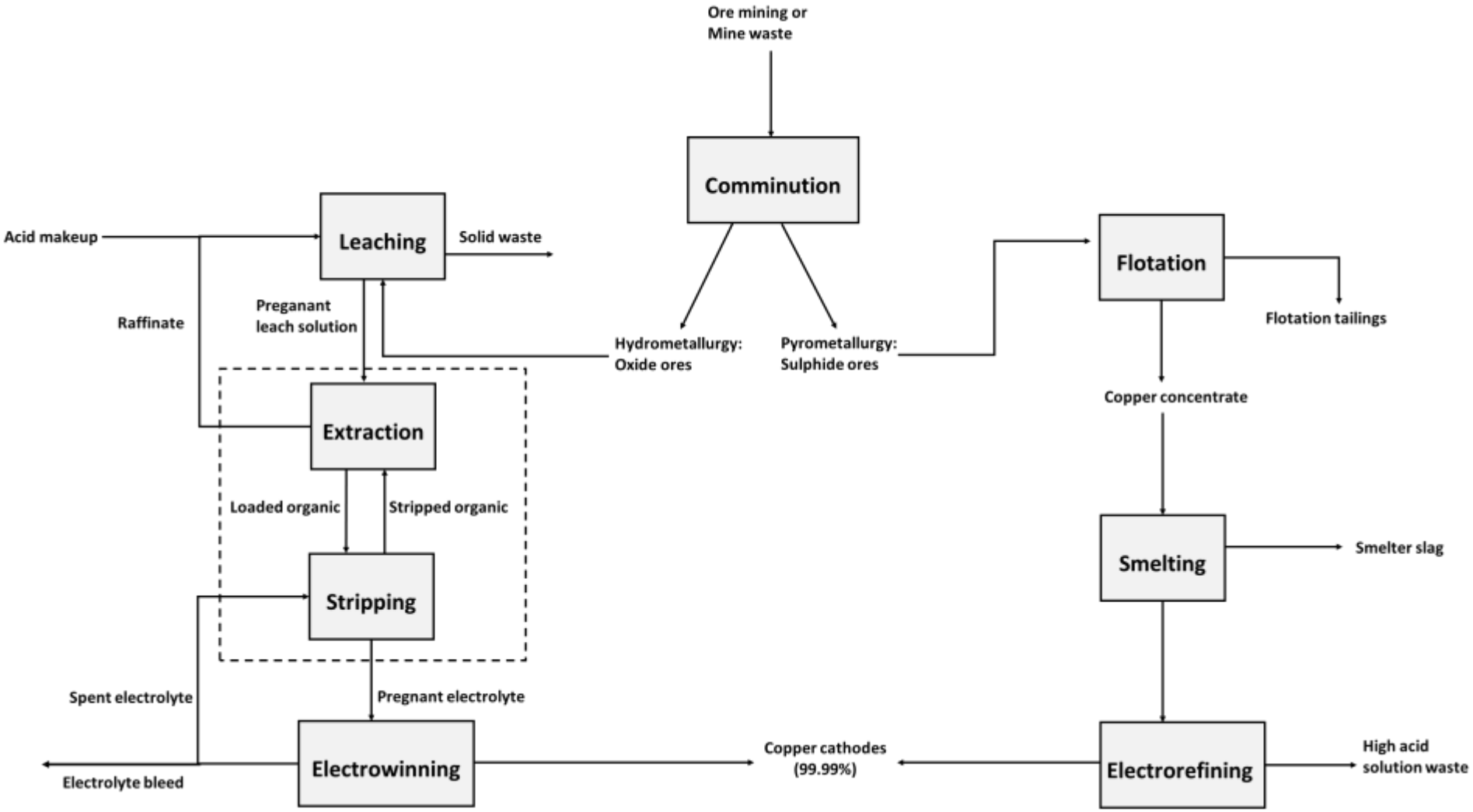

Figure 2.1: Block flow diagram of processing copper ores (Cruz, 2019).

2.2 ELECTROCHEMICAL CELL PRINCIPLES

2.2.1 Process description

In an industrial operation which produces high tonnages of copper, the electrowinning process takes place in a tankhouse which is made up of several hundreds of cells in parallel or series depending on the configuration. Each cell consists of multiple anode and cathode electrodes which are immersed into the electrolyte. Typically, the electrolyte continuously flows into each cell through a manifold at the bottom, and the overflow out of the cell is through one of the sides. Less common configurations also exist in the industry which include the electrolyte flowing horizontally across the EW cell (Tucker, 2020). A simplified electrolytic cell showing the fundamental electrochemistry of copper plating by electrowinning is shown in Figure 2.2. The cell comprises of two electrodes (anode and cathode) which are immersed in the electrolyte and an external power source which connects to the electrodes allowing the flow of electric current to reverse the process of metal dissolution when the voltage is applied to the cell.

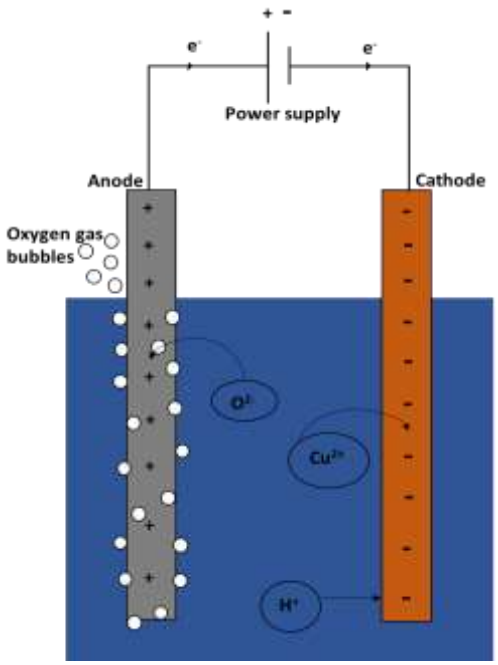

Figure 2.2: A simplified diagram of a copper electrowinning cell (Bard and Faulkner, 2001).

There are two principal reactions that occurs during copper electrowinning; the oxidation reaction occurs on the anode, while the reduction reaction takes place on the cathode. When voltage is applied to the EW cell, electrons flow towards the cathode and attract the positively charged Cu^{2+} ions present in the electrolyte. A reduction reaction shown by Equation 2.1 will then occur between the negatively charged electrons and Cu^{2+} ions producing a solid/metal copper plated on the cathode surface. Simultaneously, anions will move towards the positively charged anode.

The oxidation reaction will take place on the anode whereby water decomposes producing oxygen and hydrogen ions as it can be seen from Equation 2.2. The oxygen gas produced bubbles out through the electrolyte to the atmosphere from the top of the cell as shown in Figure 2.2. When the gas bubbles containing sulphuric acid hit the liquid/air interface they rupture, releasing acid mist into the air. The formation of acid mist results in hazardous environments in the tankhouse including

equipment corrosion and serious health effects to the operators (Liow et al., 1992; Sigley et al., 2003; Shakarji et al., 2011). To complete the electric circuit in the EW cell the electrons flow via the anode to the negatively charged cathode.

$$Cu^{2+}_{(aq)} + 2e^- \rightarrow Cu_{(s)} \qquad E^\circ = +0.337\,V \qquad Equation\ 2.1$$

$$H_2O_{(l)} \rightarrow \frac{1}{2}O_{2(g)} + 2H^+_{(aq)} + 2e^- \qquad E^\circ = -1.229\,V \qquad Equation\ 2.2$$

The net copper electrowinning reaction (Equation 2.3) in the presence of sulphate ions is given by the sum of Equation 2.1 and Equation 2.2.

$$Cu^{2+}_{(aq)} + SO^{2-}_{4(aq)} + H_2O_{(l)} \rightarrow Cu_{(s)} + \frac{1}{2}O_{2(g)} + 2H^+_{(aq)} + SO^{2-}_{4(aq)} \qquad E^\circ = -0.89\,V \qquad Equation\ 2.3$$

The reaction products include a solid plated copper, oxygen gas and regenerated sulphuric acid. Solid plated copper is stripped off from the stainless-steel cathode blanks, washed, packed, and then strapped into bundles. The strapped copper bundles can then be sent to the market. The acid present in the spent (Cu-depleted) electrolyte is recycled to the SX stage.

2.2.2 Faraday's law

The amount of copper plated on the cathode surface during electrowinning can be related to the quantity of electricity supplied to the process and this can be calculated using the Faraday's law. The Faraday's law of electrolysis states that the amount of species that reacts in a redox reaction is directly proportional to the quantity of charge that passes as presented in Equation 2.4 (Beukes and Badenhorst, 2009). In copper electrowinning the oxidizing agent (cupric ions) are reduced and the reduction reaction for producing a copper metal is shown by Equation 2.1.

$$Q = n.F.M \qquad Equation\ 2.4$$

Where: Q is the charge.

n is the number of electrons involved in reaction.

F is the Faraday's constant.

M is the molar mass of copper.

Differentiating Equation 2.4 with relation to time produces Equation 2.5 which can be used to determine the charge spent per unit time.

$$\frac{dQ}{dt} = I = n.F.\frac{dM}{dt} \qquad Equation\ 2.5$$

2.2.2.1 Weight of copper deposit

The most useful form of Faraday's Law for application in electrowinning is provided in Equation 2.5, indicating the mass of a species that reacts as a function of applied current, or charge passed per time (Newman and Thomas-Alyea, 2004).

$$m = \frac{I.t.M}{n.F} \qquad Equation\ 2.6$$

Where: m is the weight of copper metal plated.

I is the intensity current

t is the electroplating time

n is the number of electrons.

M is the molar mass of copper.

F is the Faraday's constant

Equation 2.6 provide a fundamental understanding of the theoretical amount of copper that can be produced in terms of the applied current during copper electrowinning and can be used to calculate the current efficiency.

2.2.2.1 Thickness of copper deposit

The Faraday's law can also be used to calculate the thickness of copper deposit. To calculate the thickness of copper deposited layer, the weight of copper metal plated (m) is determined first using Equation 2.6. Thereafter, Equation 2.7 can be used to calculate the thickness of copper deposit.

$$T = \frac{m}{A \times \rho} \qquad Equation\ 2.7$$

Where: T is the thickness of copper deposit.

m is the weight of copper metal plated.

A is the plated area.

ρ is the density of copper.

2.2.3 Electrode polarization and overpotential

Once the Faradaic current is passed through the electrolyte, the system shifts from its equilibrium state. The difference in the applied potential from the equilibrium condition is known as polarisation. The extent of which polarization takes place in the system is measured by the overpotential, which can be calculated by using Equation 2.8. Overpotential is the additional energy required to shift the forward reaction (copper reduction reaction) at the intended rate from their equilibrium state (Moats et al., 2016).

$$\eta = E_{cell} - E_{equ} \qquad Equation\ 2.8$$

Where: η is the overpotential.

E_{cell} is the applied cell potential.

E_{eq} is the equilibrium potential.

Polarizing the electrode to a potential higher than its equilibrium potential a positive overpotential (anodic overpotential) will result in the oxidation reaction. If the overpotential is negative (cathodic overpotential) it means the electrode potential is less than its equilibrium potential which then causes reduction of the electrochemical species (Hibbert, 1993). The total overpotential consists of both activation overpotential and concentration overpotential. Concentration overpotential is the energy used to drive mass transfer of ions to or from the cathode surface, while the activation overpotential is the energy required to drive the charge transfer reaction (Bard and Faulkner, 2001).

2.2.4 Electrochemical kinetics

Electrochemical kinetics explain the rate at which chemical reactions occurs. The Butler-Volmer (B-V) equation given in Equation 2.9 expresses the rate of reaction by relating current density with the overpotential and temperature. The overpotential ensures a sufficient supply of voltage to drive the forward reaction and sufficient temperature is also required to promote the reduction reaction. The rate of reaction also known as the mass of species reacted per unit time is measured in terms of current density. Current density is defined as current per electrode surface area perpendicular to the flow of current (Newman and Thomas-Alyea, 2004). The B-V equation shows that the exponential changes to the current density can result from changes to the potential (Beukes and Badenhorst, 2009).

$$i = i_o\left(\exp\left(\frac{\alpha_a nF\eta}{RT}\right) - \exp\left(\frac{-\alpha_c nF\eta}{RT}\right)\right) \qquad Equation\ 2.9$$

Where: i is the current density.

i_o is the exchange current density.

α_a is the anodic charge transfer coefficient.

α_c is the cathodic charge transfer coefficient.

η is the overpotential.

n is the number of electrons transferred.

R is the gas constant.

T is temperature.

F is the Faraday's constant.

It is important to measure and monitor the applied voltage in the tankhouse since the overpotential required to shift the copper deposition reaction from its equilibrium state at a specific rate depends on several operating parameters (e.g., copper concentration and smoothing agents). Smoothing agents will either polarize or de-polarize the copper deposition process and this directly affects the energy consumption and copper deposit morphology (Adcock et al., 2004). In this study guar is used as a smoothing agent to improve the morphology of copper deposits. Coetzee (2018) found that the addition of guar in the electrolyte decreased the overpotential required for initiating copper nucleation and slightly depolarized copper deposition on the cathode surface.

2.2.5 Limiting Current Density

The limiting current density is a maximum current density that can be applied in the system, after which any increase in potential does not result in an increase in the reaction rate (Bard and Faulkner, 2001). The limiting current density results from a mass transfer limiting step. This limiting current density (i_L). is also referred to as the diffusion controlled current density since it is governed by the diffusion rates of the dissolved copper ions in the electrolyte. At the diffusion limiting current (DLC) the concentration of species on the surface is zero. This means that all species are consumed as quickly as they are supplied to the electrode. Increasing concentration of species in the bulk electrolyte will increase the limiting current density as shown by Equation 2.10 (Beukes and Badenhorst, 2009).

$$i_L = \frac{n.F.D.(C_{bulk})}{\delta} \qquad Equation\ 2.10$$

Where: i_L is the diffusion limited current.

n is the number of moles.

$C_{(bulk)}$ is the concentration of species in the bulk.

F is the Faraday's constant.

D is the diffusion coefficient.

δ is the boundary layer thickness.

Enough current must be applied in operation of the electrowinning cell to ensure that the desired copper metal is produced through the reduction reaction while maintaining the current density below its limiting current density. The current density should be operated at about 50% of the limiting current density (Winand, 1992). If current density of the reduction reaction is operated above its

limiting current density the electrowinning process becomes energy inefficient and the copper deposit produced will become powdery.

2.3 ELECTRODEPOSITION PROCESS FUNDAMENTALS

The electrodeposition process of copper takes place in an electrochemical cell which contains a conductive electrode (cathode) and an inert electrode (anode) immersed in an ionic conducting electrolyte. During the electrodeposition process a copper metal is deposited on the cathode surface once an electric current is applied to the electrochemical cell (Fabian, 2005). The stages involved in the electrodeposition process of copper are presented in Figure 2.3 and can be explained as follows (Budevski et al., 1996; Beukes and Badenhorst, 2009):

a) Mass transfer of copper ions from the electrolyte via migration, diffusion, and convection from the electrolyte to the electrolyte/electrode interface.
b) Transformation of copper ions into adatoms on the cathode surface after the charge transfer step. The adatom formed adsorb to the cathode surface and then travel to a nucleation site through diffusion.
c) The formation of grains (copper metal phase) on the cathode surface overtime via two-dimensional (2D) or three-dimensional (3D) growth depending on the process conditions.

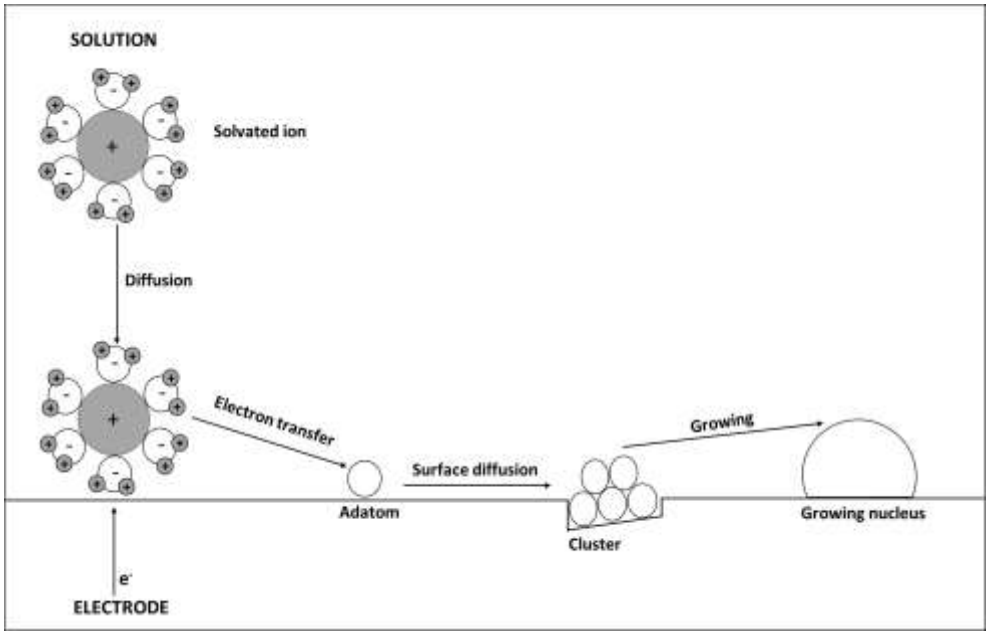

Figure 2.3: Electrocrystallization steps during metal deposition adapted from Pasa and Munford (2006).

2.3.1 Mass transfer in electrolyte

For the electrochemical reactions to take place copper species in the electrolyte are transported to the electrode surface through three basic mass transport mechanisms: convection, diffusion, and migration (Beukes and Badenhorst, 2009). There are two forms of convection mass transfer which are termed natural and forced convection. Natural convection is present in any solution and movement

of species occurs through density/temperature gradients while forced convection occurs by hydrodynamics (i.e., mechanical stirring or pressure gradient). Natural convection will be dominant in static solutions or when the flowrate is low.

Diffusive mass transfer occurs due to a concentration gradient from the electrolyte to the electrode surface (or from the electrode out into the electrolyte). The concentration gradient drives the movement of species in the electrolyte from a position of high concentration to a position of low concentration. Migration is the type of mass transport where the movement of charged particles is based on an electrical potential gradient (Bard and Faulkner, 2001). Migration is induced due to the application of voltage on the electrodes. This creates a difference in charge between the electrode and the electrode interface. The electrostatic forces which are caused by the charge difference initiates the movement of any charged species near the electrode interface to be attracted or repelled from it and this mechanism is known as migration (Chang, 2009).

2.3.2 Thermodynamics of electrochemical nucleation and growth

Nucleation of copper is the first stage that occurs in the formation of a crystal from an electrolyte in the metal electrodeposition process. It is usually initiated when the adatom travels to a nucleation site which can be a surface imperfection on the cathode through surface diffusion (Pasa and Munford, 2006). A nucleus is formed when the adatom encounters other already diffused adatom, followed by grain formation and eventually growth as depicted previously in Figure 2.3.

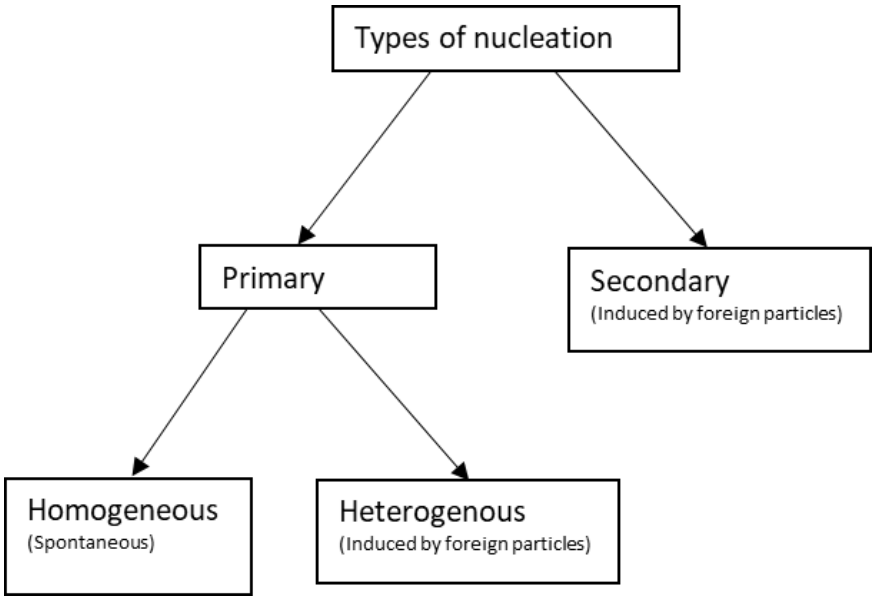

Figure 2.4: A graphic diagram of the types of crystal nucleation (Doran, 2013).

Nucleation can be divided into primary and secondary nucleation as shown in Figure 2.4. Primary nucleation occurs when a nucleus forms on the depositing surface where no crystalline material was previously formed. Primary nucleation can be classified as either homogenous or heterogenous nucleation. Homogeneous nucleation occurs when there is a spontaneous formation of small clusters of molecules on the depositing surface without the aid of any favourable nucleation site (foreign materials or defects). In the industry, homogeneous nucleation is not relevant because it is practically impossible to attain a perfectly clean electrolyte solution (Doran, 2013).

When atoms accumulate at a foreign substrate/defect and then form a nuclei heterogeneous nucleation is induced, while some foreign substrates act as nucleation sites some may alternatively inhibit nucleation (Gebbie, 2013). Heterogeneous nucleation is more favourable than homogeneous nucleation since it requires a lower overpotential which translate to lesser energy needed for promoting nucleation on the electrode surface. This may be attributed to the presence of a foreign material on the electrode surface promoting growth resulting in a lower surface free energy. The second category of nucleation is termed secondary nucleation. Secondary nucleation occurs when a seed crystal is introduced to the system to act as a nucleation site allowing the growth of a new crystal (Gebbie, 2013). Secondary nucleation is more favourable compared to primary nucleation since it requires less energy due to nucleation occurring on the existing growth on the depositing surface.

The process of nucleation can occur instantaneously or progressively. Instantaneous nucleation occurs when the nucleation rate is faster compared to the crystal growth rate. This will allow the formation of nuclei at all nucleation sites available on the electrode surface in a very short time. On the other hand, if the nucleation rate is very slow and occurs in concurrence with crystal growth progressive nucleation will occur on the depositing surface. The granularity of the deposit is determined by the competition between nucleation and growth (Budevski et al., 2000). Faster rates of nucleation during the electrodeposition process favours the formation of smaller crystals. The shape of crystals growing influences the physical appearance and structure of metal deposit on the electrode surface (Fabian, 2005). A more fibrous crystal structure will be produced if higher growth rate of the crystal grains perpendicular to the depositing surface is observed. However, if the crystal grains grow parallel (lateral) to the depositing surface a brightening effect can be achieved on the metal deposit (Budevski et al., 2000).

It is said that during electrowinning organic additives can be used to promote progressive nucleation rather than instantaneous nucleation by inhibiting the deposition of metal on high-active energy sites on the cathode surface (Winand, 1994). Coetzee (2018) presented evidence that electrodeposition without the addition of organic additive produced instantaneous nucleation. The plate produced from the electrolyte without organic additive showed rough dendrite peaks which are undesirable since they can cause short circuits in the tankhouse. Furthermore, it was concluded that the addition of guar as an organic additive in the electrolyte allows for progressive nucleation which produced a deposit with a smoother surface compared to the deposit produced without guar addition.

2.4 DENDRITE GROWTH IN METAL ELECTROLCRYSTALLIZATION

2.4.1 Dendritic growth on electrodes

A morphological structure is formed when a metal crystallizes on the depositing surface during the electrodeposition process. Frequently, as the metal growth continues the morphological structure eventually becomes unstable leading to the formation of dendrites. A dendrite as shown in Figure 2.5 is a protruding branched structure which is made up of a stem and branches (primary, secondary, etc) resembling a tree or flower in the 3-D case and a fern in the 2-D case (Wranglen, 1960).

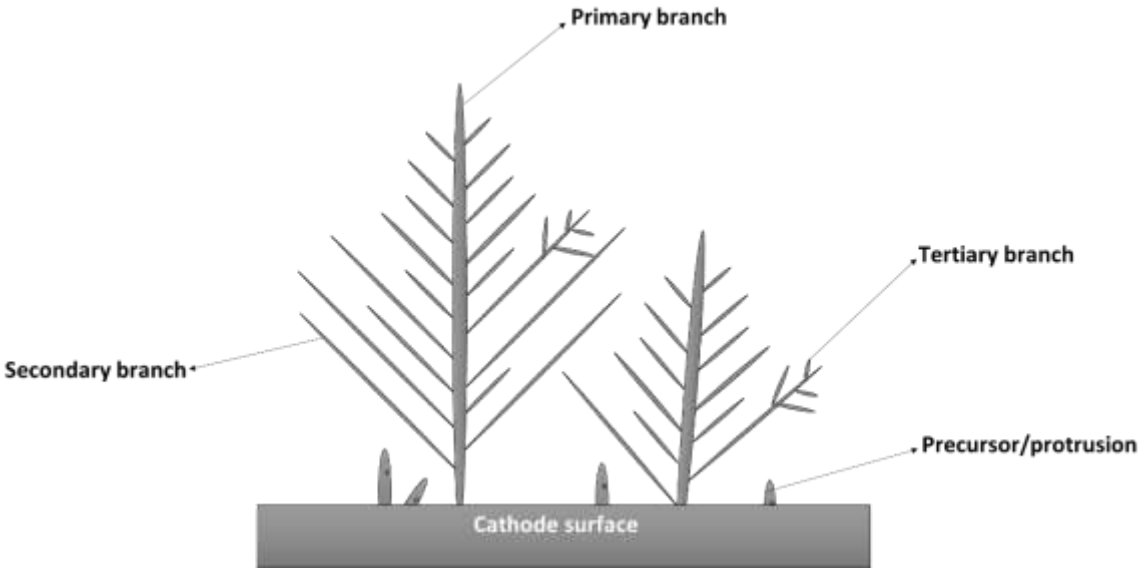

Figure 2.5: A schematic diagram of a dendrite layer growth during the electrodeposition process.

Barton and Bockris (1962) proposed a summary of the quantitative theory of dendrite growth during the electrodeposition process based on several observations. These observations were made from the investigation of dendritic growth of Ag from molten KNO_3-$NaNO_3$ at different amounts of $AgNO_3$ and can be categorised into two groups including dendrite initiation and dendrite growth:

Dendrite initiation

a) The concentration of species to be deposited on the cathode surface must not be larger than a certain maximum for a given current density.
b) The ratio of minimum current density to maximum concentration an approximately constant.
c) The overpotential (total surface, diffusion, and ohmic drop) must be greater than a certain minimum for any current density or concentration.

Dendrite growth

a) For a given overpotential the velocity of dendrite growth is constant.
b) Dendrites initiated at high overpotentials grow the fastest.
c) Increasing overpotential during deposition increase the rate of growth at first, then the dendrite tip splits into a fern-like structure which grows at a slower rate.
d) An induction period is required before a dendrite becomes visible.

2.4.2 Mechanism of dendrite growth

Dendrite growth can be initiated by a protrusion which can be a crystal dislocation, an imperfection of the surface or a co-deposit of a foreign species on the depositing surface. Dendrite growth is favoured at the tip of the precursor because it is a region of higher electrical field density, spherically predominant and has faster deposition rates of metallic ions from the electrolyte as it takes less time to reach the tip compared to those relatively flat deposits on the cathode surface (Devos et al., 2007; Bockris and Razumney, 1967; Werner, 2017). When the protrusion has grown to a size comparable to the average diffusion layer, spherical diffusion conditions rather than linear diffusion conditions are favoured. The spherical diffusion condition effect on the dendrite growth cannot become effective if the growing surface remains in a region where the concentration gradient is controlled by the diffusion

layer of the larger cathode electrode (Popov et al., 1981). It will only become a significant influence when the limiting current at the tip is reached and this condition can be achieved as the protrusion grows further and further into the diffusion layer (Popov et al., 1981). Hence, the tip will form its own diffusion layer outside the overall diffusion layer. Under these conditions an adsorbed species (i.e. organic additives) as discussed further in section 2.5 could be used to prevent further growth of the dendrites.

2.4.3 Metallurgical short circuits

Dendrite growth on the cathode surface during copper electrowinning usually causes metallurgical short circuits (hotspots) especially if the cell is operated at high current densities and there is also misalignment of electrode as shown in Figure 2.6 (Shukla, 2013). As the dendrites grows, they deteriorate the quality of copper deposit forming a rough copper deposit surface. If the dendrite grows further on the copper surface until it reaches the anode it will establish a metallic contact between the electrodes causing a short circuit. Short-circuits will then reduce the equivalent resistance between the electrodes in contact disrupting the flow of current within and between the cells. In this case, an electrical path instead of an electrochemical path occurs between the anodes and cathodes whereby the electric current produces heat in the short-circuited electrodes (very hot cathode bars) and in the current distributing system instead of plating copper (Makipaa et al., 1999; Wiechmann et al., 2006).

The electrical disturbance caused by short-circuits alters the current dispersion among the anode-cathode pairs increasing electrical waste which causes a decrease in current efficiency (Wiechmann et al., 2006; Moongo and Michael, 2021). Short-circuits must be eliminated as soon as possible since they have a detrimental effect on the current efficiency and quality of copper deposit produced during the electrowinning process. According to Moongo and Michael (2021) the root causes of the metallurgical short circuits include old corroded anodes, poor anode maintenance in terms of missing insulator replacement, poor spent electrolyte copper concentration and poor cathode smoothing agent control. Measures to eliminate short-circuits include optimization of the plating rate and time, and also addition of smoothing agents to the electrolyte (Tucker, 2019). In industrial tankhouses, faults caused by short circuits can be detected using various technologies to measure the voltage between the anode and cathode, the temperature of the cathode bars or the magnetic field of the cathode bars produced by the electrode current (Makipaa et al., 1999).

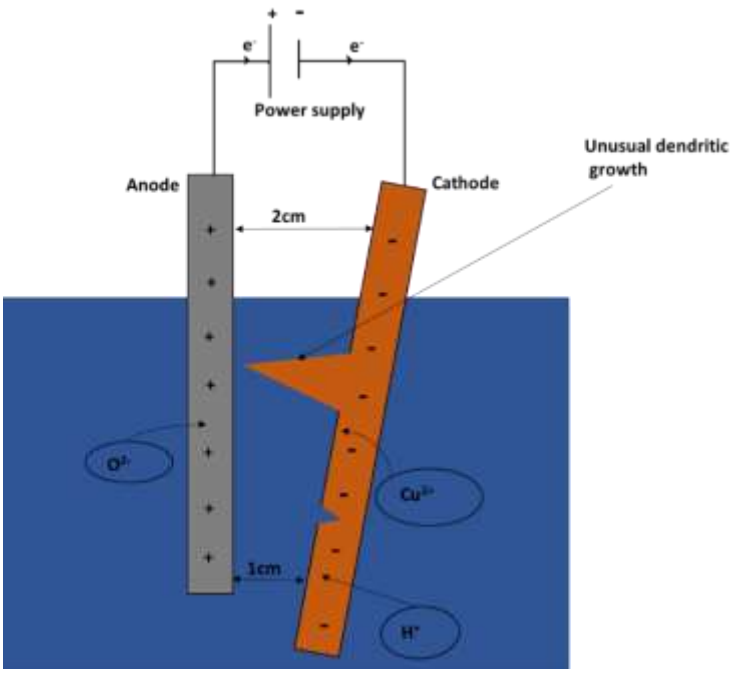

Figure 2.6: EW setup for electrodes that are not completely parallel to each other and unusual dendritic growth.

2.5 ORGANIC ADDITIVES IN COPPER ELECTROWINNING

2.5.1 Introduction

In tankhouses organic additives are dosed during the copper electrowinning process to improve the quality of copper plates by ensuring that the copper deposit produced is smooth and dense without voids or porosity. Organic additives will either act to depolarize or polarize the copper electrodeposition process. Depolarization enhances the rate of reaction while polarization initiates a decrease in the rate of reaction at a fixed potential (Moats et al., 2016; Coetzee, 2018). Additives that polarize or inhibit the copper electrodeposition reaction are believed to adsorb on the cathode surface, thereby increasing the effective current density resulting in an increase in the overpotential. The great importance of organic additives is attached to the correct dosing during copper electrowinning in tankhouses. This thesis explores the idea of reducing unusual dendritic growth on the cathode surface under various operating conditions to develop an understanding for guar requirements in copper electrowinning.

2.5.2 Classification of organic additives

As already mentioned in section 2.5.1 organic additives will either depolarize or polarize the electrodeposition process. This clearly shows that organic additives have an influence on the properties, electrochemistry, and morphology of the copper deposit on the cathode surface. Organic additives can generally be classified as follows (Coetzee, 2018; Oniciu and Muresan, 1991):

a) Brighteners
b) Levellers

c) Suppressors

Brighteners aid in orientating crystallographic changes on the copper deposit where the growth rates at different crystal faces becomes uniform making the deposit to appear brighter and shinier (e.g., Thiourea and Bis (sodium sulfopropyl) disulfide (SPS)). Levellers are added into the electrolyte during the electrowinning process generally to achieve a geometric change on the surface of the copper deposit. This tends to redistribute the growth rates that will eliminate micro-and submicro-roughness producing a smoother surface with less protrusions or edges. Common additives used as levellers in copper electrodeposition are polyacrylamides, glue, guar, thiourea, benzotriazole and janus green B (JGB). Suppressors also known as carriers or inhibitors are polarizing agents which are believed to affect both the copper dissolution and deposition process. They control the vertical growth to produce smooth deposits by conferring preferential adsorption on the peaks of active sites eliminating/reducing short circuits caused by the peaks (dendrites). Some additives used as carriers in copper electrodeposition are polyethylene glycol (PEG), polyalkylene glycol (PAG), glue, gelatin and polyacrylamides. Generally, additives can be placed in one or more of these classes and sometimes may also have synergistic properties. Chloride ion act as a depolarizing agent known to depolarize or accelerate the rate of copper plating improving plant productivity. The addition of chloride ion is important in any copper electrowinning circuit because it assist in interactions between the copper surface and suppressors.

2.5.3 Effects of organic additives on nucleation and growth

After addition of organic additives into the electrolyte there will be an effect on the current-potential relationship because of the competition that exists between organic additives and copper ions for surface coverage on the cathode. As already mentioned in section 2.3.2, nucleation and growth control are important in the electrodeposition process because they determine the resulting morphology of the copper deposit. Hence, the type of organic additive used must be selected based on its role to control nucleation and growth at the metal/electrolyte interface.

The competition for surface coverage between the various ions existing in the electrolyte is represented by the schematic of the electrical double layer shown in Figure 2.7. The electrical double layer is a region near the cathode electrode surface to the bulk electrolyte which comprises charged species close to the electrode/electrolyte interface. The layer which is closest to the electrode is termed the Inner Helmoltz plane (IHP). This layer contains solvent molecules and specifically adsorbed ions. The Outer Helmoltz plane (OHP) contains non-specifically adsorbed solvated ions which can approach the electrode surface only to a distance (X_2). The OHP is primarily comprised of ions with an opposite charge of the electrode. The ions present in the region from OHP to the bulk solution undergo diffusion.

The interaction of the solvated ions (Cu^{2+}) with the charged metal surface to produce copper metal during electrowinning through the reduction reaction is only through long range electrostatic forces and essentially independent of the chemical properties of non-specifically adsorbed solvated ions. The presence of adsorbed electroactive species in the electrical double layer affects the rate of reduction reaction. Chloride anions are specifically adsorbed on the electrode and binds with Cu^{2+} resulting in an overall acceleration of the copper reduction reaction (Shao et al., 2007). Sulphate ions are non-specifically adsorbed on the copper surface (Hope and Woods, 2004). Based on literature the presence of organic additives changes the interaction of the solvated copper cations and specifically adsorbed anions in this electrical double layer region on the cathode (Fabian 2005; Bard and Faulkner, 2001; Coetzee, 2018). Since guar contains repeating units of OH^- (hydroxyl) in the molecule chain it is

concluded that it is non-specifically adsorbed on the high-active energy sites (e.g., nodules/dendrites) on the electrode inhibiting the growth of copper dendrites.

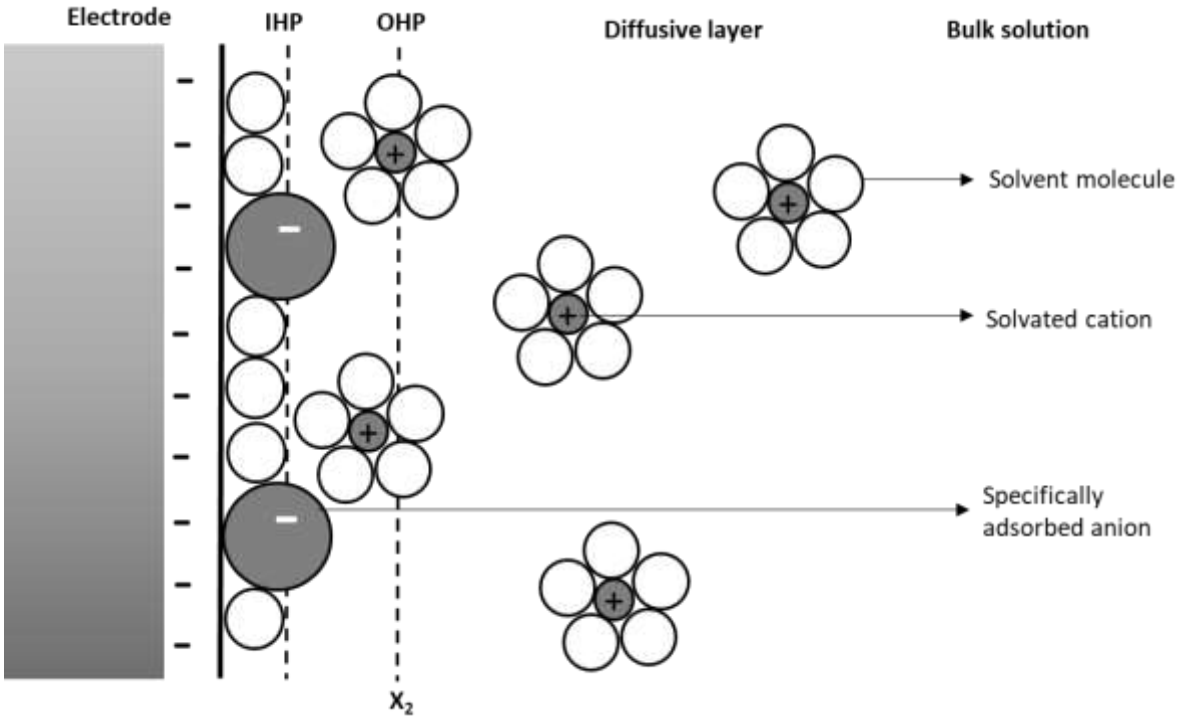

Figure 2.7. Schematic diagram illustrating the electrical double layer regions under conditions where certain anions are specifically adsorbed (Bard and Faulkner, 2001).

Inhibitors (guar, glue, polyacrylamides, etc) as discussed in section 2.5.2. can be added to control nucleation and growth of deposit during copper electrodeposition. The interaction between copper cations and specifically adsorbed anions will be hindered by the presence of inhibitors in the electrical double layer. These inhibitors do not cover the whole cathode electrode surface area but favour high active energy sites and can either be physically adsorbed (physisorption) or chemically adsorbed (chemisorption). Coetzee (2018) proposed that guar interacts near the Outer Helmholtz layer with the electrode surface via long range electrostatic forces while polyacrylamides interact on the hydrophobic copper electrode surface via hydrogen bonding (short range interactions) with their apolar backbone. This indicates that both guar and polyacrylamides are physically adsorbed on the cathode electrode surface. There is no charge transfer between the additive molecules and the substrate for physical adsorption process, and this renders the process as an almost zero current process.

Different types of deposit growth can be expected on the cathode surface during the electrodeposition process in relation to the level of inhibition provided by the organic additive in the electrolyte and the magnitude of the ratio between current density and DLC current (J/J_d) as shown in Figure 2.8 (Winand, 1992; Fisher, 1969; Winand, 1994):

- FI: Field oriented isolated crystals type
- BR: Basis oriented reproduction type
- FT: Field oriented texture type
- UD: Unoriented dispersion type

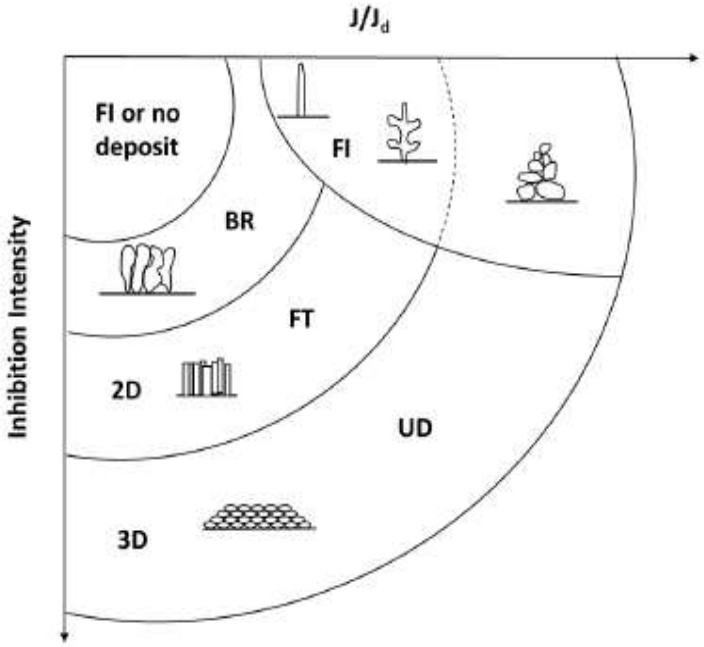

Figure 2.8. A simplified diagram showing the different types of deposit growth as a function of inhibition intensity and ratio J/J_d adapted from Winand (1992).

The competition between growth perpendicular and parallel (lateral) to the cathode surface as well as the frequency of two-dimensional (2D) nucleation influences the possible type of deposit achieved. During the electrodeposition process the thickness of growth layers will increase with current density and decreases with increasing the inhibition level (Winand, 1994). Hence, the speed of lateral growth decreases with increasing the current density at constant inhibition level favouring the formation of isolated crystals or dendrites alone the x-axis of the Winand's diagram. Alternatively, the speed of lateral growth on the cathode surface increases with increasing the inhibition level at constant current density allowing the formation of dense and coherent deposits along the y-axis. If there is insufficient energy two-dimensional nucleation might not be possible to occur. This effect is dominant at very low inhibition levels and magnitudes of J/J_d. However, if the magnitude of J/J_d ratio and/or the level of inhibition are high enough, new crystals are developed via three-dimensional (3D) nucleation (Winand, 1994). The ratio (J/J_d) can also be written in terms of current density and concentration of copper in the bulk solution (J/C_{bulk}) since DLC current and concentration of copper in bulk solution have a linear relationship.

2.5.4 Physicochemical properties of guar

Guar is a naturally occurring galactomannan polymer, a polysaccharide, which is widely used as a flocculant or coagulant in various industrial applications with average molecular weight ranging from 1 to 2 million Da. Guar is a linear D-mannose sugar with D-galactose sugar side chains on every other mannose backbone as shown in Figure 2.9 (Coetzee, 2018). Depending on the variation of its

geographical origin the average ratio of mannose to galactose unit (M/G) is 2:1 (Mudgil et al., 2014; Wang et al., 2000).

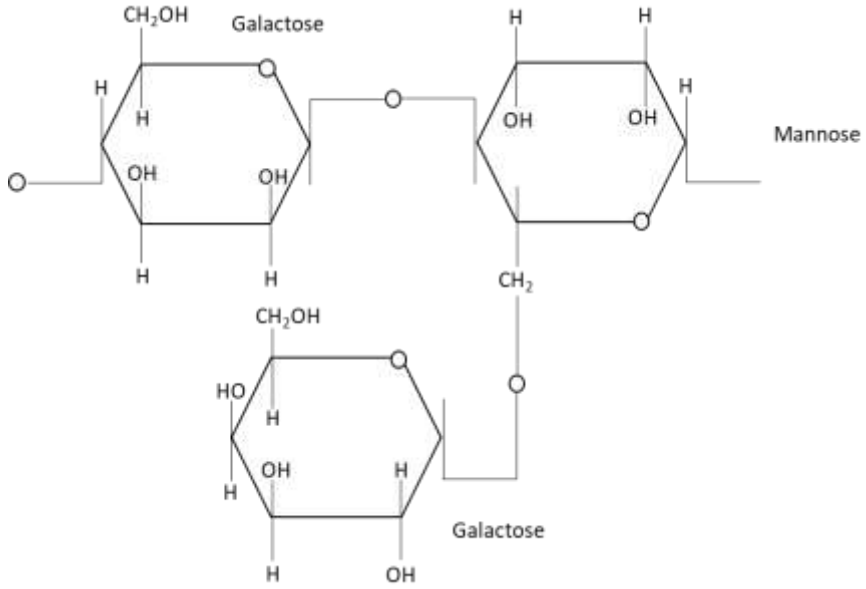

Figure 2.9: The molecular structure of guar adapted from Fabian et al. (2007).

Guar is derived from a guar plant (Cyamopsis tetragonolobus) which is usually found in South Africa, Indian subcontinents, southern hemisphere in semi-arid zones of Brazil and Australia or in the southern part of USA, like Texas or Arizona (Sharma et al., 2018). India and Pakistan combined produce a total of 90% guar of which 80% is produced by India only. The availability of guar can be impacted by geopolitics and natural catastrophes like monsoon related to the climate of India leaving the industry without an alternative. Furthermore, the price of guar can be extremely volatile due to demand and supply constraints (Sharma and Gummagolmath, 2014). The manufactured guar powder appears whitish to yellowish in colour and it is odourless. Guar is widely used in industrial applications because of its physical, chemical, and biological properties which includes the following (Hasan and Abdel-raouf, 2018):

a) High viscosity.
b) It is soluble in water but insoluble in all organic solvents.
c) High ability for chemical modification and cross linking.
d) Gel and film forming ability.
e) Ability to maintain its polymeric properties or intended function when exposed to chemicals.

2.5.5 Guar hydrolysis mechanisms

The degradation rate of guar is influenced by physicochemical conditions (temperature, pH, and concentration) and the conformation of molecules (Hjerde et al., 1994). Generally, galactomannans exist as random coiled single-stranded chains in solutions and for such conformation a non-specific degradation (random scission) can be expected. From the published literature there is very little information on the kinetics of acidic hydrolysis of guar and modified saccharides reported. Increasing temperature of guar solutions causes the water molecules around the guar molecules to lose their

ordering, because of which conformation gets disturbed resulting in reduced viscosity. Wang et al. (2000) reported that guar and similar polysaccharides are readily hydrolysed to shorted organic molecules (monosaccharides) in strong acidic solution (i.e., 12 M sulphuric acid). But in milder conditions guar can either remain undegraded or be partially degraded.

2.5.6 Adsorption mechanisms of guar.

Similar to the guar hydrolysis mechanism, there is also limited information from the published literature on the studies regarding the adsorption mechanism of guar on copper metal during the electrodeposition process. According to Stankte (1999) the adsorption of guar during the electrodeposition process can be explained based on the adsorption mechanism of glue. The electro adsorption of guar on the cathode surface mainly occurs at locations with high field strength (edges/needles/nodules/dendrites). In these areas, the guar molecules form an isolating layer which causes a decrease in the electric field strength. This prevents further growth of the dendrites which could result in short-circuiting. After the normal copper deposit layer has grown up to the peak of the dendrite inhibited, the guar molecule is desorbed and can be adsorbed again at another area with a high field strength. The surface adsorption of guar during metal deposition at protrusions may be represented by Figure 2.10 which was proposed for adsorption of organic additives such as glue.

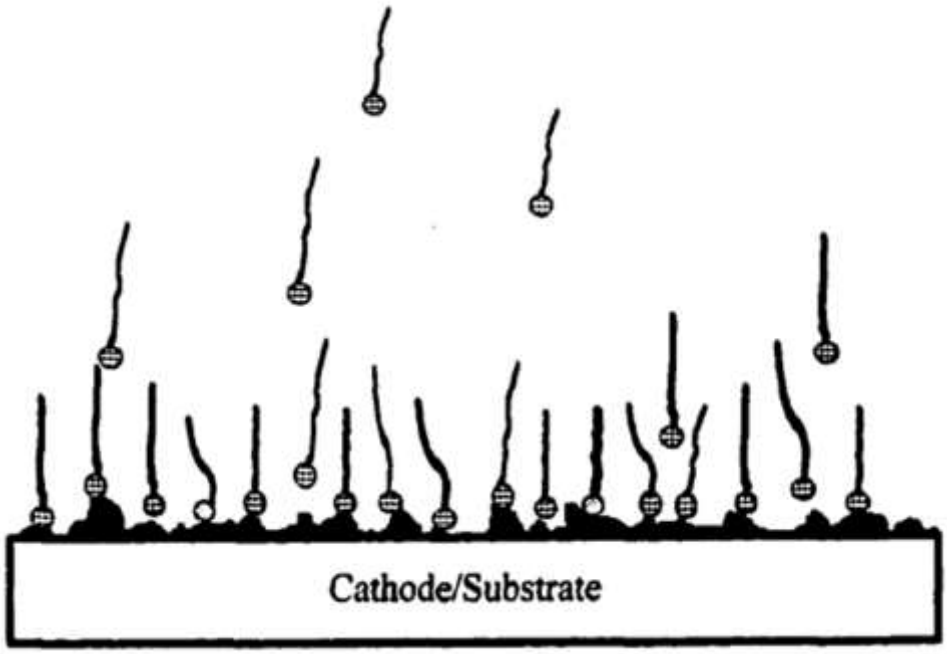

Figure 2.10: A Proposed surface adsorption of organic additives such as glue during metal deposition at protrusions adapted from Collins (2001).

2.6 KEY PERFORMANCE INDICATORS (KPI's)

Operational problems which result from interactions of several parameters are a major concern in the copper EW tankhouse because they directly affect the key performance indicators (KPI's), namely current efficiency, quality of cathode deposit, and the specific energy consumption. The main aim during copper EW is to maximize the current efficiency while ensuring that a high-quality cathode deposit is produced at reduced energy consumption. To achieve this aim various monitoring systems

have been developed to establish the actual status of different operating parameters during EW which directly affect the KPI's (Aqueveque et al., 2015). Some of the important operating parameters in the EW process are discussed in section 2.7.

2.6.1 Current efficiency

Current efficiency (CE) is the ratio of the current used to produce a metal copper to the total current which is actually applied to the EW cell. It is one of the most important measures of tankhouse proficiency in producing electron metal and it is normally expressed in percentage (Alfantazi and Valic, 2003). To determine the current efficiency once the EW process is completed, Equation 2.11 can be used whereby the actual weight of metal copper produced is divided by the theoretical weight of copper deposited.

$$CE\ (\%) = \frac{m_{actual}}{m_{theoretical}} \times 100 \qquad Equation\ 2.11$$

The theoretical weight of copper is represented by Equation 2.6 which is described by the Faraday's law discussed in section 2.2.2 of this report. Current efficiencies for operations where electrowinning is coupled with solvent extraction can be as high as 95% (Beukes and Badenhorst, 2009). The current is wasted through (Beukes and Badenhorst, 2009; Wiechmann et al., 2010; Shukla, 2013):

a) Stray currents to the ground.
b) Short circuits of the electrode caused by the dendritic growth of copper during deposition.
c) Side reactions such as the reduction of Fe^{3+} to Fe^{2+} at the cathode and the re-oxidation of Fe^{2+} to Fe^{3+} at the anode.

High current efficiency is desirable during copper EW for the reason that it maximizes copper deposition rate and minimizes the specific energy consumption, but it does not provide a direct measure of the quality of the copper metal produced. Production of poor quality of copper deposit can still be observed at high current efficiencies (Alfantazi and Valic, 2003).

2.6.2 Copper deposit quality

Physical and chemical measurements can be done to determine the quality of copper plates produced during the copper electrowinning process. A chemical analysis on the copper sheets is done in the laboratory after sampling to determine the grade of copper for quality control purposes. The quality of copper deposit produced is normally specified by the client (Beukes and Badenhorst, 2009). Generally, high purity cathodes that are 99.99% copper are produced during electrowinning (Aqueveque et al., 2015), and the remainder consists of solid particles reported as impurities which are physically entrapped on the cathode deposit (Schlesinger et al., 2011). Major entrapped impurities analysed are iron, sulphur and lead. Scanning electron microscopy or X-ray photoelectron spectroscopy can be used in the laboratory to assay for sulphur, lead, iron, etc from the copper sheets produced (Aqueveque et al., 2015). The results obtained will only indicate whether changes in the chemical section are required for the next EW cycle since corrective measures cannot be done on the copper sheets already produced. The LME Grade A specifications in copper cathode production are given in Table 2.1.

Table 2.1: LME chemical specifications for a commercial copper cathode.

Element	LME Grade A (ppm)
Pb	5
S	15
Fe	10
As	5
Sb	4
Ag	25
Te	2
Cu	99.99%

Physical measurements on the copper sheets can also be done to analyse and classify the morphology in which the copper has been deposited. The surface roughness and grain orientation of the copper deposit produced must uphold a certain standard to conform with regards to downstream physical handling and market acceptance (Alfantazi and Valic, 2003). Formation of dendrites on the cathode surface from copper deposition is a persistent problem in copper electrowinning, especially where high current densities are applied (Cifuentes et al., 2015). Thus, it is important to ensure that the deposit surface roughness always conform to the required standard to avoid affecting the plant performance. Since the cathode plates are immersed inside the EW cell it is difficult to detect the formation of dendrites instantly (Aqueveque et al., 2015). Dendrites have a tendency to trap suspended solids, which has a negative effect on the conductivity and ductility of copper deposits (Cifuentes et al., 2015). In extreme cases the deposits become so brittle to an extent that the copper sheets break during stripping and results in production of large amounts of scrap copper which causes significant delays in stripping as plant operators struggle to clear the scrap. Short-circuiting and a loss in current efficiencies can also result from dendrites on the copper plates. After the electrowinning process, a machine is used to analyse for dendrites on the copper sheets produced thereafter the cathodes can be weighed.

2.6.3 Specific energy consumption

The specific energy consumption (E.C) is a measure of the power used during the electrowinning process. In copper electrowinning operations the power requirements are high, ranging between 1300 kWhr/tonne and 2400 kWhr/tonne (Shukla, 2013). The power requirement is primarily dependent upon the applied voltage, which can be calculated using Equation 2.12:

$$P = V.i.A \qquad Equation\ 2.12$$

Where: P is the power requirement.

V is the applied voltage.

i is the current density.

A is the total area of electrowinning surface.

From basic physics of electricity, electrical energy can be calculated as per Equation 2.13:

$$E = P.t \qquad Equation\ 2.13$$

Where: E is the electrical energy.

P is the power requirement.

t is time.

Combining Equation 2.6, Equation 2.12 and Equation 2.13 shows that the specific energy consumption (E.C), in kilowatt hours per tonne of copper produced can be calculated per Equation 2.14:

$$E.C\ \left(\frac{kWhr}{tonne}\right) = \frac{V.n.2680}{(C.E(\%).M_w)} \qquad Equation\ 2.14$$

2.7 FACTORS AFFECTING COPPER ELECTROWINNING

2.7.1 Temperature

Most electrowinning operations are performed within the temperature range of 45°C to 55°C (Beukes and Badenhorst, 2009;). From the 2013 world operating tankhouse survey data for copper electrowinning, the lowest temperature that was observed from one of the plants was 38°C while the highest operating temperature was 60°C (Robinson et al., 2013). There is no truly ideal temperature for the electrowinning process. Therefore, the best operating temperature for achieving optimum rate of copper production and deposit quality is dependent on the other operating parameters specific to each plant. In industry, a heat exchanger is therefore placed before and after the electrowinning cell to control the circulating electrolyte temperature. The spent electrolyte temperature must be maintained below 40°C to prevent degradation of the SX organic phase when contacted with the recycled spent electrolyte.

Temperature is an important parameter for copper electrowinning process which affects the physico-chemical properties and mass transfer of the electrolyte. Ultimately, temperature also affects the energy efficiency of the electrochemical process. According to Owais (2009) operating the electrowinning cell at a higher temperature causes a decrease of electrolyte viscosity and consequently enhanced ion diffusion rate through the electrolyte bath, which reduces the concentration polarization (improves current efficiency) and consequently decreases the cell voltage

(lower energy demand). However, elevated temperatures are also reported to supress additive adsorption rendering them ineffective (Ngandu, 2016).

It has been reported that the change in temperature of the electrolyte affects the copper cathode deposit and its structure. According to Andersen et al. (1983) and Panda and Das (2001) the quality of copper deposit improves as the temperature increases. This was attributed to accelerated mass transfer rates enabling constant smooth growth of copper crystals. However, if the temperature is too high, a rough cathode surface (along with dendritic structures) will result because faster reaction kinetics causes insufficient time for a smooth crystal structure to be formed (Ehsan et al., (2016). This effect of temperature is also supported by Pradhan et al. (1996) whereby it was observed that increasing temperature from 30-60°C resulted in rougher copper cathode deposits. In conclusion, Ehsani et al. (2016) suggested that temperature should be controlled effectively to establish a balance between the deposit quality, current efficiency, and specific energy consumption.

2.7.2 Copper concentration

Copper ore grade and upstream processes influences the concentration of copper in the feed electrolyte. The concentration of copper in the feed electrolyte can range from 25 g/l to 70 g/l (Robinson et al., 2013). Fundamentally, copper in the electrolyte should not be depleted too low during the electrowinning process as this will cause hydrogen formation at the cathode leading to fire and explosion hazards (Abbey, 2019). Furthermore, the formation of nodules can be observed because of the limiting mass-transfer rate of copper to the cathode surface whereby copper ions cannot be supplied locally to the cathode surface at the rate in which it is being depleted from the boundary layer solution by plating (Leahy and Schwarz, 2010).

Moats and Khouraibchia (2009) and Das and Krishna (1996) observed that the current efficiency slightly increases with increasing copper concentration. Owais (2009) also observed the same trends and explained that increasing the copper concentration in the electrolyte will constantly supply a sufficient amount of copper ions to the cathode surface improving the deposition rate and consequently the efficiency. Owais (2009) and Das and Krishna (1996) observed that the power consumption increased with decreasing copper concentration. The increase in energy consumption can be due to higher tendency for stray currents at lower copper concentration.

2.7.3 Sulphuric acid concentration

In the industry, sulphuric acid concentration ranges between 160 g/l and 200 g/l for electrowinning plants which are coupled with the solvent extraction stage (Robinson et al., 2013). According to Davenport et al. (2002), most electrowinning tankhouses commonly operate at 170 g/l. The variation of sulphuric acid concentration during the electrowinning process highly influences the anode and cathode polarization.

According to Owais (2009), increasing the sulphuric acid concentration from 50 g/l to 300 g/l will result in an increase in current efficiency whereas the cell voltage and specific energy consumption decrease. Moats and Khouraibchia (2009) similarly observed that increasing sulphuric acid concentration from 160 g/l to 220 g/l will lead to a slight increase (1% increase) in current efficiency. The main drawback of increasing sulphuric acid concentration in the electrolyte include the increase of viscosity and a decrease of diffusion of ions to the cathode surface (Owais, 2009). However, according to Panda and Das (2001) the variation of sulphuric acid concentration in the range 30 g/l to 150 g/l had no significant effect on the current efficiency and power consumption. On the other hand, the direct result of the sulphuric acid concentration on the pH of the system means that the more acidic the solution, the

more conductive the electrolyte becomes, thereby lowering electrical resistance and hence the higher the energy efficiency (Davenport et al., 2002; Hayes, 2003).

The higher the concentration of sulphuric acid, the more likely the quality of the copper deposit is compromised (Dini and Snyder, 2011). The effect on the quality can be due to the sulphate anion specifically adsorbing to the cathode surface. Brown and Hope (1995) also investigated the adsorption of HSO_4^- and SO_4^{2-} ions at a copper cathode in sulphuric acid solution. The results showed that the adsorption of anion at the copper cathode is dominated by SO_4^{2-} while HSO_4^- ions exist primarily as solution species even though a residual amount of HSO_4^- can weakly interact with the copper cathode surface. The adsorption is improved at large cathodic potentials and it is not observed at positive potentials where copper dissolution occurs (Brown and Hope, 1995). These specifically adsorbed anions inhibit the nucleation of new copper crystals and causes the existing crystals to increase in size (Panda and Das, 2001).

The presence of acid in the electrolyte has a negative impact on the operation of the electrowinning plant since it causes acid mist. Acid mist is inevitably generated in electrowinning tankhouses when sulphuric acid particles trapped in the ascending bubbles of oxygen that were formed when the water molecules are electrolyzed on the anode burst at the free surface of the solution (Weichmann et al., 2016; Msindo, 2010). The production of acid mist during electrowinning is affected by such factors as current density, electrolyte temperature, ambient temperature, electrolyte composition and ambient pressure (Hiskey, 1999). Acid mist has detrimental effects in the tankhouse as it causes extensive corrosion of equipment and unfavourable labour conditions (Aqueveque et al., 2015). In an attempt to eliminate or minimize acid mist in copper electrowinning tankhouses chemical and physical methods have been used. According to Pfalzgraff (2009), acid mist can be controlled by covering the cells and ventilate the mist somewhere else. The second physical method to control acid mist is to float a layer of beads or balls on top of the electrolyte. This creates a more convoluted path of acid mist so that they can burst less violently (Aqueveque et al., 2015; Shakarji et al, 2011). To control the acid mist chemically, chemical suppressants can be added into the electrolyte. Alternatively, surfactants or foaming agents which stabilise the oxygen bubbles into foam layer can also be used to control acid mist (Aqueveque et al., 2015; Pfalzgraff, 2009).

2.7.4 Current density

Current density is one of the important parameters which influences the current efficiency and quality of the copper deposit produced during electrowinning (Alfantazi and Valic, 2003). In the industry, current densities are usually operated between 250 A/m^2 to 300 A/m^2 for operations where copper electrowinning is coupled with the SX stage (Beukes and Badenhorst, 2009). From the 2013 world tankhouse operating tankhouse survey data, the lowest current density observed was 189 A/m^2 while the highest operating current density was 400 A/m^2 (Robinson et al., 2013). Normally, copper cathodes with improved quality are produced at higher current density in operations where SX precedes electrowinning than in direct electrowinning operations.

According to Alfantazi and Valic (2003) and Moats and Khouraibchia (2009) current efficiency increases with an increase in current density. Operating at high current densities will result in an increase in current efficiency, however, operating at too high current density will result in a low-quality copper deposit produced. Increasing current density results in finer grains and more dendrites on the cathode surface (Akbarzadeh and Shakib, 2011). This may be attributed to faster reaction kinetics occurring at higher current densities allowing less time for the formation of large crystals. Furthermore, if the current density is increased until it exceeds the limiting current density (i_L) of the system the deposit will become powdery (Davenport et al., 2002; Panda and Das, 2001). Hence, the

norm in the electrowinning tankhouses is to operate at around 50% of the limiting current density. Winand (1992) also concludes that the copper deposits become powdery when current density is operated above the limiting current density. An increase in power consumption was observed with an increase in current density (Panda and Das, 2001; Das and Krishna, 1996).

2.7.5 Guar concentration

To promote the plating of smoother copper deposits with minimal entrapments of impurities, organic smoothing agents are added in the electrolyte (Schlesinger et al., 2011). For several decades, guar gum has become the standard smoothing agent for copper electrowinning. Guar is added in the electrolyte to keep the rate of copper crystal growth constant and help reduce the formation of dendrites which can cause short-circuiting as discussed in section 2.6.3 (Murray et al., 2016). Typically, guar is added at a range of 200-700 g/t cathode during copper electrowinning (Robinson et al., 2013).

Stankte (1999) presented information on the measurement of guar using the CollaMat system. The electrochemical activity of various amounts of guar was established. The response rate versus time as a function of sulphuric acid concentration and temperature were studied using the CollaMat system. For all the tests it was observed that guar did not reach maximum activity for some time. Based on these results, Stankte concluded “that the most active species (molecules) of guar are generated by hydrolysis reaction” and guar was a weak polarizer. Wang et al. (2000) also support these results based on the study of guar gum degradation in acidic solutions where it was found that temperature and pH had an effect on the degradation of guar gum, both separately and synergistically when considered together.

From a laboratory scale experiments to examine guar and activated polyacrylamides (APAM), guar plus chloride was found not to be effective in smoothing the cathode when compared to APAM plus chloride prepared at the same concentration (Fabian et al., 2007). The interaction of guar and chloride on the copper deposit crystal structure in concentrations of 15 mg/l to 30 mg/l with 30 mg/l Cl^- improved the quality of copper deposit (Aragon and Camus, 2011).

Very little literature was found on the performance of guar as a smoothing agent at varying concentrations with other parameters to control dendrite growth during bench-scale copper electrowinning experiments.

2.7.6 Chloride Ions

Chloride ions often occur naturally in the electrolyte as a result of chloride transfer from the solvent extraction circuit. According to Robinson et al. (2013) most industrial copper electrowinning tankhouses operates with a chloride concentration between 20 mg/l to 30 mg/l in the electrolyte. If the leach operations contain high concentrations of Cl^- in their leach liquors the SX circuit is coupled with a wash stage to prevent excessive Cl^- transfer to the feed electrolyte (Schlesinger et al., 2011). However, if there is insufficient chloride concentration in the electrolyte it can be added as either hydrochloric acid or sodium chloride (Schlesinger et al., 2011). The most beneficial effects of chloride ions in the electrolyte are to promote the growth of dense, fine-grained, low-impurity copper deposits on the cathode. However, if the chloride concentration is above 30 mg/l it will lead to detrimental effects such as pitting corrosion on the stainless-steel cathode blank at the air/electrolyte interface which causes the depositing copper to stick and resist detachment from the cathode during the process of stripping (Schlesinger et al., 2011).

In the copper electrodeposition process, chloride ions are known to act as de-polarizers (accelerators) and grain refiners (Ilgar and O’Keeffe, 1997; Cui, 2014; Moats et al., 2016). In other words, chloride

ions increase the rate of charge-transfer, consequently increasing surface roughness since they enhance growth rate rather than nucleation rate (Fabian et al., 2017). According to Sun and O'Keefe (1992) at 40 mg/l chloride the rate of reaction will be increased possibly due to the formation of copper-chloride. Furthermore, it was observed that increasing chloride concentration in the electrolyte enhances the surface roughness and impurity levels on the cathode deposit. Thus, chloride should be used in conjunction with a polarizing agent to prevent compromising the cathode quality from its reaction accelerating benefits as was proved by Fabian (2005).

2.7.7 Flowrate of electrolyte

As already discussed in Section 2.3.1 during copper electrodeposition the copper ions are transported to the cathode surface through three mechanisms: diffusion, convection and migration. According to Newman and Thomas-Alyea (2004), the transportation of copper ions to the cathode surface through convection is largely dependent on the flowrate of the fluid.

Najminoori et al. (2015) conducted a study whereby the actual experimental conditions of an industrial electrowinning cell were compared to a CFD simulation model. From the study, it was observed that increasing the electrolyte flowrate from 8 m^3/hr to 11 m^3/hr caused an increase in the vertical velocity near the cathode surface. A 0.2% increase in the concentration of copper ions was measured between cells at 11 m^3/hr compared to 8 m^3/hr due to the change in the electrolyte hydrodynamic behaviour. However, current density was kept constant while varying the flowrates and thus, according to the Faraday's law the deposition rate of copper to the electrode surface remained the same. In conclusion, it was suggested that current density should also be increased in order to improve the copper deposition rate from the electrolyte to the depositing surface at an increased flow rate. At an increased flowrate, the Nernst boundary layer thickness decreases which in turn increases the limiting current density (Najminoori et al., 2015).

2.7.8 Cathode

During copper electrowinning, copper ions migrate towards the cathode where they react with electrons to form a copper metal on the cathode surface. Traditionally, copper starting sheets have been used as cathode material; however, with the development in electrometallurgy, 78% of tankhouses surveyed uses permanent cathode technology whereby copper metal is electrodeposited onto 316 stainless steel blank cathodes (Robinson et al., 2013; Schlesinger et al., 2011). The permanent stainless-steel blanks are re-usable and less labour intensive since the technology facilitates automated cathode stripping. To prevent the risk of short-circuiting due to dendrite growth the minimum spacing acceptable for cathode centre to cathode centre for copper electrowinning operations is 95 mm (Beukes and Badenhorst, 2009).

2.7.9 Anode

Most tankhouses employ lead alloy anodes as positive terminals in copper electrowinning operations containing acidic sulphate-based electrolyte. Lead is usually alloyed with other elements which include tin, calcium and antimony to improve its mechanical and structural properties so as to increase its life expectancy (Beukes and Badenhorst, 2009; Mirza et al., 2016). Lead is preferred as a material of construction since it is inert and hence there is no copper electrodeposition at the anode as the only reaction taking place is the evolution of oxygen as shown by Equation 2.2. Lead has the ability to form a stable regenerative oxide layer (PbO_2) on its surface which is insoluble. This oxide layer impedes corrosion and cathode degeneration (Mirza et al., 2016).

Cobalt can exist naturally or physically added as cobalt sulphate to maintain a concentration of 80 to 250 mg/l Co in the electrolyte (Robison et al., 2013). The presence of Co^{2+} stabilizes the PbO_2 layer that forms on the anode, promoting oxygen evolution by decreasing the anode potential, rather than lead oxidation at the anode. As a result, cobalt remarkably mitigates the corrosion of lead anode, thereby, reducing lead contamination on the copper deposit improving the cathode quality and extending the anode life (Nikoloski and Nicol, 2008; Robinson et al., 2013). The average life expectancy of the lead-alloy anodes is typically 7 to 9 years (Beukes and Badenhorst, 2009). The life cycle of anodes is affected by tankhouse operating conditions and maintenance of the anodes, as well as the frequency and duration of power failures (Robinson et al., 2013). Current efficiency is also found to be higher in the presence of Co^{2+} in the electrolyte (Shukla, 2013). According to Moats and Khouraibchia (2009) cobalt has an insignificant effect on the current efficiency and energy consumption when operating the copper electrowinning process with cobalt concentration varied from 100-200 mg/l.

2.8 SURFACE ROUGHNESS CHARACTERIZATION TECHNIQUE

As already discussed in Section 2.4.3, undesirable roughness can cause short-circuiting between cathodes and anodes. Hence, it is importance to evaluate the surface roughness of each copper plate and compare it to determine which experimental conditions are best to control dendrite formation on the copper depositing surface during electrowinning. The variance in the height of a surface is the obvious quantifiable parameter that can be measured when studying rough surfaces.

Surface roughness parameters can be calculated using a line-profiling method (2D roughness) or areal topography method (3D roughness). Two-dimensional (2D) profile analysis has been widely used to evaluate the surface texture of various products in science and engineering industry and laboratory environments (Adamczak and Zmarzly, 2019). Such parameters are easy and quick to measure using portable measuring devices. The arithmetic average height (R_a) parameter is the most common used 2D roughness parameter. This roughness parameter is used to measure the vertical characteristics of the surface deviations for general quality control (Adamczak and Zmarzly, 2019). The R_a parameter can be defined as the average absolute deviation of the roughness irregularities from the mean line over one sampling length as shown in Figure 2.11.

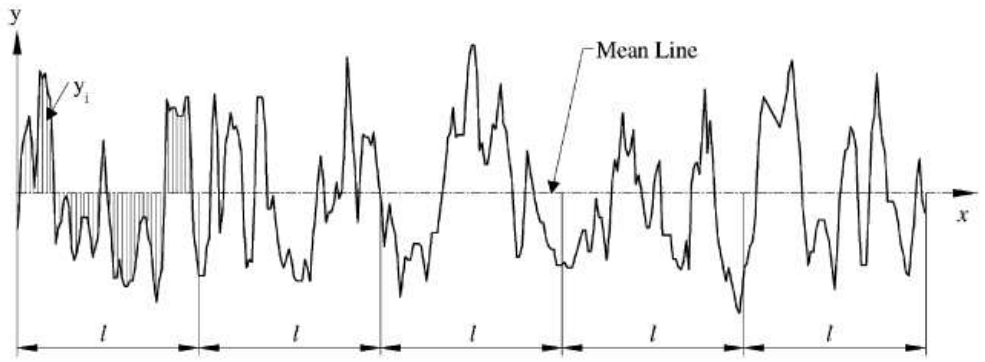

Figure 2.11: Definition of the arithmetic average height (Ra) adapted from Gadelmawla et al. (2002).

The R_a parameter is easy to define and measure. Furthermore, it gives a good general description of height variations. Mathematically, the arithmetic average height parameter can be defined as per Equation 2.15.

$$R_a = \frac{1}{l}\int_0^l |y(x)|dx \qquad Equation\ 2.15$$

Even though the arithmetic average height (R_a) parameter is commonly used it is only limited to providing numerical values that describe the variance in surface height and does not allow for the calculation of the unevenness of the surface (Mathia et al., 2011; Williams et al., 1994). Hence, the data provided from the individual profile measurements solely are not sufficient to describe the actual surface texture. Measurements of completely different shapes can give the same roughness parameter R_a value as shown in Figure 2.12. This provides further evidence for the requirement of other possible measures for investigating the surface roughness (Jansons et al., 2016).

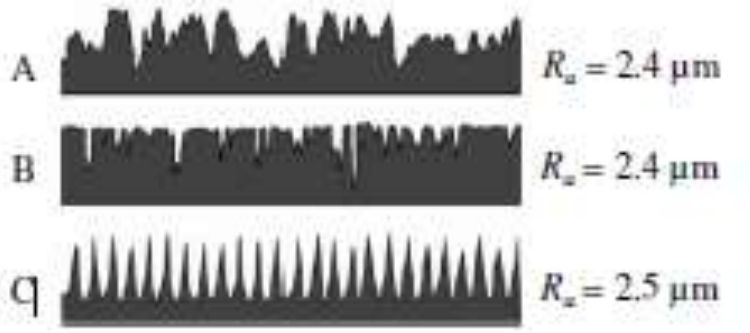

Figure 2.12: Roughness profile examples (Jansons et al., 2016).

Three-dimensional (3D) roughness measurements can be used to describe the surface texture instead of just measuring 2D profile in order to improve the surface roughness characterization precision. In recent years, an increase in the use of 3D surface analysis was observed in the science and engineering applications (Gadelmawla et al., 2002; Lancashire, 2017). A software computer vision package which considers an area from the surface to be tested and divides it into a number of sections can be used to calculate the 3D roughness parameters. To measure the 3D roughness of a single surface might take several hours. Furthermore, advanced knowledge is required to interpret the results of such measurements. Hence, highly qualified personnel must be employed to interpret the results (Adamczak and Zmarzly, 2019).

Several 3D roughness parameters exist which can be used to characterise surface topography (Jansons et al., 2016). In this study the arithmetic mean height (S_a) was used for characterizing the surface of copper plates produced during the copper electrowinning experiments.

The arithmetical mean height (S_a) is the extension of the arithmetical mean height of a line (R_a) to a surface. It expresses, as an absolute value, the difference in height of each point compared to the arithmetical mean of the surface as defined in the new standard ISO 25178 Surface Texture. An

example of a surface demonstrating the measurement of the arithmetical mean height is shown in Figure 2.13. On a perfectly flat surface S_a=R_a=0.

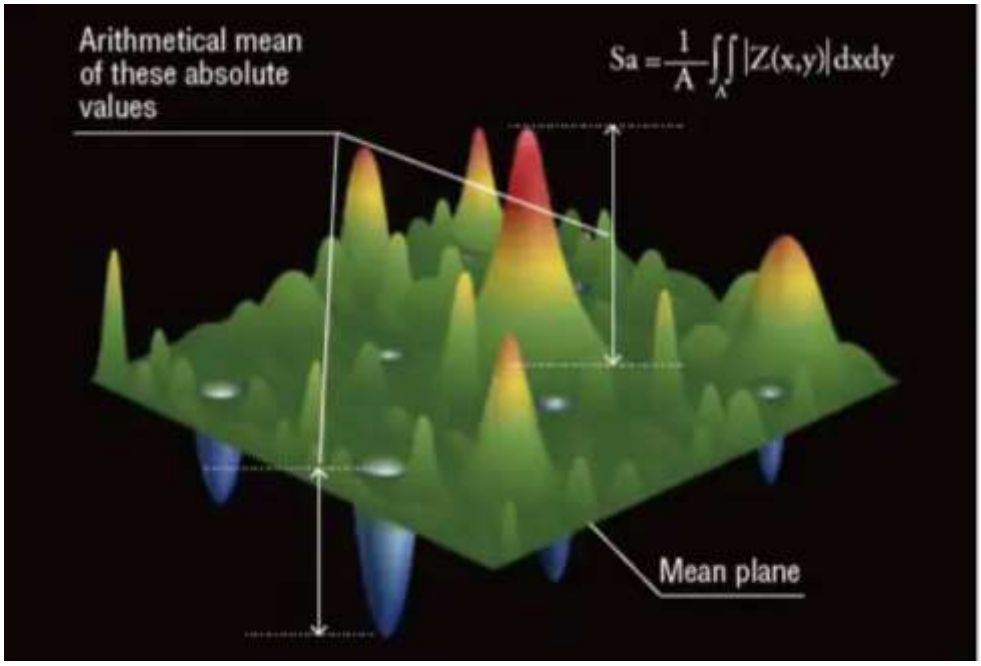

Figure 2.13: A figure demonstrating how the S_a value is measured on the copper cathode deposit.

Mathematically, the arithmetic mean height (Sa) parameter is defined as per Equation 2.16.

$$S_a = \frac{1}{A}\iint |Z(x,y)|\,dx\,dy \qquad Equation\ 2.16$$

To calculate the S_a value of each copper plate the absolute values of the deviation values are calculated, and then multiplied by the corresponding surface area to each such deviation, thereafter the total is divided by the total surface area (Du Plessis et al., 2018).

In the current study, the measurement of surface roughness on the copper plates includes the use of an Artec Spider surface scanner for areal surface parameters and to produce high resolution image of copper plate surface. Since 3D roughness parameters are calculated for an area of the surface instead of a single line the high-resolution image of the copper plate surface was analysed on Volume Graphics VGStudioMax 3.1 software to estimate a mean surface deviation which is a surface roughness factor. A detailed description of measuring the surface roughness value (S_a) for each copper plates produced during copper electrowinning experiments is discussed in Section 3.2.2.

2.9 COPPER DEPOSIT ACID DIGESTION

Acid digestion is a method for dissolving constituents from solid metallurgical products (i.e., copper cathode plates) into solutions. Dissolution can be done by adding acids and heating the sample until complete decomposition. In general, acid digestion depends on the following factors: reaction time, the acid used and its concentration, reaction conditions (temperature, solid-liquid ratio, etc.), driving forces (heat, agitation, etc.) as well as the chemical form of the metals present in the solid matrix (Guven and Akinci, 2011). Analysis techniques including ICP, ICP-MS, AA, or AFS instruments are the ideal companion for acid digestion.

The choice of an acid or acid mixture to be used for digestion is critical and is largely dependent on the nature of the metals present in the metallurgical product to be dissolved (Ramanathan and Ting, 2015). Several studies have reported the use of nitric acid (HNO_3), sulphuric acid (H_2SO_4), hydrochloric acid (HCl) and aqua regia (HNO_3/HCl) for the recovery of metals from waste PCB's (Mecucci and Scott, 2002; Tuncuk et al., 2012). The copper metal is oxidized by the concentrated acid to produce Cu^{2+} ions. As a reference, the acid digestion methods used to recover copper from waste PCB's was used to leach the copper plates produced during the copper electrowinning experiments in this study.

Hydrochloric acid

Hydrochloric acid (HCl) is a non-oxidising acid and thus there is no significant reaction expected between Cu and HCl. For a significant copper dissolution to be achieved when using HCl an oxidative environment is required as represented by Equation 2.17.

$$Cu + 2HCl_{(aq)} \rightarrow CuCl_2 + H_{2_{(g)}} \qquad \Delta G^o_{80} = 92.58\,{}^{kj}/_{mol} \qquad Equation\ 2.17$$

However, if oxygen is available to take part in the reaction, Cu dissolution can be achieved as shown by Equation 2.18.

$$4Cu + 4HCl_{(aq)} + O_{2_{(aq)}} \rightarrow 4CuCl_{(aq)} + 2H_2O \qquad \Delta G^o_{80} = -63.5\,{}^{kj}/_{mol} \qquad Equation\ 2.18$$

Sulphuric acid

Sulphuric acid (H_2SO_4) is used together with hydrogen peroxide (H_2O_2) as an oxidising agent for copper dissolution. Oxygen produced from the decomposed hydrogen peroxide (Equation 2.19) reacts with the metallic copper forming cupric oxide (CuO) which is shown by Equation 2.20. The cupric oxide further reacts with sulphuric acid to produce copper sulphate ($CuSO_4$) as shown by Equation 2.21. Combining Equation 2.19-Equation 2.21 gives the overall reaction of copper dissolution as represented by Equation 2.22.

$$H_2O_2 \rightarrow H_2O + \frac{1}{2}O_2 \qquad Equation\ 2.19$$

$$Cu + \frac{1}{2}O_2 \rightarrow CuO + H_2O \qquad Equation\ 2.20$$

$$CuO + H_2SO_4 \rightarrow CuSO_4 + H_2O \qquad Equation\ 2.21$$

$$Cu + H_2O_2 + H_2SO_4 \rightarrow CuSO_4 + 2H_2O \qquad Equation\ 2.22$$

Nitric acid

Nitric acid is a strong acid and has the ability to corrode most base metals. Furthermore, nitric acid dissociates completely according to reaction represented by Equation 2.23.

$$HNO_3 \rightarrow NO_3^- + H^+ \qquad Equation\ 2.23$$

The nitrate ions may act as oxidising agents by accepting electrons according to the half-reactions represented by Equation 2.24 and Equation 2.25:

$$NO_{3_{(aq)}}^- + 4H_{(aq)}^+ + 3e^- \rightarrow NO_{(g)} + 2H_2O_{(l)} \qquad E^o = 0.96V \qquad Equation\ 2.24$$

$$NO_{3_{(aq)}}^- + 2H_{(aq)}^+ + e^- \rightarrow NO_{2_{(g)}} + 2H_2O_{(l)} \qquad E^o = 0.80V \qquad Equation\ 2.25$$

The reduction of nitrate (see Equation 2.24 and 2.25) can electrochemically sustain the oxidation of most base metals (Cu, Pb, Fe, etc.) due to its higher relative reduction potential. The reduction potential of copper is provided in Equation 2.1.

Aqua regia

Different acids may be combined to improve the dissolution of the desired material. Castro and Martins (2009) reported an improved copper recovery when using a dilute mixture of nitric acid and hydrochloric acid when compared to using only hydrochloric acid or sulphuric acid. The mixture of nitric acid and hydrochloric acid is known as aqua regia. Aqua regia is made by mixing one part concentrated nitric acid and three parts concentrated hydrochloric acid (Rossouw, 2015). Aqua regia has the ability to dissolve to completely dissolve most base metals and precious metals since it has strong reducing and oxidising properties. The dissolution action of aqua regia is due to the formation of nitrosyl chloride and chloride according to the mechanism represented by Equation 2.26-Equation 2.29.

$$HNO_3 + 3HCl \rightarrow NOCl + 2H_2O \qquad Equation\ 2.26$$

$$Cl^- \rightarrow \frac{1}{2}Cl_2 + e^- \qquad Equation\ 2.27$$

$$4H^+ + NO_3^- + 3e^- \rightarrow NO + 2H_2O \qquad Equation\ 2.28$$

$$NO + \frac{1}{2}Cl_2 \rightarrow NOCl \qquad Equation\ 2.29$$

In this study, aqua regia was used to conduct the acid digestion tests as it allows for complete dissolution of copper.

2.10 SUMMARY

Copper electrowinning is the application of an electrolytic cell, whereby current is applied in the system to allow the reduction of copper ions to copper metal deposit at the cathode and the evolution of water at the anode. It has been shown in this literature review that the use of organic additives in copper electrowinning plays a significant role in the copper electrodeposition process to facilitate the formation of smoother, brighter, and denser copper cathode deposits. It has been reported that organic additives interact with the cathode surface by competing with copper atoms for adsorption on high energy nucleation sites (i.e., dendrites). Thus, the organic additives inhibit the growth of dendrites by promoting progressive nucleation rather than instantaneous nucleation. In the industry, guar has been used as a standard organic additive in copper electrowinning, and in acidic solutions guar degrades by hydrolysis. It is essential to constantly monitor the guar concentration in the electrolyte and ensure that it is maintained at optimum level. Thus, if guar addition is not controlled it can lead to reduced electrowinning performance as a result of insufficient suppression of dendrite formation of the copper cathode surface. Dendrites result in an undesirable rough cathode surface and can decreases current efficiency due to short-circuiting.

Fabian (2005) studied the effectiveness of guar and APAM in controlling dendrite growth in a continuous bench scale copper electrowinning system. However, the surface roughness of copper deposits was unable to be measured. Recently, Coetzee (2018) conducted a study comparing guar and polyacrylamides molecular characteristic in the copper electrodeposition process showing that different cathode morphologies were achieved. However, little literature has been published on process interaction and the relationship between operating conditions and optimal guar dosage as well as their implications on the key performance indicators (KPI's). The KPI's in electrowinning are current efficiency, quality of the copper deposit, and specific energy consumption. Some of the operating parameters which directly affect the key performance indicators include temperature, copper concentration, sulphuric acid concentration, current density, and organic additive concentration. With the recent trend of using less expensive modified polysaccharides and polyacrylamides to replace guar, it is thus evident that a better understanding on the operation for organic additives in copper electrowinning will be valuable as organic additives can be dosed on a more informed schedule to avoid its overdose in the tankhouse. Since guar has been used as a standard organic additive it can be used as a benchmark for the performance of newer organic additives in copper electrowinning.

Therefore, process interaction and the relationship between operating conditions and optimal guar dosage as well as their implications on the quality of copper deposit and current efficiency can be investigated by conducting bench scale copper electrowinning test work. The quality of copper deposit can be described by the cathode morphology developed from each experimental condition in the presence of various guar concentrations. Furthermore, the quality of the copper deposit can be described by determining the amount of sulphur by dissolving the copper plates achieved through conducting acid digestion tests. The statistical analysis of copper deposits achieved by Shukla (2013) provided the significant effect of the operating parameters on the surface roughness of copper

deposits. Therefore, there is scope for determining the significant effect of the individual, 2-way interactions, and 3-way interactions of the operating parameters on the copper deposit quality and current efficiency data through statistical analysis.

3. EXPERIMENTAL

The experimental work conducted in this study is divided into three categories:

I. Electrowinning tests
II. 3D scanning tests for morphology determination
III. Acid digestion tests

Electrowinning tests were conducted to investigate the effect of guar dosage on the cathode morphology under various experimental conditions. The surface roughness of copper cathodes was analysed using a 3D surface scanner and a Volume Graphics VGStudioMax 3.1 software to allow for analysis of the surface morphology of all the copper plates that were produced in the presence of guar at various experimental conditions quantitively and qualitatively. Acid digestion tests were carried out in order to determine the chemical composition of each copper plate produced during the electrowinning experiments. The chemical composition was analysed using an Inductively Coupled Plasma Atomic Emission Spectroscopy (ICP-AES). Details on the experimental design, materials, experimental equipment setup, sample preparation, experimental methodology and sample analysis for each test are provided in this chapter.

3.1. BENCH SCALE COPPER ELECTROWINNING EXPERIMENTS

3.1.1. Materials

The electrowinning experiments were conducted using a synthetic copper sulphate solution prepared from analytical grade reagents and de-ionized water to simulate the primary constituents for standard industrial electrolyte. A commercial grade guar powder (Sendep Opt43) purchased from an industrial reagent manufacturing company (SENMIN) was added in the synthetic electrolyte as an organic smoothing agent for all the electrowinning experiments to improve the quality of copper cathodes produced. Literature indicated that the molecular weight of guar varies significantly, depending on the analytical technique used to determine this, however, when using the most recent technique the average molecular weight of guar was determined to be between 1 and 2 million Da (Mudgil et al., 2014). The chemicals used for the electrowinning experiments are listed in Table 3.1. The concentrations of the reagents were chosen based on the typical concentrations in electrowinning operations, determined from literature (Alfantazi and Valic, 2003; Coetzee, 2018; Cui, 2014; Fabian, 2005; Robinson et al., 2013). Calculations for the exact amount of chemicals required for the sulphate-based electrolyte and other concentrations are provided in Appendix A-Sample calculations.

Table 3.1: List of chemicals used in bench-scale copper electrowinning experiments.

Reagent name	Supplier	Grade	Molecular weight (g/mol)
Copper sulphate pentahydrate ($CuSO_4.5H_2O$)	Labchem	AR	249.68

98% Sulphuric acid (H_2SO_4)	Scienceworld	AR	98.08
32% Hydrochloric acid (HCl)	Scienceworld	AR	36.46
Guar (Sendep Opt43)	SENMIN	AR	1×10^6-2×10^6

3.1.2. Experimental Design

In this study the electrowinning tests were carried out by employing a mixed-level full factorial experimental design approach to fully understand the relationship of guar dosage with other electrowinning parameters and their effect on the copper deposit quality and current efficiency. A mixed-level factorial experimental design was chosen as it allowed for simultaneous study of several parameters and the interaction effects of each factor on the electrowinning performance (i.e., copper deposit quality and current efficiency). According to Alfantazi and Valic (2003) important parameter interactions may remain undetected without the use of factorial experiments. The experimental design approach was chosen to include copper electrowinning experimental investigations at two levels of current density, sulphuric acid concentration and initial copper concentration, as well as three levels of guar concentration as indicated in Table 3.2. Three levels instead of two levels of guar concentration were chosen to provide more detailed information on the possible interactions of guar with the other factors.

Table 3.2. Level values for operating parameters tested during the electrowinning experiments.

Factors	Units	Levels		
Initial copper concentration	g/l	35	45	
Sulphuric acid concentration	g/l	150	180	
Current density	A/m^2	180	300	
Guar concentration	mg/l	2	10	18

The electrowinning experiments were conducted in the absence and presence of organic additive (guar) in the electrolyte. The experiment conducted in the absence of organic additive was labelled the “Base case”. A base case scenario experiment was tested for the following experimental condition: no organic additive, 35 g/l initial copper concentration, 150 g/l sulphuric acid concentration, 30 mg/l chloride and 300 A/m^2 current density. A complete experimental design matrix for the bench-scale electrowinning experiments conducted in the presence of guar is provided in Appendix B-Experimental procedure.

Current density, copper concentration and sulphuric acid concentration were selected because they are widely considered to be the most important factors in copper electrowinning (Alfantazi and Valic, 2003). However, the low-level current density value was chosen to be much lower than in the industry

because a conservative current density might provide insight on the effects of copper concentration, sulphuric acid concentration and guar concentration more easily by not being dominated by the effect of high current density. The theory presented in Section 2.2.4 showed that current density has a direct relationship with the rate of reaction and may dominate the system because it was found that it had the largest impact on the Butler-Volmer equation. Thus, increasing current density increases the rate of reaction which significantly affects the deposition mechanism of copper and the morphology of the metal deposit (Collins, 2001; Kruyswijk, 2009). For the chosen levels of copper concentration, a drop in copper concentration in the electrolyte is expected during the test work especially at high-level current density.

Temperature is also an important factor that influences the effectiveness of copper electrowinning and the degradation rate of guar in acidic solutions (Alfantazi and Valic, 2003; Wang et al., 2000). However, in this study temperature was kept constant to understand the effect of guar interaction with other parameters on the surface roughness and current efficiency at 40°C. This temperature was chosen to investigate the performance of guar at its lower rate of degradation while interacting with other electrowinning parameters to improve the copper cathode morphology. It can be recommended to consider the effect of varying temperature on the interaction of operating variables in future work to determine whether the effect of temperature on degradation and ion mobility influences the morphology of the copper deposit.

The aim of the study was to understand the performance of guar at varying concentrations with other parameters to control localized growth (dendrites) during bench-scale copper electrowinning experiments. A detailed description of how additives interact with the cathode surface and why they are so imperative in copper electrowinning is presented in Section 2.5 of this report. Guar was chosen as an organic additive in the current study since it has been used in the copper electrowinning industry as a standard smoothing agent to produce smoother copper cathodes (Moats and Free, 2007; Moats et al., 2016). The typical dosage of guar concentration used in bench-scale copper electrowinning experiments to investigate the influence of guar on the cathode quality is 2 mg/l (Coetzee, 2018; Fabian et al., 2016). In the current study, three levels of guar concentration were investigate (2 mg/l, 10 mg/l and 18 mg/l) as shown in Table 3.2. The low-level guar concentration is 2 mg/l and the medium level of guar concentration (10 mg/l) were identical to the one used in the electrochemical tests from the study conducted by Coetzee (2018). An additional higher level of guar concentration (18 mg/l) was also investigated. This high guar concentration (18 mg/l) is within the range of guar concentrations used to examine guar in copper electrodeposition (Aragon and Camus, 2011; Moats and Derrick, 2012). The presence of impurities in the electrolyte not only have a detrimental effect on cathode quality but also has an effect on the current efficiency (Ngandu, 2016; O'keefe, 1984; Shukla, 2013). Therefore, in order to determine the sole performance and comparison of various guar concentrations without interferences, impurities we not added in the synthetic electrolyte in this current study.

3.1.3. Reproducibility

Validation with literature

Coetzee (2018) conducted copper electrowinning experiments for the base case scenario (no organic additive) and 2 mg/l guar concentration in the electrolyte. In the current study the experimental procedure used by Coetzee (2018) was employed for conducting the copper electrowinning study. To validate the accuracy of the experimental procedure and the results achieved the copper deposits obtained for the base case scenario and 2 mg/l guar concentration were compared to the copper

deposits achieved by Coetzee (2018). The results of the copper deposits can be found in appendix C-Electrowinning supporting results.

Experimental validation

In the current study one of the experiments was repeated to show reproducibility of results. The repeat experiment was conducted for the following operating conditions: 35 g/l initial copper concentration, 30 mg/l chloride, 180 A/m^2, 10 mg/l guar concentration, and 150 g/l sulphuric acid concentration. The repeatability was determined by calculating the standard deviations of surface roughness, current efficiency and mass of copper plated for the validation electrowinning experiments. The results of these experiments were reported in Chapter 4 of this report.

3.1.4. Equipment setup and electrowinning cell configuration

The major equipment used in this study for conducting the copper electrowinning experiments is listed in Table 3.3.

Table 3.3: Equipment used during electrowinning experiments.

Equipment	Purpose
Electrowinning cell (EW cell)	Electrowinning
Stock solution bottle	Feed electrolyte storage
Laboratory scale peristaltic pump	Pump feed electrolyte to the EW cell
Waste bottle	Spent electrolyte collection
DC power supply	Supply current to the electrowinning cell and record voltage with time
Thermostat	Heat and maintain feed electrolyte at desired temperature value
Thermometer	To measure electrolyte temperature

All the constituent equipment used for the bench-scale electrowinning experimental set up is illustrated in Figure 3.1. The setup consisted of an EW cell which was made of a polyvinyl chloride (PVC) material (see photo in Figure 3.2) and has a total volume of 5 L. PVC material was chosen because of its resistance to acid corrosion at electrowinning operating temperatures. The EW cell was constructed with inlet and outlets pipes connected to it using pipe connectors. The design of the inlet and outlet pipes facilitates the even distribution of feed and spent electrolyte throughout the EW cell. The stock solution bottle containing the feed electrolyte was placed in a water bath, which was heated and maintained at the desired temperature value using a thermostat shown in Figure 3.1. A peristaltic pump was used to transfer the feed electrolyte from the stock solution bottle to the EW cell. The feed electrolyte enters the cell from the bottom passing through a perforated horizontal plate and is dispersed inside the cell until it reaches the outflow weirs in two opposite side walls near the top of the cell where it leaves the cell by overflow as shown in Figure 3.2. During the electrowinning process bubbles are also forming, thus, a mixture of the bulk flow and evolving oxygen takes place in the EW cell. In industry, the flow between plates is largely driven by convection through the evolving oxygen

and not by the upward flow of bulk electrolyte. The net electrolyte volume in the electrowinning cell was 5 L (before plates) and the flowrate of the circulating electrolyte was 0.0064 m^3/hr which was achieved at a pump speed setting of 25% of the maximum. The flowrate translates to an interfacial velocity of 0.2 m^3/hr.m^2 over the total surface area of the cathode plate available for plating.

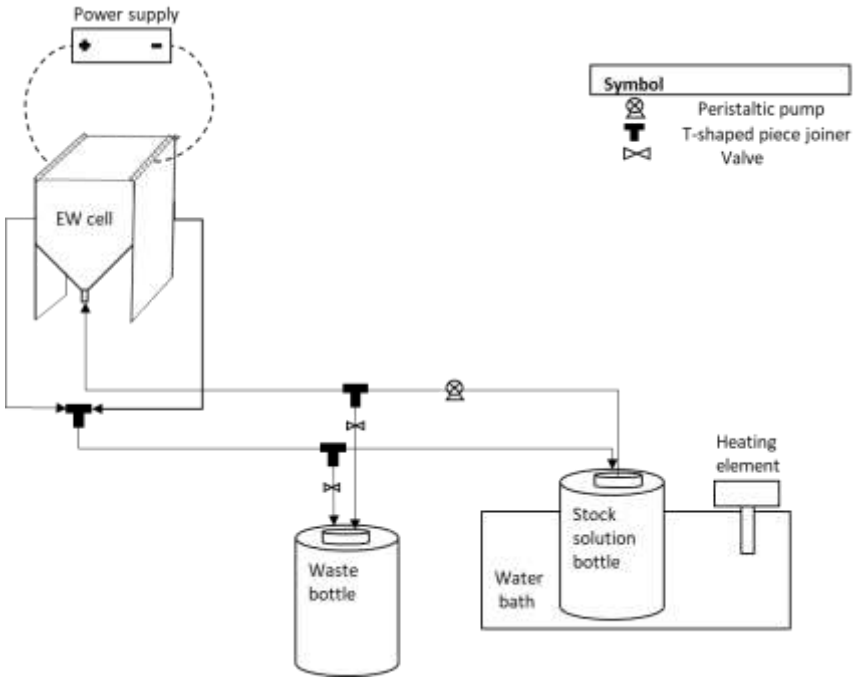

Figure 3.1: A schematic diagram showing pipe connection of the electrowinning cell setup.

The bench scale copper electrowinning experiments were conducted in an electrowinning system using three parallel plate electrodes (one cathode and two anodes). The cathode plate was a grade 304 stainless steel with thickness of 1 mm with cathode area dimensions of 15 × 12 cm. The anode plates used were cold-rolled lead alloy purchased from Polymer Concrete Industries with thickness of 3 mm and dimensions equivalent to the cathodes. The EW cell was designed to have grooves cut at the top in which the electrodes can be inserted. To ensure that the electrodes remain in a fixed position throughout the electrowinning experiment they were bolted to copper hanger bars which fit into the grooves cut on the EW cell as shown in Figure 3.2. For each experiment, a new stainless steel cathode blank was placed in between the same two anodes to ensure that the electrodeposition of copper occurs on both sides of the cathode electrode surface. The distance between the electrodes was 25 mm for all the experiments.

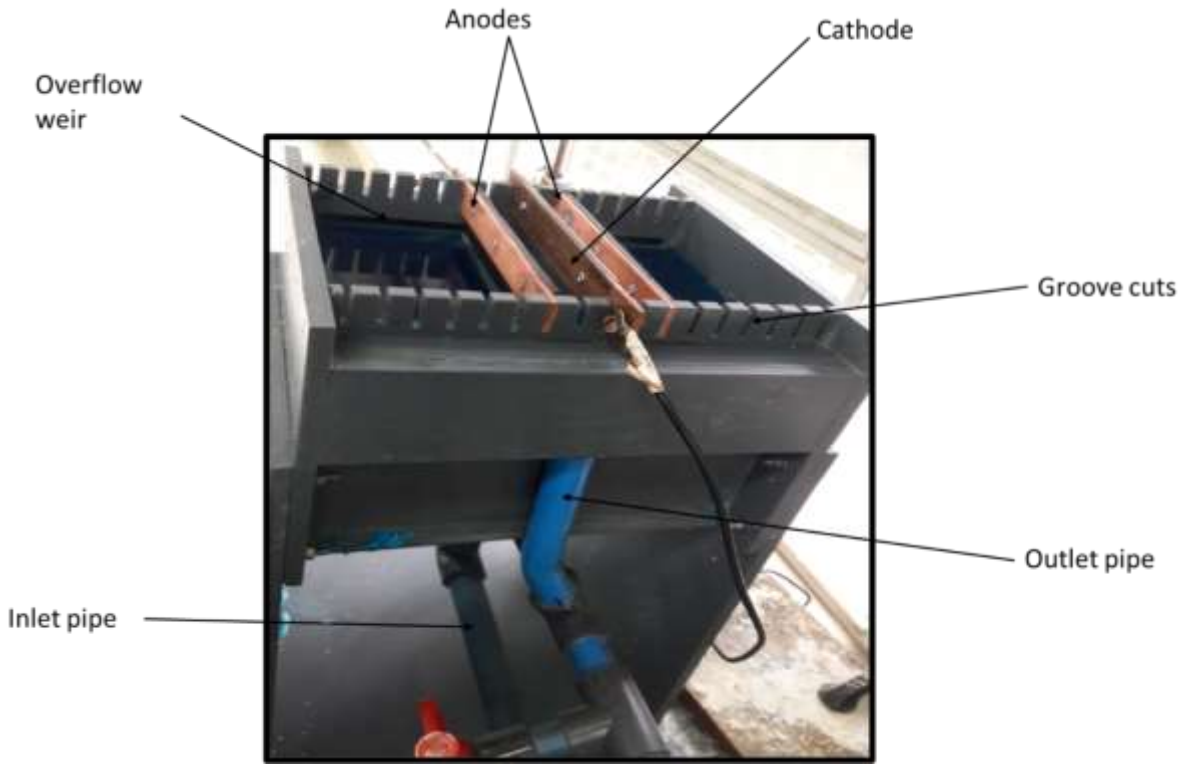

Figure 3.2: Actual EW cell showing groove cuts with inlet outlet piping.

The electrowinning experiments were conducted by feeding a constant current through the power source (current control), the cell voltage was not monitored throughout the tests. The electrical wires connecting the power source (a Manson Switching Mode Power Supply, 1-16 VDC, 60 A) to the electrodes were attached to ring terminal lugs and bolted to each electrode hanger bar to ensure a fixed contact resistance. The positive terminal wires of the power source were then bolted to both anode hanger bars, and the negative terminal wire of the power source was bolted to the cathode blank as shown in Figure 3.3.

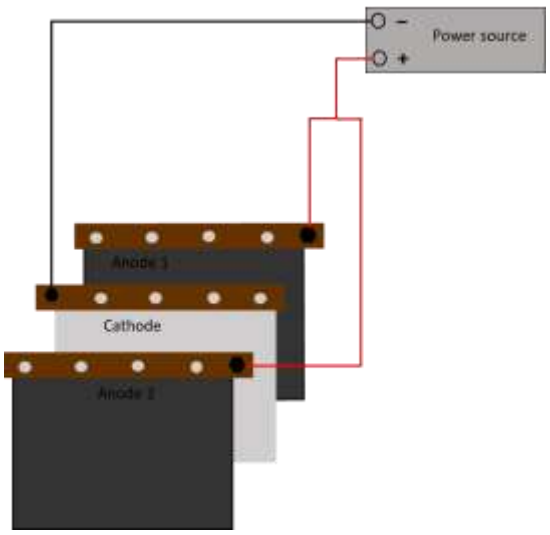

Figure 3.3: A schematic diagram representing the electrical wires connection to the power supply.

3.1.5. Methodology

3.2.4.1 Guar preparation

Guar was freshly prepared before every electrowinning experiment to eliminate the risk of guar degradation. Guar solution preparation equipment is shown in Figure 3.4. 400 mg guar powder was measured and added into a conical flask containing 200 ml of de-ionized water to make up a stock solution. The solution was then placed on a heater stirrer at a temperature of 40°C for 2 hours to allow guar to dissolve. A glass stopper was used to prevent the evaporation of guar solution. Guar formed a viscous, colloidal dispersion solution which is consistent with literature (Coetzee, 2018; Fabian, 2005). Insufficient hydration time and agitation for guar solution preparation results in guar gelling and forming lumps (Cifuentes et al., 2015). The hydration time and agitation for guar preparation in this study was sufficient since no lumps were observed in the solution. After the preparation of guar, the required concentration of guar was removed from the prepared guar stock solution via a pipette and added to the stock solution bottle containing the feed electrolyte. Guar was then left in the electrolyte for another 30 minutes prior the commencement of electrowinning experiment to allow time for guar to hydrolyze in the acidic solution (Coetzee, 2018). A detailed guar solution preparation procedure is provided in Appendix B-Experimental procedure.

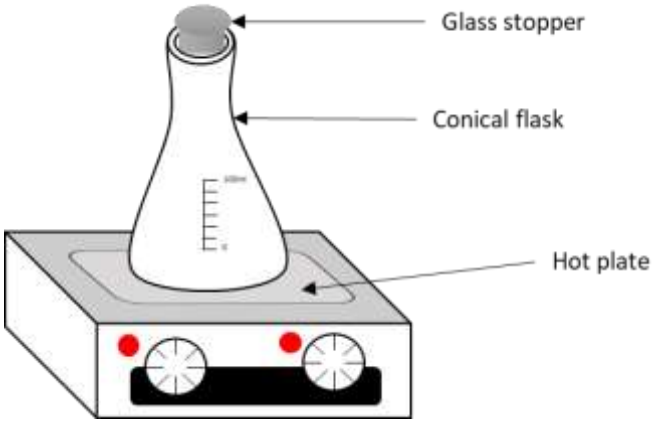

Figure 3.4: Guar solution preparation setup.

3.2.4.2 Cathode and anode preparation

As already mentioned in Section 2.4.2, imperfections on the cathode surface can initiate dendrites growth which causes a rough deposit surface. Hence, before each electrowinning experimental run, the stainless-steel cathode blank with smoothened edges was prepared by thoroughly rinsing the surface sequentially with acetone and de-ionized water as a cleaning medium to remove any contaminants (dirt or other materials) on the surface. Thereafter, the cathode plate was allowed to air dry prior to inserting into the EW cell. The cathode surface was washed on both sides since electrodeposition is allowed on both sides of the plate. The anode plates were washed using de-ionized water to remove loose oxidation products and solid matter which might have been deposited on the anode surface during the electroplating process.

3.2.4.3 Electrolyte preparation

Before the commencement of each electrowinning experiment a 15 L synthetic electrolyte was prepared using the analytical grade reagents described in Section 3.1.1. The electrolyte was prepared by weighing out the desired amount of copper, sulphuric acid and chloride ion into de-ionized water.

Chloride ion concentration was kept constant for all the experiments and was introduced by adding HCl resulting in 25 mg/l chloride. A step-by step electrolyte preparation procedure is outlined in Appendix B-Experimental procedure which was adapted from Coetzee (2018).

3.2.4.4 Experimental method

The schematic diagram of the bench scale electrowinning setup shown in Figure 3.1 will be used as a reference for the following methodology description. A step-by-step methodology for the copper electrowinning experiments is provided in Appendix B-Experimental procedure.

Initially, only 10 L of the 15 L electrolyte prepared was heated in a water bath to a desired temperature value which ensured that the electrolyte temperature in the EW cell was at 40°C. The inlet and outlet pipes were inserted into the stock solution bottle. Every experimental run was conducted using a new cathode plate with a deposition area of 0.0318 m^2. After ensuring that the cell is clean and free from any solids or solutions, the prepared cathode blank was weighed and then inserted in the EW cell between the two lead alloy anodes. Thereafter, the pump was switched on and set to the desired pump speed to fill the cell with the feed electrolyte until there was an overflow of solution into the spent electrolyte (outlet) pipe. The electrolyte was circulated through the EW cell and stock solution bottle until the temperature of electrolyte inside the EW cell was maintained at 40°C. Once this steady state was achieved (after about 20 minutes of electrolyte circulation), guar was added to the stock solution bottle and immediately thereafter the remaining 5 L synthetic electrolyte was also added to the stock solution bottle to mix with the electrolyte/guar solution. The final electrolyte/guar solution had a volume of 15 L and was allowed to further circulate until steady stated was achieved. The time allowed for guar to unfold in acid (approximately 30 minutes) and for the additional solution to reach the operational temperature before the power supply was switched on to initiate the deposition process. The power supply was set to a current translating to the desired operating current density and the experiment was performed for 24 hours to allow enough time for multilayer copper electrodeposition on the cathode surface. The electrolyte temperature in the cell was monitored as well was the current during the electrowinning experiments.

To safely remove acid mist produced during the electrowinning experiment a vent with an extraction fan was placed over the EW cell. After each experiment, the power supply and pump were switched off and the positive terminal wires were unbolted from the cathode hanger bars. Thereafter, the copper cathode was then harvested from the electrolyte bath, rinsed with de-ionized water, and hung to dry completely by air on a drying rack. The dry copper cathode was then weighed to determine the mass of copper deposited with reference to the mass of the cathode blank and stored for further analysis. The copper plates were weighed before and after each experiment to be able to calculate and compare the current efficiency in each experimental condition as described in Section 2.6.1. A sample of the spent electrolyte was taken for analysis of its composition. Thereafter, the spent electrolyte in the EW cell was drained and collected using the waste bottle after the experimental run. In preparation for the next experiment the electrowinning system was flushed with water.

3.2. SAMPLE ANALYSIS

3.2.1. Visual analysis of copper deposits

The physical appearance of the resultant cathode plates for all the electrowinning experimental conditions were investigated visually to conduct a qualitative analysis of the plates. The difference between rough dendrite-like localized growth and uneven copper growth is clearly drawn from the

visual analysis of the copper cathode plates. Uneven copper growth refers to an uneven plate surface topography while a smooth appearance is maintained on the cathode surface. This type of plate morphology can be visualized as a smooth plate with gradually altering surface gradients (Coetzee, 2018). Dendrite-like nodular growth or localized growth refers to a rough topography with a jagged like surface copper deposit. As previously discussed in Section 2.5.3, Winand (1992) developed a Winand's diagram to show the different possible types of electrodeposit growth and structure as a function of the ratio between current density and DLC density, and the inhibition intensity as shown in Figure 2.8. The growth types described from the Winand's diagram were used as a reference to suggest possible growth types at various experimental conditions in the presence of guar from the visual examination of the copper deposits in this study.

3.2.2. Surface scanning analysis

The morphology of each copper cathode plate harvested after the electrowinning experiments was analysed qualitatively and quantitatively by investigating images produced from scanning the surface of each plates using an Artec Spider surface scanner at the CT scanner facility, Stellenbosch University.

An Artec Spider surface scanner is a hand-held 3D surface scanner which was developed particularly to be used in conjunction with a computer aided design (CAD). The scanning of small items with complex surface structure up to 1 million points per second can be allowed using this scanning system (Kersten et al., 2016). This scanning system works with a linear field of view between 90×70 mm^2 and 180×140 mm^2 with a measuring range between 0.17-0.35 m. For texture mapping of the objects the Artec Spider uses a structured light technology with blue LED as the light source combined with a colour camera which has 1.3 megapixels with a 3D resolution which normally ranges between 0.01 mm and 0.1 mm (Kersten et al., 2016).

After scanning the surface of each copper plate, the high-quality 3D volumetric data generated were then imported and analysed in Volume Graphics VGStudioMax 3.1, which is a 3D data viewing and analysis software program. The 3D volumetric data generated were analysed quantitatively by measuring the surface roughness of each plate using a technique as described by Du Plessis et al. (2018).

Six areas of interest were selected on the image of each copper plate relative to the regions of interest (ROI) chosen for acid digestion tests. These regions of interest (ROI) were consistently selected on the same place for each plate in order to measure the surface roughness. The six squares selected as regions of interest were considered to be representative of each copper cathode plate (sample) and relative to the equivalent areas of interest of all the other samples. For each square region selected, a best fit plane (geometry element) was created by selecting approximately 15 points along each edge of the region. Thereafter, the best fit plane was fitted with a mesh of surface elements. The ROI and their corresponding best fit plane for one of the cathode plates produced during bench scale electrowinning experiments is represented by Figure 3.5.

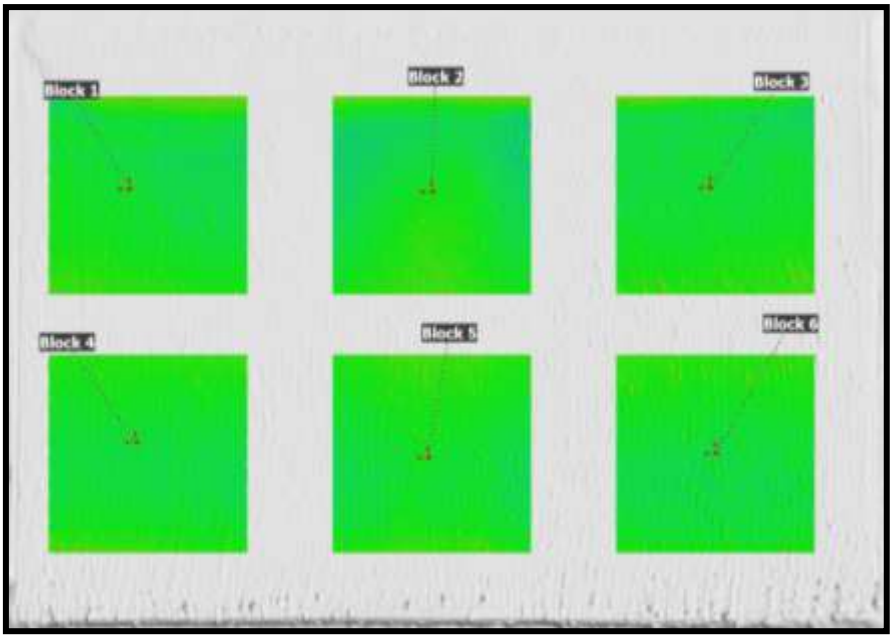

Figure 3.5: Example of surface topography of a copper plate showing the 6 selected ROI with their respective geometry elements.

The deviation data generated could then be extracted via the software as a comma-separated values (CSV) file in the format of two columns. One column contains deviation values (distance from the best fit plane to the copper deposit surface) ranging from minimum (negative) to maximum (positive) values. The second corresponding column represents the number of surface elements at which that specific deviation from the best fit plane was measured. Equation 2.16 was used to calculate the arithmetic mean (S_a value) of the distance from the reference plane (best fit plane) to the copper deposit surface measured at each of the regions of interest. The final S_a value will increase with an increase in the overall surface roughness.

The deviation values obtained from the reference plane to the copper deposit surface were used to plot density distribution curves for each copper plate produced during copper electrowinning at various guar dosage and operating conditions. From the density distribution curves, the position with the maximum deviation density (i.e., the peak of the curve) represents the flattest part of the copper cathode surface. The position of the reference plane was normalized for all selected ROI on the copper plates by making the flattest part on each of the plates to be the "new" reference plane (Coetzee, 2018). This allows comparison of the distribution of surface deviations away from the new reference plane between each copper plates produced during electrowinning on the same axis. The surface roughness evaluation of each copper cathode also included the analysis of variance (ANOVA) to statistically analyse the effect of individual parameters and interactions between the operating parameters by ANOVA.

3.2.3. Statistical analysis of data

As already mentioned in Section 3.1.2 a mixed-level factorial design of experiments was established in order to explore the effect of individual parameters including copper concentration, sulphuric acid concentration, current density and guar concentration on the electrowinning performance. The values of main effect parameters and interactions are indicative of how strong an individual factor affect the response variable (surface roughness, current efficiency, and chemical composition). The initial copper

concentration was varied during the bench scale copper electrowinning experiments, but the average copper concentrations were reported/employed for statistical analysis since copper depletes in the bulk solution during the operation. Statistical analysis of data was carried out by analysis of variance (ANOVA) to determine the statistical significance of the main parameters and interactions between these parameters on the response variables using a confidence interval of 90%. The statistical significance was considered when p-value was typically less than 0.1.

3.3. COPPER DEPOSIT ACID DIGESTION TESTS

3.3.1. Materials

All the acid digestion tests were carried out using the copper sheets produced from the copper electrowinning experiments as well as aqua regia solution prepared from analytical grade reagents without further dilution. The chemicals used to prepare the aqua regia solution are listed in Table 3.4.

Table 3.4: Reagents used for acid digestion tests.

Reagent name	Supplier	Grade	Molecular weight (g/mol)
32% Hydrochloric acid (HCl)	KIMIX	AR	36.46
55% Nitric acid (HNO_3)	Scienceworld	AR	63.01

3.3.2. Plan

After the surface scanning analysis of each copper cathode plate as discussed in Section 3.2.2, acid digestion was then conducted for the copper plates. Acid digestion tests using aqua regia allow for the complete dissolution of copper plate. Thereafter, the chemical composition of the leach liquor is determined using the ICP analysis technique. The required amount of aqua regia for every acid digestion test was based on a 1:10 solid to liquid ratio (Dehghanpoor et al., 2016; Rossouw, 2015). The amount of aqua regia required for each digestion test based on the weight of the copper sheets to be dissolved is given in Appendix B-Experimental procedure.

3.3.3. Sample preparation

Harvested copper sheets were stripped from the stainless-steel cathode blank and cut into six equivalent square pieces (2 pieces on the left, 2 pieces on the centre, and 2 pieces on the right). The six areas selected on each cathode plate were relative to the regions of interest (ROI) chosen for cathode plate surface scanning analysis. These ROI were selected on the same places for each copper plate and were marked before cutting to dimension of 2.6 cm × 3.4 cm as shown in Figure 3.6. The six square pieces of copper sheets were once again cut into four smaller square pieces with equivalent dimensions of 1.3 cm × 1.7 cm.

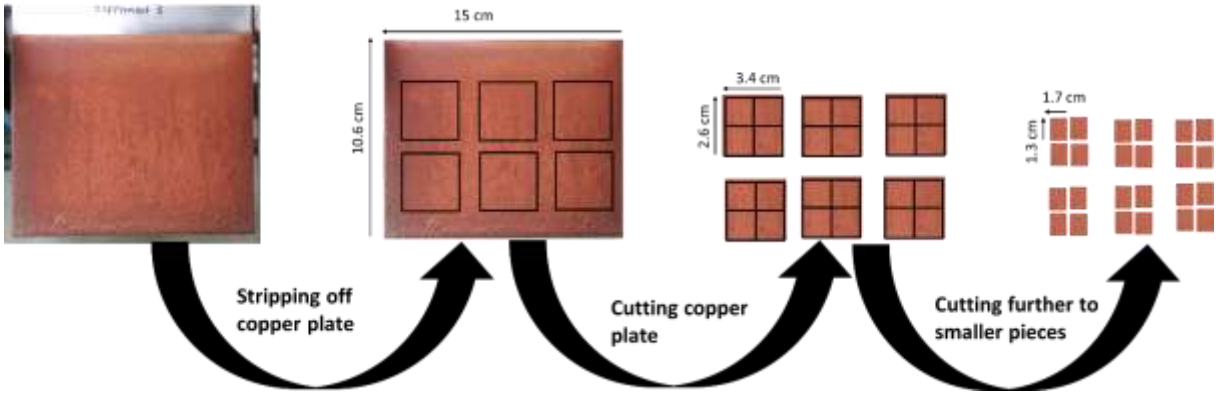

Figure 3.6: Positions of areas selected on experimental copper plate for acid digestion tests.

3.3.4. Experimental procedure

Acid digestions tests were conducted under a fume hood. A fresh solution of aqua regia was prepared before every acid digestion test to avoid storing it for long periods of time as it quickly loses its effectiveness due to oxidation of its reactive components. Aqua regia was prepared by mixing concentrated hydrochloric acid and concentrated nitric acid at a volumetric ratio of 3:1 in a 500 ml glass beaker. Therefore, it is 3 parts of hydrochloric acid to 1 part nitric acid. Firstly, the required amount of hydrochloric was measured using a glass measuring cylinder into the mixture glass beaker, and then the required nitric acid was also measured and slowly added to the hydrochloric acid.

A 250 ml conical flask was filled with the required volume of prepared aqua regia based on the weight of the smaller piece copper sheets cut at a region of interest to be dissolved as shown in Figure 3.7. The conical flask containing the mixture of aqua regia, and copper sheet pieces was then placed on a hot plate set at a temperature of 55°C. A thermometer was used to confirm the temperature. To ensure that there is adequate agitation of solution a magnetic stirrer bar was added in the conical flask and the solution stirred at a slow rate. The conical flask was closed using a watch glass to prevent the loss of liquid during the digestion test. The acid digestion tests were carried out for 24 hours to allow sufficient time for complete dissolution of copper sheets. After the completion of each test, the stirring was stopped, and the hot plate was switched off. The conical flask was then removed from the hot plate, allowed to cool and thereafter the magnetic stirrer bar was removed from the leach solution. A detailed step-by-step methodology for the acid digestion test is provided in Appendix B-Experimental procedure.

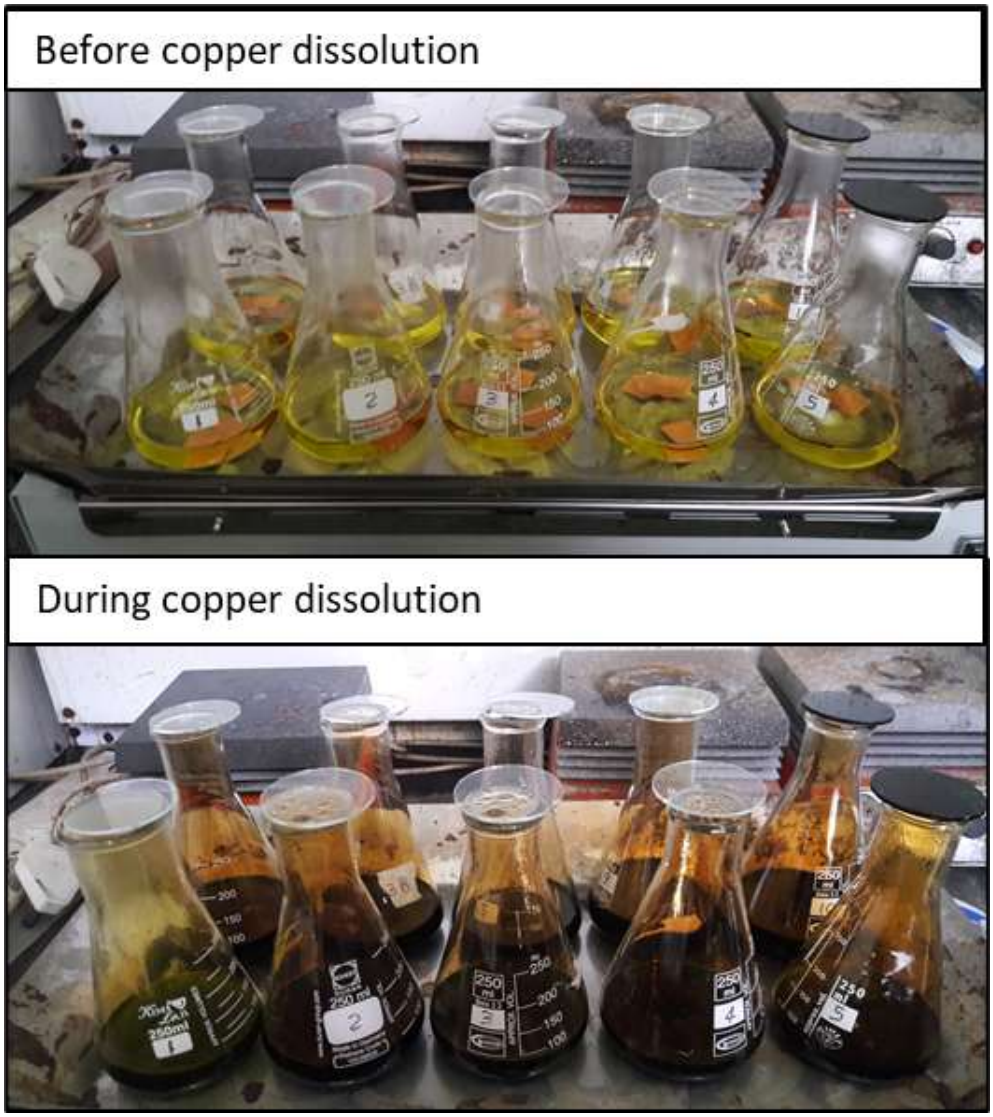

Figure 3.7: Before and during the copper dissolution process.

3.3.5. ICP analysis

The samples of copper leached solution from acid digestion tests were analysed to determine the concentration of impurities entrapped in the copper cathodes produced during the electrowinning experiments. As already mentioned in Section 2.6.2, the major entrapped impurities analysed in copper cathode include iron, sulphur, and lead. However, since the synthetic electrolyte used for all the electrowinning experiments in this study was free from impurities only sulphur and lead were analysed on the copper cathodes produced. The concentration of sulphur and lead was determined by using the ICP analysis technique. After the impurity concentration was measured on the sections investigated on each cathode deposit, the average concentration data were calculated, compiled, and thereafter, analysis of variance (ANOVA) was used to statistically analyse the effect of individual parameters and interactions between the operating parameters. A detailed method for the preparation of solution for ICP analysis is given in Appendix B-Experimental procedure.

4. RESULTS & DISCUSSION

In the current study, a semi-batch experimental system was used to evaluate the interactions between guar concentrations and other parameters to enable improved control of guar addition in copper electrowinning. This investigation was achieved by conducting copper electrowinning experiments using parallel cathode and anode plates, 15 L electrolyte solution, and the solution was recycled as mentioned in Section 3.1.4. As mentioned in Section 3.3.2, copper cathode plates produced during the copper electrowinning experiments were analysed using an Artec Spider surface scanner and Volume Graphics VGStudioMax 3.1 software to study the surface morphology. The chemical composition of copper plates dissolved through acid digestion tests were studied by using ICP analysis technique. This chapter discusses the results obtained from the copper electrowinning experiments and acid digestion tests, through comparison of the surface roughness, current efficiency, and chemical composition of each plate at various operating conditions as well as a summary of ANOVA from the statistical analysis of data from the experiments. A statistical analysis of data was performed to develop statistical relationships between various parameters to see the statistical effect of varying operating conditions on guar requirements in copper electrowinning. The validation of experiments was done by repeating experiment 11 as discussed in Section 3.1.3. The surface roughness, current efficiency, and mass of copper plated for the experiments used for validation are presented in Table 4.1. The repeatability of both experiments was determined by calculating the standard deviations. The experiments can be considered valid as the calculated standard deviations are less than 1 showing that there is little variation between the experiments. The surface topography of the copper deposits achieved for each experiment were compared to validate the reproducibility of the experiments as provided in Appendix C-Electrowinning supporting results.

Table 4.1: Reproducibility of experiment using standard deviation.

	Mass of Cu plated (g)	Current efficiency (%)	Surface roughness (µm)
Experiment 11	157.1	98.0	34.1
Experiment 11-repeat	157.3	98.1	32.8
Standard deviations	0.18	0.12	0.96

4.1. ELECTROWINNING TESTS: DEPOSIT SURFACE ROUGHNESS

The morphology of each copper plate produced after the electrowinning experiments was quantified for a more accurate comparison of the effect of varying operating conditions on the performance of guar at various dosages to enable improved control of guar addition allowing for control of localized growth (dendrites) on the cathode surface. The methodology for producing the 3D cathode images and the average surface deviations which were converted into S_a values (measure of roughness) was discussed in Section 3.3.2 of this report. In this section, the quantitative and qualitative analysis of the morphology of copper plate achieved at various operating conditions is discussed. The following data

of the copper deposit surface roughness from the bench scale electrowinning experiments were utilized and discussed in the results and discussion:

- Visual images of the copper plates.
- Images of the plates indicating the changes in surface deviation (from a reference plane) to ± 0.3 mm with a colour scale.
- Surface deviation values (minimum to maximum) which were converted into S_a values.
- Interactive effects of operating parameters from the S_a values.

4.1.1. Visual analysis of copper deposits

In this section of results, photographs showing the physical appearance of copper deposits produced during the bench-scale copper electrowinning are presented and discussed. From the physical appearance of the copper deposits achieved at various operating conditions a clear distinction is drawn between uneven copper growth and rough dendrite-like growth types.

4.1.1.1. Effect of guar addition

The colour images that show the effect of guar addition on electrodeposition from the physical appearance of copper deposits produced during the 24-hour electrowinning experiments are presented in Figure 4.1 (a-d). The copper deposit achieved from the Base case electrolyte (absence of guar) is presented in Figure 4.1 (a). The physical appearance of copper deposit achieved in the absence of guar shows a rough surface topography. This is evident from the nodules and dendrites covering the copper cathode surface. Localized growth (dendrites) is unpredictable in nature, this type of growth is thus the most unwanted surface morphology since it poses a high risk of short-circuiting in the cell during electrowinning (Coetzee, 2018). Severe dendrite growth tends to trap suspended solids and electrolytic solution which has a negative influence on the copper deposit's ductility and conductivity. As already mentioned in the literature review section, in extreme cases nodular growth lead to shattering of the copper plates during the stripping procedure (Cifuentes et al., 2015). This growth type can be classified to be FI growth type when described using the Winand's diagram in Figure 2.8. According to Winand (1992) FI growth type can be expected at low inhibition levels with whiskers, then dendrites, and finally powder forming when the current density is increased. Therefore, this classification is justified since low inhibition levels are expected in the absence of additives in the electrolyte.

It can be observed that the resultant copper deposit in the presence of 2 mg/l guar in the electrolyte was much smoother compared to the copper deposit achieved from the Base case scenario. This is indicated in Figure 4.1 (b), whereby in the presence of guar less rough needle-like (dendrite) copper deposit developed on the cathode surface. Coetzee (2018) investigated the plate morphologies of copper electrowinning in an electrolytic solution in the presence of guar and polyacrylamides (PAM). In Coetzee's study the resultant plate morphology in the presence of 2 mg/l guar in the electrolyte was described as having less dendrite formation and localized growth, however, the copper cathode surface was still classified as rough and irregular. A similar description was given by Fabian et al. (2007) for a copper deposit in the presence of 2 mg/l of guar. In that study a rough-needle-like copper deposit was developed, and the plate morphology described as "dendritic and discontinuous". Furthermore, Coetzee (2018) classified this type of growth to be UD growth type. UD growth type is attainable at low inhibition levels and high current density or at very high inhibition levels and low current density (Winand, 1992). According to literature, it is believed that organic additives achieve a levelling/smoothing effect on electrodeposits by preferentially adsorbing onto the active sites,

thereby inhibiting further development and growth of the dendrite structure (Collins, 2001). Based on these results, it is concluded that in the presence of guar the formation of dendrites on the copper plate is reduced due to guar molecules adsorbing onto the active sites compared to copper plate achieved in the Base case electrolyte. However, guar molecules do not completely adsorb on all the active sites because there is still some roughness observed on the copper plate achieved (Figure 4.1 (b)).

Figure 4.1 (c) shows that in the presence of 10 mg/l guar concentration in the electrolyte the physical appearance of copper deposit produced a plate morphology that is smoother than copper deposit produced from the electrolyte without the addition of guar. Similarly, Figure 4.1 (d) shows that increasing guar concentration to 18 mg/l resulted in less dendrites formation on the cathode surface compared to the copper deposit achieved from the Base case scenario. It can be concluded from the visual analysis of copper deposits that the addition of guar in the electrolyte during copper electrowinning is important since the Base case scenario produced a copper deposit with a rougher surface compared to copper cathodes achieved in the presence of guar in the electrolyte. Furthermore, increasing guar concentrations in the electrolyte is more effective in producing smooth copper electrodeposits. The classification of the growth types cannot be identified by direct external observation of the copper deposit except for the FI growth type (Winand, 1992). Thus, it is necessary to conduct cross-section metallographic examination on the copper deposits to identify the type of growth achieved during copper electrowinning.

It is also important to discuss the brightness of copper plates since organic additives are added in the electrolyte to ensure that not only a smooth but also a bright copper deposit is produced during copper electrowinning. The copper deposit that developed in the absence of guar in the electrolyte appears to be the dullest when compared to the plates produced in the presence of guar. This provides evidence that it is important to add organic additives in the electrolyte to produce a bright copper deposit. Coetzee (2018) hypothesized that in the absence of a smoothing agent a porous copper deposit structure developed, enabling electrolyte entrapment and crystallization in the pores. Therefore, the discolouration observed in the base case scenario in this work may be attributed to the entrapped crystallized electrolyte.

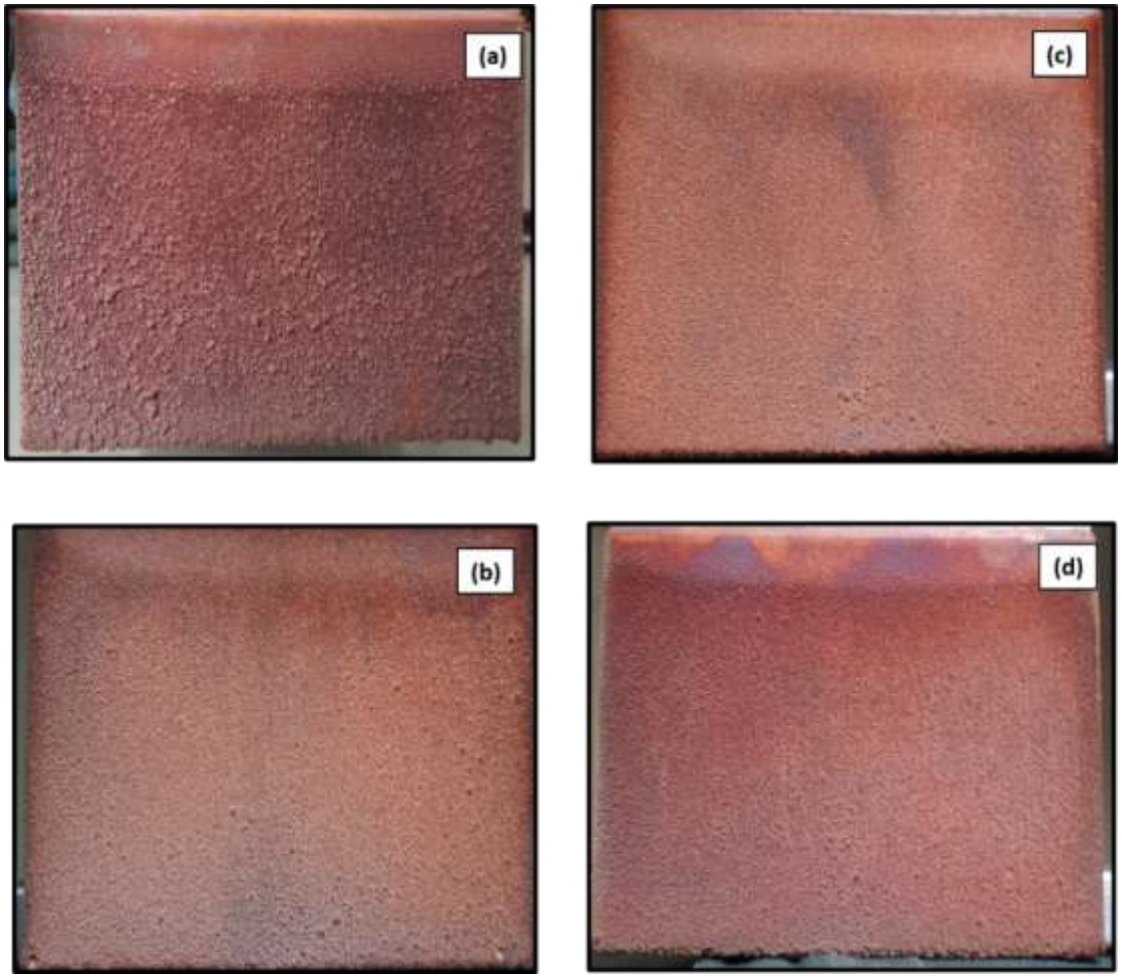

Figure 4.1: Visual images of copper plates obtained at 35 g/l initial copper concentration, 300 A/m^2 current density, 150 g/l sulphuric acid concentration and guar concentration of (a) base case scenario, (b) 2 mg/l, (c) 10 mg/l and (d) 18 mg/l.

4.1.1.2. Effect of current density

At low current density (180 A/m^2) the plating of copper on the cathode surface during the electrowinning process will achieve only about 60% of the thickness after 24 hours compared to the high current density (300 A/m^2). For this study, the copper cathode surface roughness between these experiments were compared based on anomalies in growth of copper deposit which could potentially lead to dendrite formation. It is expected that these anomalies would be sustained as the copper deposit thickness increases relative to the plating time.

It can be observed from Figure 4.1 (b-d) that a rougher copper deposit was produced at a higher current density than the copper deposit produced at low current density as shown in Figure 4.2 (a-c). The same trend was observed for all the copper plates achieved at experimental conditions comparing high and low current density. The evidence of a rougher copper deposit at high current density is the localised growth or dendrites observed (Figure 4.1 (b-d)). Copper electrodeposition at high current density allows for faster reaction kinetics showing that the nucleation rate is faster than the rate of crystal growth on the cathode surface. Jacobs and Groot (2019) investigated the deposit morphologies over a wide range of current densities in the presence of Magnafloc 333 as the organic additive in an electrolytic solution. In this study, poor morphologies were observed with powdery and dendritic

deposits, due to deposition occurring at, or close to, cathode surface boundary layer diffusion control for copper ions at high current densities. The effect of current density on the surface roughness of copper deposits will be discussed further in Section 4.1.4 of this report.

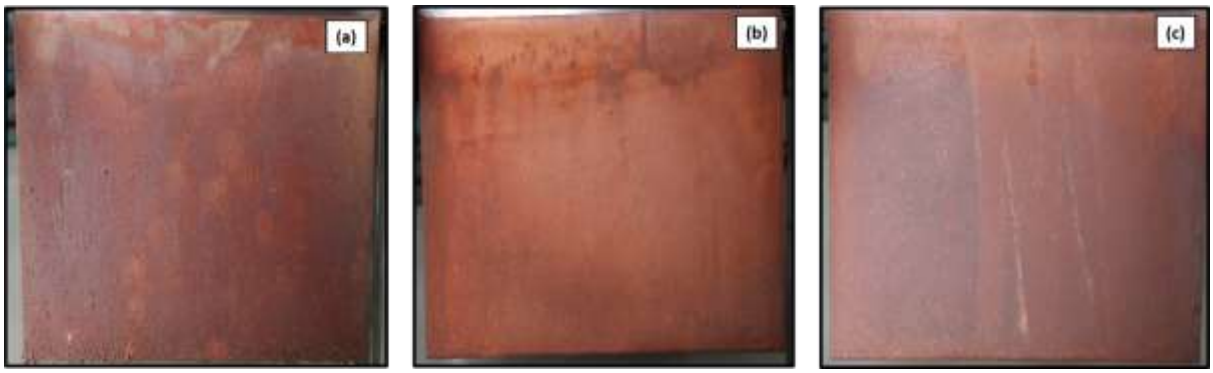

Figure 4.2: Visual images of copper plates obtained at 35 g/l initial copper concentration, 180 A/m^2 current density, 150 g/l sulphuric acid concentration and guar concentration of (a) 2 mg/l, (b) 10 mg/l and (c) 18 mg/l.

In contrast, it can be observed from Figure 4.2 (a-c) that the morphology of the copper deposit produced at low current density is smoother than copper deposits produced at high current density. The physical appearance of copper deposits observed at low current density is desirable in electrowinning facilities. As indicated in Figure 4.2 (a), little to no nodules prevailed in the presence of 2 mg/l guar but the surface can still be classified as smooth. The deposit morphology achieved at low current density is consistent with the finding of Jacob and Groot (2019). It was observed from the findings that at low current densities, deposition will occur under activation-control conditions, which is expected to result in fairly smooth deposits. Furthermore, it is proposed that early electrowinning tankhouses did not add smoothening agents because of low current densities employed (Moats et al., 2016). This suggest that copper deposits with smooth surface can be achieved at low current densities in the absence of organic additives in the electrolyte. However, at low current densities low production rates occur as will be discussed in Section 4.2. Within the range investigated, the effect of guar concentration on the copper deposit surface is not visible at low current density as shown in Figure 4.2 (a-c).

Figure 4.1 (b-d) and Figure 4.2 (a-c) show that more significant dendrite growth occurred at the bottom-edges than at the centre of the copper deposits at high current density compared to copper deposits produced at low current density. According to Popov et al. (2011), thick deposits at the edge of electrode are due to higher current densities experienced at the edges than at the centre. This is also in agreement with the findings of Filzwieser (2005), that suggested that in the case of rapid growth (high current density) the build-up of crystals takes place primarily at the edges and corners of the copper plate.

From Figure 4.1 (b-d) and Figure 4.2 (a-c) it was also observed that copper deposits achieved at low current density are smoother and guar concentration had an invisible effect compared to copper deposits produced at high current density. The effect of guar concentration at low current density can be clearly compared in terms of an overall surface roughness factor (S_a value) as presented in Section 4.1.4.4. Therefore, only copper deposits achieved at high current density will be discussed further to

determine the conditions which shows the most efficient guar concentration that can be added in the electrolyte to ensure a desirable copper plate at various experimental conditions.

4.1.1.3. Effect of copper concentration

Visual images showing the effect of copper concentration on the physical appearance of copper deposits in the presence of guar at high sulphuric acid concentration (180 g/l) are presented in Figure 4.3 (a-f).

Figure 4.3: Visual images of copper plates obtained at 300 A/m^2 current density, 180 g/l sulphuric acid concentration for 35 g/l initial copper concentration with guar concentration of (a) 2 mg/l, (b) 10 mg/l, (c) 18 mg/l and for 45 g/l initial copper concentration with guar concentration of (d) 2 mg/l, (e) 10 mg/l, (f) 18 mg/l).

It can be seen from Figure 4.3 (a-f) that the physical appearance of copper deposits achieved with low initial copper concentration (35 g/l) were rougher than those obtained at high initial copper concentration (45 g/l) at high sulphuric acid concentration. At low initial copper concentration, it is evident that the copper deposits produced have more localized growth or needle-like appearance throughout the plates (Figure 4.3 (a-c)). Shreir and Smith (1953) suggested that this effect may be attributed to the reduced mobility or insufficient supply of copper ions to the cathode surface. A semi-batch experimental system was used in the current study; thus, the initial copper concentration decreases in the electrolytic solution as the electrodeposition process proceed. A decrease in the initial copper concentration in the electrolyte leads to insufficient supply of copper ions to the cathode surface which contributes to the production of a rough copper deposit. At low initial copper concentration, the surface roughness of copper deposit is marginally higher compared to copper deposit achieved at high initial copper concentration due to a high depletion of copper ions in the electrolyte. This effect of reduced mobility of copper ions on surface roughness of copper cathode deposits will be discussed further in Section 4.1.4.3 of this report.

Figure 4.3 (a-f) also shows that increasing the guar concentration results in copper deposits with little to no localized growth, compared to copper deposits achieved at low guar concentration, which is desired in operating copper electrowinning facilities. This shows that high guar concentrations have the ability to effectively prevent the formation of dendrites on the copper deposit surface than low guar concentration under the current experimental conditions. As already discussed, guar molecules adsorb on the active sites to inhibit further development and growth of dendrites. Thus, the addition of high guar concentrations allows a larger number of guar molecules to adsorb on the active sites reducing the formation of dendrites compared to the addition of low guar concentration. Furthermore, increasing the inhibition levels (guar concentration) at constant current density result in an increase of the speed of lateral growth on the copper deposit surface (Winand, 1992). This allows the formation of dense and coherent deposit along the y-axis as shown on the Winand diagram presented in Figure 2.8. A coherent deposit morphology is desired in copper electrowinning, and it also reduces the risk of electrolyte entrapment (Winand, 1992).

The effect of copper concentration on the physical appearance of copper deposits was also observed at low sulphuric acid concentration (150 g/l) as shown in Figure 4.4 (a-f).

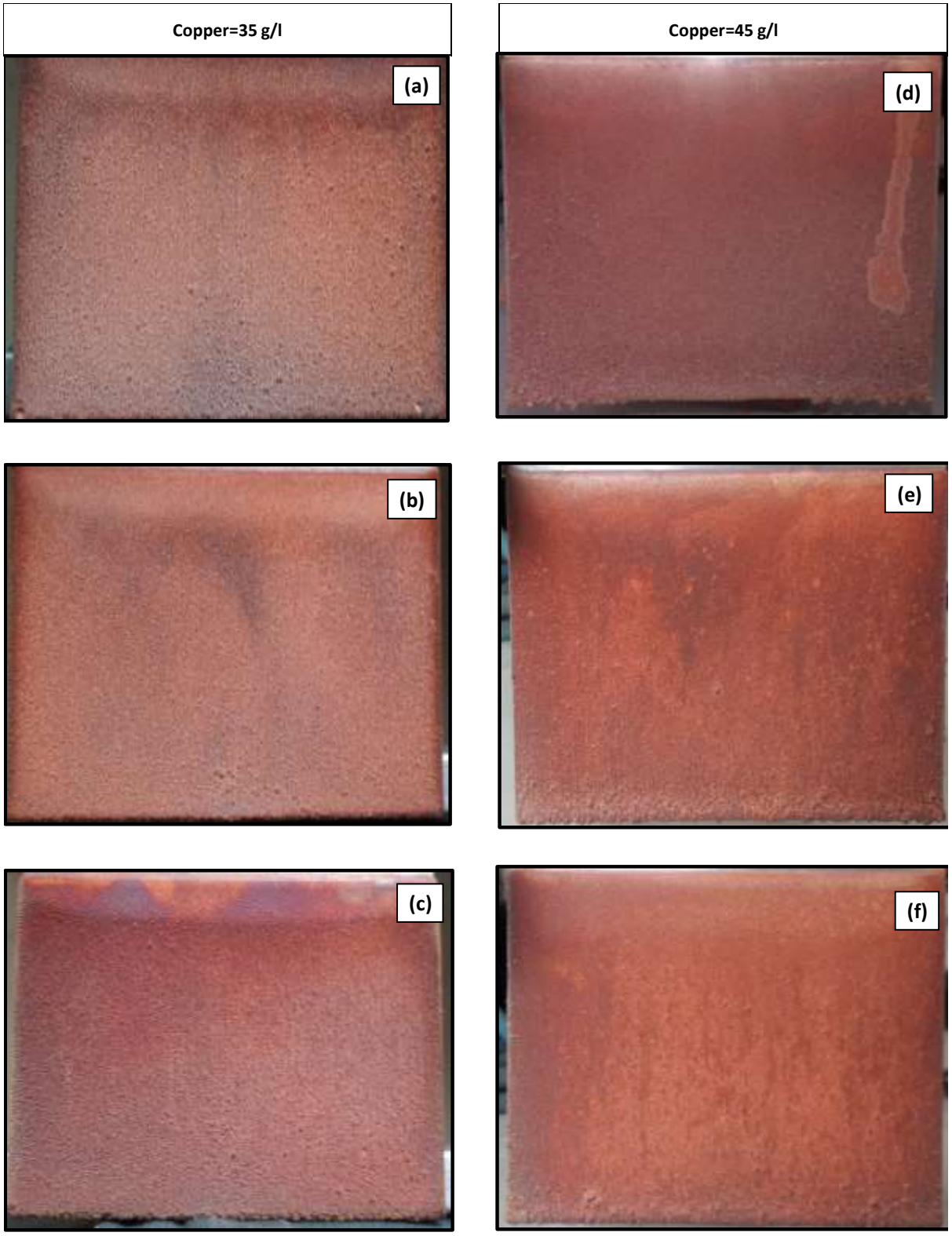

Figure 4.4: Visual images of copper plates obtained at 300 A/m^2 current density, 150 g/l sulphuric acid concentration for 35 g/l initial copper concentration with guar concentration of (a) 2 mg/l, (b) 10 mg/l, (c) 18 mg/l and for 45 g/l initial copper concentration with guar concentration of (d) 2 mg/l, (e) 10 mg/l, (f) 18 mg/l).

Varying sulphuric acid concentration in the electrolyte strongly influences the conductivity (Chibwe, 2020). Decreasing the sulphuric acid concentration will result in a decrease in conductivity due to reduced mobility of hydrogen ions to the cathode surface. Figure 4.4 (a-c) and Figure 4.4 (d-f) shows that even at low sulphuric acid concentration (150 g/l) more localized growth are still observed on the copper deposits achieved at low initial copper concentration than copper deposits produced at high initial copper concentration.

It can also be seen from Figure 4.4 (d-f) that high guar concentration result in brighter copper deposits than low guar concentrations. This trend is in agreement with the observation made from Figure 4.3 (d-f) which also shows the effect of increasing guar concentration on the brightness of copper deposit at high initial copper concentration. According to Budevski et al. (2000), if the crystal grains grow lateral to the depositing surface a brightening effect can be achieved on the metal deposit. Furthermore, the speed of lateral growth increases with an increase in the inhibition level. This explains the brighter copper deposit observed at high guar concentration than low guar concentration. This trend was also observed on copper deposits when increasing guar concentration from 2 mg/l to 10 mg/l at low initial copper concentration of 35 g/l (Figure 4.4 (a-b)). However, a dull copper deposit with localized growth was observed when the guar concentration was increased to 18 mg/l as shown by Figure 4.4 (c).

4.1.1.4. Effect of sulphuric acid concentration

The visual images of the electrowon copper plates showing the effect of sulphuric acid concentration at high initial copper concentration is shown in Figure 4.3 (d-f) and Figure 4.4 (d-f). Alternatively, the effect of sulphuric acid concentration at low initial copper concentration is shown in Figure 4.3 (a-c) and Figure 4.4 (a-c).

At high initial copper concentration (45 g/l) and low guar concentration (2 mg/l), the copper deposits produced at high sulphuric acid (Figure 4.3 (d) appears to have more prominent nodules than the copper deposit achieved at low sulphuric acid concentration (Figure 4.4 (d)). The same effect was observed from the copper deposits achieved at low initial copper concentration as shown in Figure 4.3 (a) and Figure 4.4 (a). Owais (2009) proposed that increasing sulphuric acid in the electrolyte leads to an increase in viscosity and decrease in the diffusion of copper ions to the cathode surface. Thus, copper deposits produced at high sulphuric acid had more visible nodules because a decrease in the diffusion of copper ions leads to insufficient supply of copper ions to the cathode surface which favours a higher growth rate of crystal grains perpendicular to the electrode surface than nucleation rate leading to the formation of dendrite. However, with increased guar concentration the effect of varying sulphuric acid concentration on nodule formation is not visible on the visual images produced during the bench-scale copper electrowinning experiments at low and high initial copper concentration. The effect of sulphuric acid concentration on the copper deposit morphology is discussed further in Section 4.2.4. The discoloration on the top right-hand side of Figure 4.4 (a) was due to the drying process. Since the drying process is through horizontal placement of cathode it may have allowed the electrolytic solution to pool and crystallize on the plate surface.

As already mentioned, there are visible nodules that can be observed on the copper deposit surface achieved at high sulphuric acid concentration (180 g/l) and low guar concentration (2 mg/l) as shown in Figure 4.3 (d). However, it can be seen from Figure 4.3 (e) and Figure 4.3 (f) that increasing guar concentration produce copper deposits with very little to no nodules. This implies that high guar concentrations adsorb more effectively on the active sites which is desirable in copper electrowinning facilities. Furthermore, Figure 4.3 (f) shows that increasing guar concentration to 18 mg/l results in a

brighter copper deposit. It can also be seen in Figure 4.4 (d-f) that increasing guar concentration results in brighter copper deposits with less nodules than the copper deposit achieved at low guar concentration.

4.1.2. Surface topography analysis

During copper electrowinning, short-circuiting will occur when the maximum height of nodules developed on the cathode surface reaches the anode. Each region of interest on the copper plate was analysed for the relative height of each copper nodule as previously described in section 3.2.2 of this report. The relative height of each copper nodule in each region of interest is shown by the colour scale. Figure 4.7-4.12 provides valuable insight regarding the relative distance of surface deviations from the best fit planes to ± 0.3 mm. Positive deviations (protrusions) initiate localized growth on the copper depositing surface as discussed in Section 2.4.2. On the other hand, negative deviations indicate indentations on the cathode surface. Indentations are less harmful in an electrowinning facility than irregular large protrusions.

4.1.2.1. Effect of guar addition

As already discussed in Section 4.1.1 the copper plate achieved from the Base case scenario has the roughest surface covered with nodules and dendrites when compared to copper plates achieved in the presence of guar. This is also evident from Figure 4.5 (a) which shows a flat copper plate produced from an electrolyte with no guar addition whereby irregular deviations most of which exceed 0.3 mm in height developed. This provides evidence of localized growth (nodules or dendrites), meaning selective growth of copper deposit on a certain spot or area on the cathode plate surface. This observation is in agreement with the finding of Coetzee (2018), whereby a copper plate with localized growth was produced from an electrolyte with no organic additive. However, Figure 4.5 (b-d) shows that the plate morphology did improve in the presence of guar in the electrolyte since deviations which exceeds 0.3 mm in height observed are less compared to copper plate produced in absence of guar. This further shows that the addition of guar in the electrolyte has an influence on the nucleation and growth of the copper deposit on the cathode surface.

Figure 4.5 (b) shows that the morphology of copper plate produced in addition of 2 mg/l of guar improves compared to the plate developed in the absence of guar. However, the level of gaur dosed seems like it was unable to adsorb on all the high-active sites effectively since deviations which exceeds 0.3 mm in height also developed on the copper cathode surface. According to Coetzee (2018), the inconsistent adsorption of guar supports the theory of guar molecules bonding at a weaker longer-range with the copper cathode surface from the OHP as described in Section 2.5.3 of this report. Figure 4.5 (c) shows very little negative deviations and no positive deviations from the reference plane. This may possibly imply a more consistent coverage or there are little to no protrusions which can initiate dendrites. Hence, a smoother cathode surface was observed.

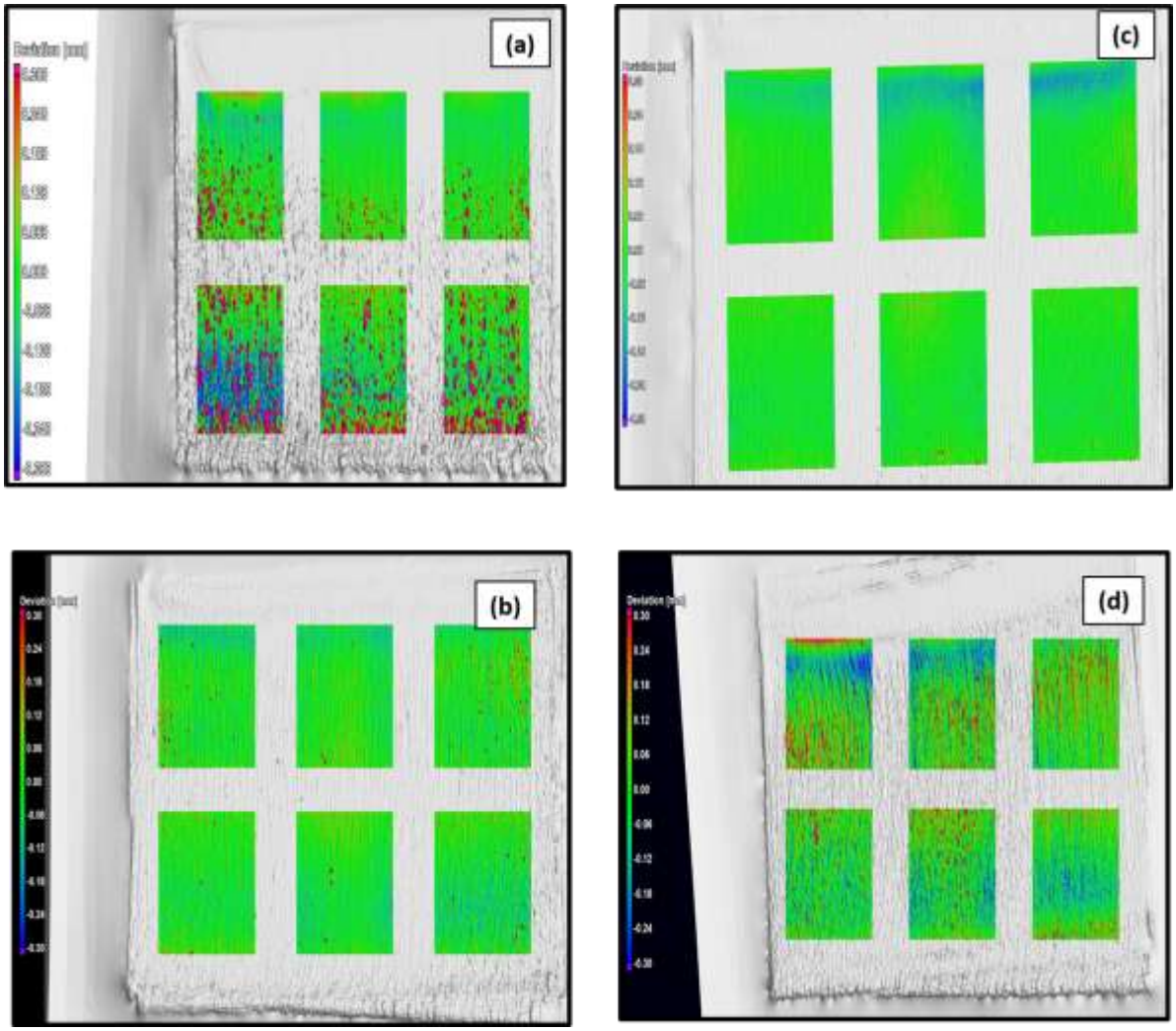

Figure 4.5: Surface topography analysis of copper plates obtained at 35 g/l initial copper concentration, 300 A/m^2 current density, 150 g/l sulphuric acid concentration and guar concentration of (a) base case scenario, (b) 2 mg/l, (c) 10 mg/l, (d) 18 mg/l.

4.1.2.2. Effect of current density

Based on the visual analysis of copper deposit produced during copper electrowinning at various experimental conditions it was observed that the copper plates produced at high current density had the most localized growth compared to copper plates produced at low current density. This is also evident in Figure 4.6 (a-c) showing that at a lower current density the cathode surface had very little to no positive deviations from the best fit plane when compared to the copper plates produced at higher current density as shown in Figure 4.5 (b-d). This shows that there are less to no protrusions which can initiate dendrites. Hence, at low current density the ensuing copper deposits were much smoother compared to copper deposits achieved at high current density.

Figure 4.6 (a) shows that 2 mg/l of guar adsorbed evenly on the cathode surface producing a smooth surface. From the visual analysis, little to no nodules were observed on the copper deposit achieved at 2 mg/l (Figure 4.2 (a)). However, Figure 4.6 (a) provides evidence that the copper plate achieved at 2 mg/l can still be considered smooth since the cathode surface shows that positive deviations with less than 0.12 mm in height developed.

Figure 4.6 (b) and (c) shows a marginal increase in the negative deviations on the cathode surface. Negative deviations (cathode indentation) are less harmful in an electrowinning facility than positive deviations (irregular large protrusions). It is important to note that the effect of guar concentration on surface roughness will depend on the various operating conditions.

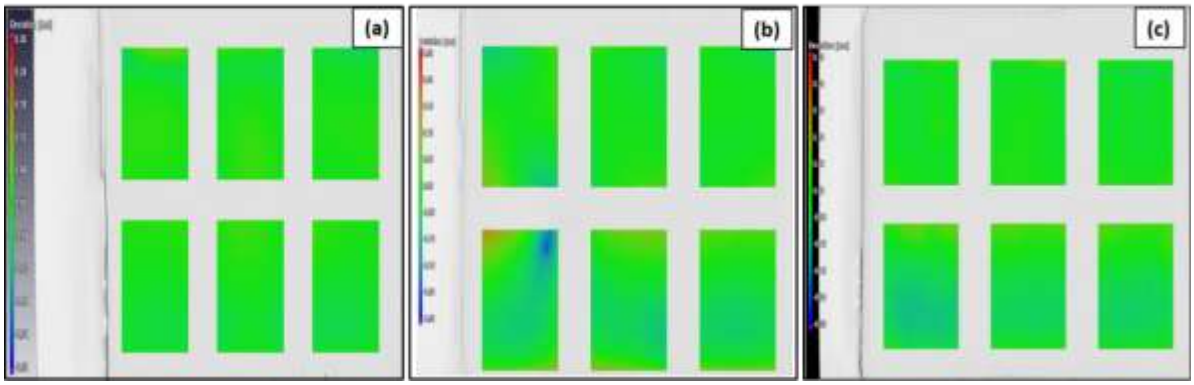

Figure 4.6: Surface topography analysis of copper plates obtained at 35 g/l initial copper concentration, 180 A/m^2 current density, 150 g/l sulphuric acid concentration, and guar concentration of (a) 2 mg/l, (b) 10 mg/l, (c) 18 mg/l.

Figure 4.5 and Figure 4.6 shows that the deviation colour scale of copper deposits achieved at low current density have no positive and very little to no negative deviations showing that guar concentration had a negligible effect compared to copper deposits produced at high current density. Therefore, only deviations scales of copper deposits achieved at high current density will be discussed further to provide evidence of the effect of guar at various experimental conditions. The deviation scales achieved at low current density at various operating conditions can be seen in Appendix C-Electrowinning supporting results.

4.1.2.3. Effect of copper concentration

The colour scale showing the effect of copper concentration on the physical appearance of copper deposits in the presence of guar are presented in Figure 4.7.

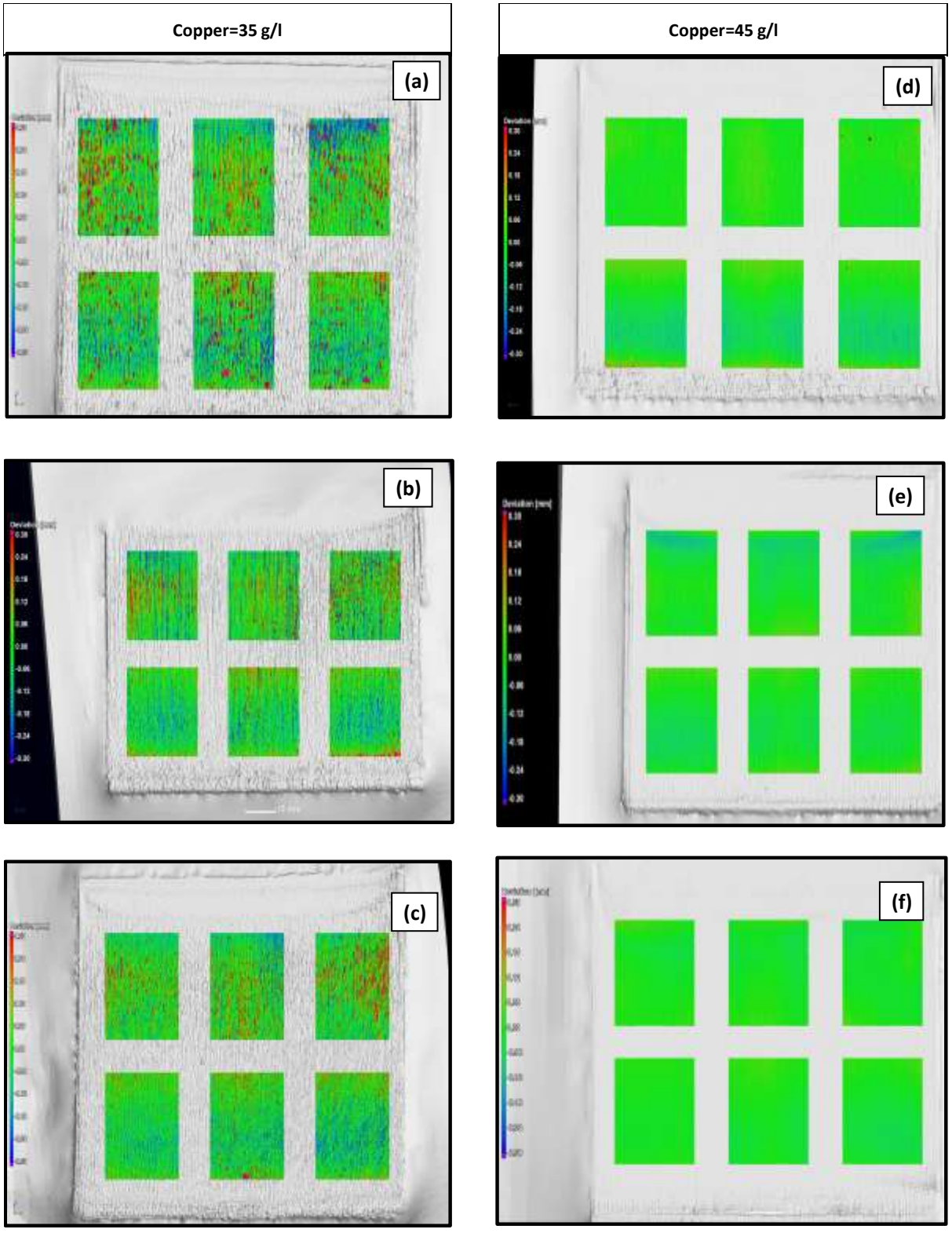

Figure 4.7: Surface topography analysis of copper plates obtained at 300 A/m^2 current density and 180 g/l sulphuric acid for 35 g/l initial copper concentration with guar concentration of (a) 2 mg/l, (b) 10 mg/l, (c) 10 mg/l) and for 45 g/l initial copper concentration with guar concentration of (d) 2 mg/l, (e) 10 mg/l, (f) 18 mg/l).

The deviation scale in Figure 4.7 (a-c) shows both positive and negative deviations from the best fit plane. This provides further evidence that at low initial copper concentration under the current experimental conditions, guar did not adsorb evenly and effectively on the cathode surface. However, it can also be seen that the positive deviations on the copper plate decreases at high guar concentration (Figure 4.7 (b-c)) than at low guar concentration (Figure 4.7 (a)).

By comparing Figure 4.7 (a-c) and Figure 4.7 (d-f) it is apparent that the copper deposits at high initial copper concentration are smoother compared to copper deposits achieved at low initial copper concentration. At high initial copper concentration, (Figure 4.7 (d) shows limited negative and positive surface deviations which implies a more consistent surface coverage of guar. Increasing guar concentration results in very little to no negative surface deviations on the copper plates as it can be seen in Figure 4.7 (e). A further increase in guar concentration to 18 mg/l produced a copper plate which virtually shows no negative and positive deviation from the best fit plane as shown in Figure 4.7 (f). This provides further evidence that high guar concentration adsorbs evenly and effectively onto the cathode surface.

The colour scales showing the effect of copper concentration at low sulphuric acid concentration in terms of the relative height of each copper nodule in each region of interest is provided in Figure 4.8 (a-f).

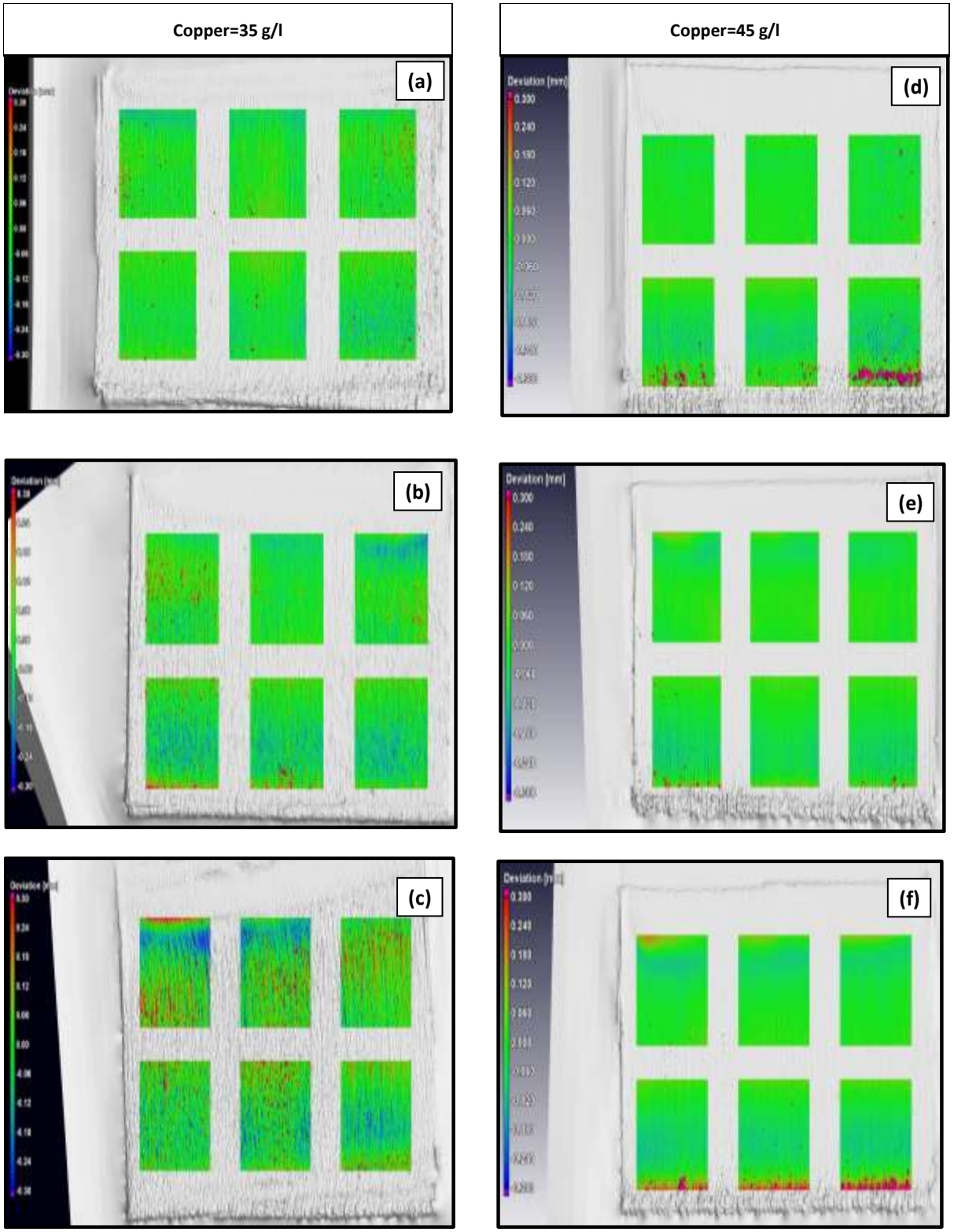

Figure 4.8: Surface topography analysis of copper plates obtained at 300 A/m^2 current density and 150 g/l sulphuric acid for 35 g/l initial copper concentration with guar concentration of (a) 2 mg/l, (b) 10 mg/l, (c) 10 mg/l) and for 45 g/l initial copper concentration using guar concentration of (d) 2 mg/l, (e) 10 mg/l, (f) 18 mg/l).

The deviation scale in Figure 4.8 (d-f) shows that the copper deposit surface with irregular deviations which exceeds 0.3 mm in height developed at the bottom of the copper deposit. This provides evidence of localized growth showing selective growth of copper at the bottom of the copper plate surface. In overall, the copper plates achieved at high initial copper concentration can be considered smooth since the localized growth were only observed at the bottom of copper plate. Therefore, copper plates achieved at high initial copper concentration are smoother when compared to copper deposits achieved at low initial copper concentration. The effect of increasing guar concentration at low initial copper concentration (150 g/l) is not visible from the deviation scales presented by Figure 4.8 (d-f). However, this effect can be compared in terms of an overall surface roughness factor (S_a value) as presented in Section 4.1.4.5.

At low initial copper concentration, Figure 4.8 (a-c), both positive and negative surface deviation is observed on the copper deposit surface. The negative surface deviation increases with increase in guar concentration; thus, it is possible that increasing guar concentration leads to uneven/preferential adsorption of guar on the plate surface. Furthermore, the positive deviations seem to increase with an increase in guar concentration. This trend is not expected since guar is added to control the formation of dendrites in copper electrowinning.

By investigating Figure 4.8 (a-c) and Figure 4.8 (d-f), it can be concluded that under the current experimental conditions the copper deposits produced at high initial copper concentration are smoother than copper deposits achieved at low initial copper concentration. The effect of low and high initial copper concentration on the copper cathode morphology will be discussed in detail in Section 4.1.4.

4.1.2.4. Effect of sulphuric acid

The deviation colour scales showing the effect of sulphuric acid concentration on the physical appearance of copper deposits in the presence of guar are presented in Figure 4.7 (a-f) and Figure 4.8 (a-f).

At low initial copper concentration (35 g/l) and low guar concentration (2 mg/l) it can been seen that the deviation colour scale of copper deposit achieved at high sulphuric acid concentration shows more positive deviations than copper deposit achieved at low sulphuric acid concentration as shown in Figure 4.7 (a) and Figure 4.8 (a).). Positive deviations provide evidence of localized growth on the plate topography which will cause short-circuiting leading to low quality copper cathode. Therefore, copper deposits achieved at high sulphuric acid are rougher and not desirable when compared to copper plates produced at low sulphuric acid concentration. This supports the results observed from the visual analysis of copper deposit as discussed in Section 4.1.1.4. However, at high initial copper concentration (45 g/l) the deviation colour scales show that varying sulphuric acid concentration has no visible effect of nodule growth as comparable positive and negative deviations from the best fit plane were observed from Figure 4.7 (d) and Figure 4.8 (d). Furthermore, Figure 4.7 (b-c) and Figure 4.8 (b-f) shows that with increased guar concentration the effect of varying sulphuric acid concentration is not visible as comparable positive and negative deviations are observed from the deviation scales of the copper deposits achieved supporting the results from the visual analysis.

4.1.3. Surface area deviations

As discussed in Section 3.3.2, the position of the reference plane on each of the selected regions of interest on each of the plates was effectively normalized by making the flattest part of the copper plate the “new” reference plane. This allowed relative comparison of the distribution of copper deposit surface deviations away from the normalized flattest surface between the plates on the same

axis as shown in Figure 4.9 and Figure 4.10. Basically, Figure 4.9 and Figure 4.10 can be explained in the following way: a narrower distribution of deviation suggests that less surface deviations developed from the flattest plane during the electrodeposition process, and hence a lower total surface roughness can be expected.

4.1.3.1. Effect of guar addition

Figure 4.9 shows that the Base case scenario resulted in the largest spread of surface area away from the reference plane compared to copper deposit produced in the presence of guar, and thus had the roughest surface area. This corresponds to the qualitative analysis of the copper deposit results already discussed in Section 4.1.1 and Section 4.1.2. It was explained that localized growth is much more unwanted and damaging during the electrodeposition process compared to smooth uneven growth. In other words, negative deviations (cathode indentations) are much less harmful in an electrowinning facility than large positive deviations (cathode protrusions) which are erratic during the electrowinning process. Therefore, deviation distributions with long tails, especially in the positive directions are undesirable.

Figure 4.9 gives useful insight: a small proportion of the plate produced in the Base case scenario can be considered smooth compared to the copper plates produced in the presence of guar which seems to have a narrower distribution around the reference plane. However, large dendrites were more prominent on the plate achieved in the Base case scenario (Figure 4.1 (a)), which is indicated in Figure 4.9 by the long distribution tail in the positive direction.

At the current density of 300 A/m^2 the average thickness of copper deposit was calculated to be about 1 mm as shown in Appendix A-Sample calculations. The relative height of copper nodules developed in copper plates achieved in the presence of guar is less than 0.3 mm. It was discussed in 4.1.2 that copper plates with deviations that exceeds 0.3 mm in height provide evidence of dendrite-like growth. This shows that in the presence of guar in the electrolyte the copper deposits achieved are smoother compared to the copper deposit produced in the base case scenario with deviations of more than 0.3 mm. The copper deposit produced from the base case scenario further shows deviations of +/- 0.5 mm which has quite a significant effect on the total growth of copper electrodeposit. The total growth of copper deposit is the sum of thickness of copper deposit and the height (deviation) of copper deposit as defined by Shukla (2013). Therefore, the base case scenario will also result in a shorter time to short-circuiting than copper deposits produced in the presence of guar in the electrolyte.

Interestingly, Figure 4.9 shows that the copper deposit achieved at high guar concentration (18 mg/l) a more even distribution of shorter deviations was observed than at lower guar concentrations which have sharper contrast between short and high deviations. The negative deviations in Figure 4.9 were eliminated to provide an interpretation of the distribution tail for the Base case scenario more clearly as shown in Appendix C–Electrowinning supporting results.

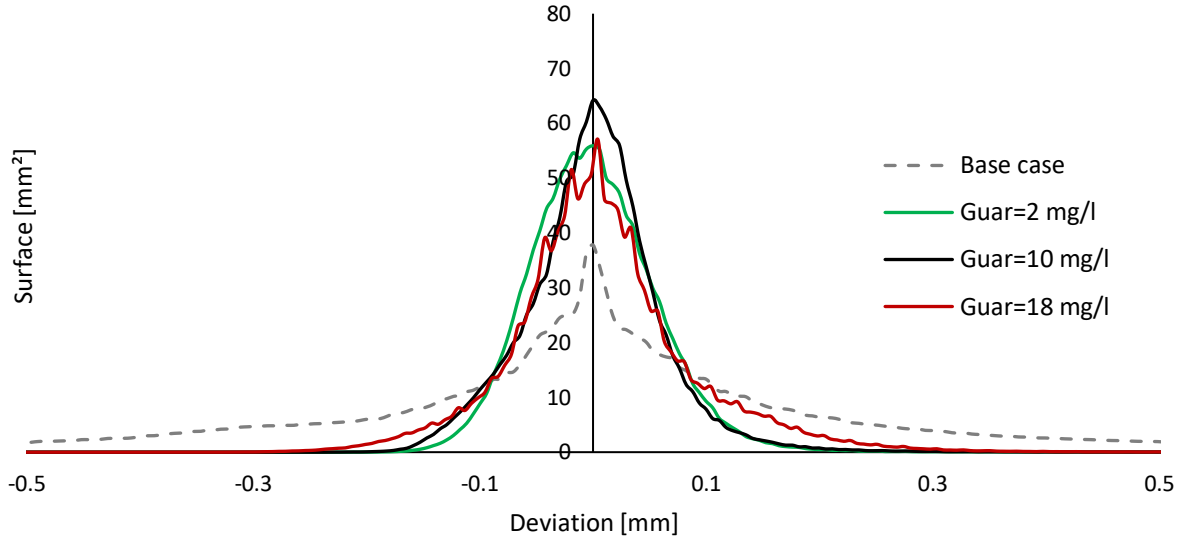

Figure 4.9: Average total surface elements (area) deviation from the flattest surface plane (normalized) for each plate achieved in the base case, 2 mg/l, 10 mg/l and 18 mg/l guar electrolyte at 300 A/m^{2}with sulphuric acid and initial copper concentration 150 g/l and 35 g/l, respectively.

4.1.3.2. Effect of current density

The effect of increasing current density from 180 A/m^2 to 300 A/m^2 on the surface deviations of each plate at various levels of guar concentration can also be quantitatively analysed as shown in Figure 4.10. These results, support the qualitative results of copper deposits as already discussed in Section 4.1.1 and Section 4.1.2. It is apparent from Figure 4.10 that operating the electrowinning experiments at higher current density resulted in the largest spread of surface area away from the reference plane. Consequently, this shows that the copper plate produced had a rougher surface area when compared to plates produced when operating at a lower current density. Copper plates at higher current densities are undesirable since deviation distributions with long tails are observed in the positive direction (cathode protrusions) than at the negative direction (cathode indentation). The explanation for the observed results on the effect of current density on the copper cathode surface roughness are discussed in section 4.1.2.

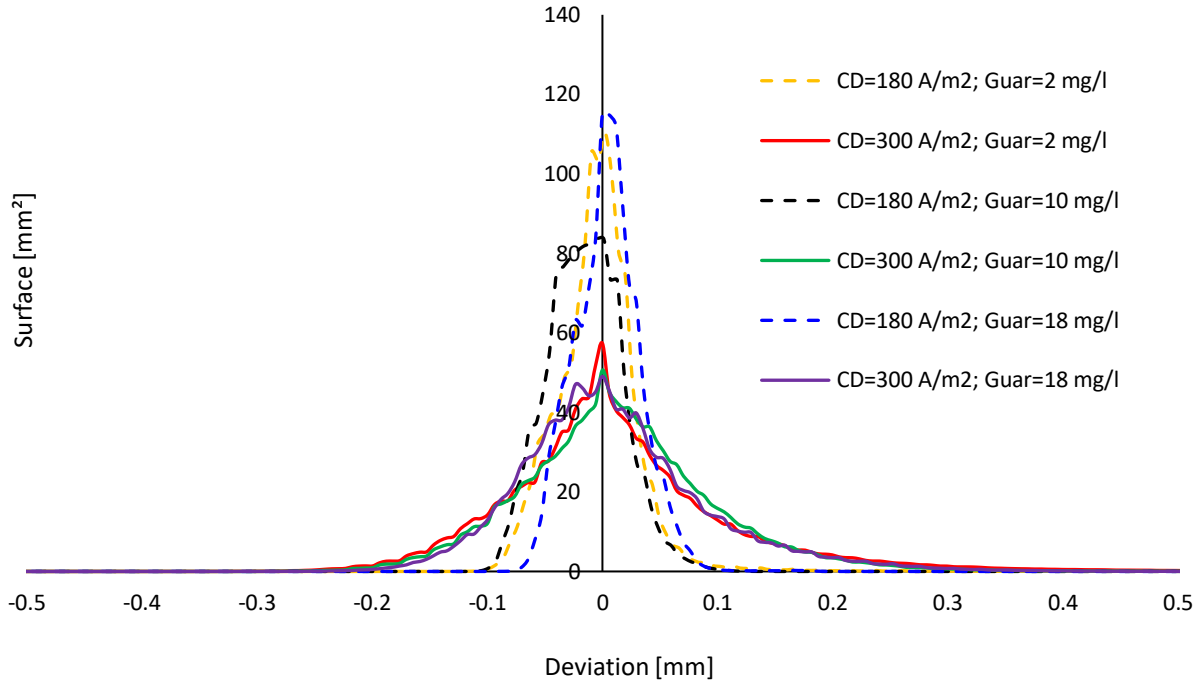

Figure 4.10: Average total surface elements (area) deviation from the flattest surface plane (normalized) for each plate achieved in the presence of guar electrolyte with sulphuric acid and initial copper concentration of 150 g/l and 35 g/l, respectively.

It is difficult to see the effect of varying the initial copper concentration and sulphuric acid concentration on the copper deposit morphology from the distribution of surface deviations since the deviations from the flattest surface plane are small to be comparable. Appendix C-Electrowinning supporting results, provides the surface deviation distribution curves showing the effect of initial copper concentration and sulphuric acid concentration.

4.1.3.3. Average deviation from the normalized reference plane (S_a value)

It is difficult to visually see variance in the spread of surface elements (area) from the density distribution of the surface deviations curves from the reference plane for some experimental conditions. For this reason, the arithmetic mean (S_a value), which encapsulates all the measured surface deviations from the reference plane to the copper deposit surface data in one numerical value, were calculated and plotted compared to each other in Figure 4.11. Both the positive (protrusions) and negative (indentations) surface deviations were considered for when calculating the S_a values for each plate produced at various experimental conditions. In order to be able to calculate the overall mean surface deviation for each copper deposit the negative deviations are converted to absolute values. Thereafter, the absolute negative deviations are combined with the positive deviations to get the overall surface mean surface deviation (S_a value) as described in Section 3.3.2 of this report. The S_a values were calculated as a measure of the surface roughness of each copper plate.

Considering both the negative and positive deviations from the flattest part of the surface it can be observed when comparing all the surface roughness values for copper deposits at a high current density, low initial copper concentration and high sulphuric acid concentration performed the worst compared to all the other copper deposits achieved at other experimental conditions. It can also be

seen that the surface roughness value decreases for all the copper plates achieved at low current density than copper plates produced at high current density. This effect of current density of surface roughness is consistent with the qualitative analysis results as discussed in Section 4.1.1 and 4.1.2. It was previously proposed, based on the qualitative evidence that at a high current density dendrite (localized growth) was observed on the copper cathode surface than at low current density. Whilst less dendrites developed on the cathode surface might have also been due to the differences in plating rates, current density is known to be a significant contributor to deports morphology (Shukla, 2013). This is also evident from the quantitative data presented in Figure 4.10 where a wide deviation distribution with long tails was observed for copper plates achieved at high current density than low current density.

Furthermore, Figure 4.11 shows that the surface roughness of copper deposits is highly influenced by the interactive effects of guar dosage with the other operating parameters at the various operating conditions. The trend showing the effect of guar concentration on the surface roughness of copper deposit for all experimental conditions at high current density correspond to the trend observed at low current density expect for the copper deposit achieved at low copper and low sulphuric acid concentrations. At high current density, the experimental conditions that produced copper deposits with low surface roughness compared to other experimental conditions is when high copper and sulphuric acid concentrations are added in the electrolyte. It can be observed further that under this experimental conditions, high guar concentration is more effective in reducing localized growth than low guar concentration. This effect was also revealed from the qualitative analysis as shown in Figure 4.7 (d-f). The interactive effects of the operating parameters will be discussed further in section 4.1.4 of this report.

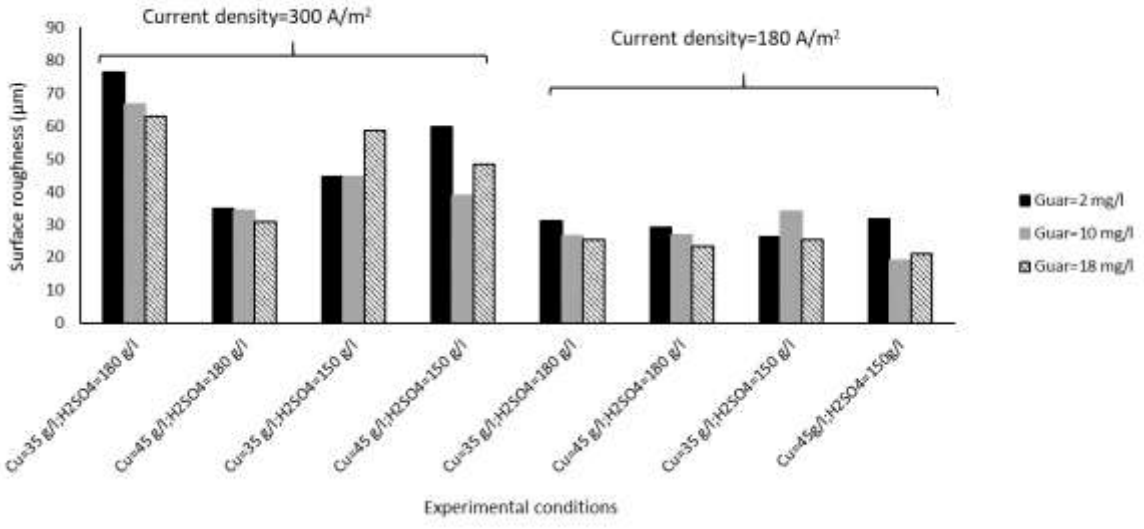

Figure 4.11: Average deviations from the normalized reference plane (S_a value) for each copper plate produced during the 24 hours of electrowinning at various experimental conditions in the presence of guar.

Equal weight is given to uneven growth and localized growth of copper deposit on the cathode surface by considering for the negative deviations when calculating the mean surface deviation from the normalized flattest part of the plane. In the context of the qualitative evidence presented in Section 4.1.1 and Section 4.1.2, negative deviations on the plate topography will not cause short-circuits. Furthermore, negatives deviations will not lead to a lower quality of copper cathode plate in terms of ductility, porosity, entrapment, and purity, whereas positive deviations (localized growth) will. Based on this, the S_a value were then recalculated to describe the copper cathode quality by giving much more weight to the localized growth. This was done by considering only the positive deviations from the reference plane, since positive deviations are directly related to nodules and localized growth. The calculated S_a values without considering negative deviations are presented in Figure 4.12.

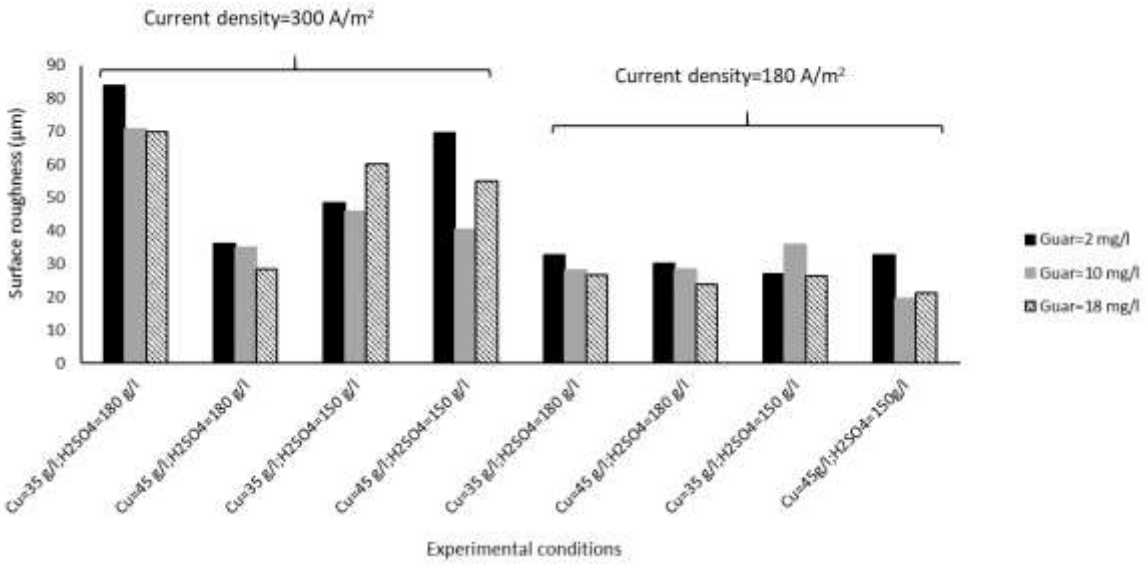

Figure 4.12: Calculated arithmetic mean surface deviation (S_a value) for each copper plate produced during the 24 hours of electrowinning at various experimental conditions in the presence of guar-considering positive deviations only.

Comparing the results presented in Figure 4.11 to the results in Figure 4.12, it can be observed that the surface roughness values for all the copper plates achieved slightly increased except for the copper plate achieved at high current density, high initial copper concentration and high sulphuric acid concentration in the presence of 18 mg/l guar concentration which showed a slight decrease in the surface roughness value. For all the plates that shows a slight increase in the surface roughness values it suggests that more positive deviations (protrusions) were captured away from the flat surface than negative deviations (indentations) for all the copper plates. However, an opposite effect was observed for the copper plate achieved at high levels of operating parameters resulting in a slight decrease in surface roughness value. Furthermore, the resulting trend in Figure 4.12 is consistent with the conclusion made for the effect of current density on the qualitative analysis as discussed in Section 4.1.1 and Section 4.1.2. However, it can be seen that the overall surface roughness of copper plates with combined negative and positive deviations as shown in Figure 4.11 and the overall surface

roughness without negative deviations as shown in Figure 4.12 presented equivalent results since there is only a slight difference in the surface roughness values.

4.1.4. Statistical analysis of operating parameters on surface roughness

Ultimately, from the visual inspection only, it is difficult to explain the interaction effects of operating parameters on the various experimental conditions on the copper deposit morphology in the presence of guar considering the evidence and arguments presented thus far. The interactive effects of operating factors on the surface roughness are based on the surface roughness values calculated from combining both the negative and positive deviations.

Analysis of variance (ANOVA) was used to determine the significant effects of the operating parameters on the surface roughness of copper deposits from the surface roughness experimental data. To quantify for the significance of each parameter (individually and interactively) the Probability value (P-value) of each parameter was returned from the statistical analysis as presented in Table 4.2 and Table 4.3. The parameters with a P-value≤0.1 suggested that the parameters or their interactions were the most significant in affecting the surface roughness of copper deposits at a 90% confidence level as discussed in Section 3.3.4 of this report. It can be seen from Table 4.2 showing the individual effects of the operating parameters that the surface roughness is significantly influenced by current density (P-value=0.00) and copper concentration (P-value=0.02). As expected, current density has the most significant effect on the surface roughness of the copper deposit compared to the other the operating parameters which have a significant effect on the surface roughness. This is in agreement with the findings of Shukla (2013) where it was observed from the statistical analysis of copper deposit obtained from electrowinning experiments that the current density has the most significant effect on the roughness of copper deposits.

Table 4.2: Analysis of variance (ANOVA) for the surface roughness of copper deposits (main effects).

Parameters	Degrees of Freedom	P-value
Intercept	1	0.31
Current density (CD)	1	0.00
Sulphuric acid (SA)	1	0.78
Copper (C)	1	0.02
Guar (G)	2	0.33

Table 4.3 shows the interactive effects of operating parameters on the surface roughness of copper deposits. It can be seen from Table 4.3 that current density (P-value=0.08), copper concentration (P-value=0.04) and the interactive term of SA*C (P-value=0.09) have a significant effect on the surface roughness of copper deposits. The significant effect of the term involving SA*C on the surface

roughness of copper deposit is well supported by the interaction plot in Figure 4.15 showing that an interaction occurs from the non-parallel lines. Furthermore, the guar concentration P-value is above 0.1 which implies that the effect of guar concentration on surface roughness is insignificant. The results are consistent with the previous EW tests conducted by Fabian et al. (2007) where the findings shows that the effect of guar had an insignificant effect to reduce surface roughness from a statistical analysis.

The influence of individual and interactions of operating parameters on the surface roughness of copper deposits produced during copper electrowinning is discussed in more detail in Section 4.1.4.1-4.1.4.5.

Table 4.3: Analysis of variance (ANOVA) for the surface roughness of copper deposits (interactive effects).

Parameters	Degrees of Freedom	P-value
Intercept	1	0.07
Current density (CD)	1	0.08
Sulphuric acid (SA)	1	0.12
Copper (C)	1	0.04
Guar (G)	2	0.44
CD*SA	1	0.61
CD*C	1	0.04
SA*C	1	0.09
CD*G	2	0.84
SA*G	2	0.58
C*G	2	0.39

4.1.4.1. Effect of current density and copper concentration on surface roughness

The effect of current density on the surface roughness of copper electrodeposit was studied at a range of 180 A/m^2 to 300 A/m^2 at a temperature of 40^{o}C with results illustrated in Figure 4.13 and Figure 4.14. The effect of current density on the surface roughness follows the expected trend. Increasing the current density resulted in an increase in the surface roughness. High surface roughness on copper deposits at increased current density shows that dendrite-like nodular growth is favoured more than at lower current densities as already discussed from the qualitative analysis in Section 4.1.1 and Section 4.1.2. An increase in current density results in a higher overpotential that increase the nucleation rate (Rashidi and Amadeh, 2008). This leads to faster deposition rate of copper ions to the

cathode surface promoting the formation of smaller crystals. Therefore, with a higher growth rate of the crystal grains perpendicular to the electrode surface instabilities are more likely to occur leading to the formation of dendrites on the copper deposit surface (Winand, 1992; Budevski et al., 2000).

Figure 4.13 also shows the interactive effect of current density and copper concentration on the surface roughness of copper electrodeposits. Increasing the average copper concentration decreases the surface roughness of the copper deposits. This effect is more significant at higher current density than at low current density. The low cathode deposit quality observed at a lower average copper concentration was due to the faster rate at which copper cations are removed from the vicinity of the electrode exceeding the rate at which copper ions are replaced from the bulk electrolyte (Alfantazi and Valic, 2003). Therefore, increasing the average copper concentration in the electrolyte will improve the quality of copper deposit since sufficient copper will be supplied to the electrode surface at higher current density. This further explains the results observed from the qualitative analysis (Section 4.1.1 and Section 4.1.2.) showing the effect of copper concentration on the copper deposit surface achieved during copper electrowinning. It was observed from the qualitative analysis that a smoother copper deposit is achieved at a higher average copper concentration compared to copper deposit produced at lower average copper concentration.

The effect of current density and copper concentration can also be explained using the Winand's diagram. From the Winand's diagram as shown in Figure 2.8, increasing current density causes the ratio of current density to limiting current density (i/i_L) to increase and shift the electrodeposition conditions towards the region where the possibility of dendrite formation is increased along the x-axis. At increased current density, the deposition rate of copper ions on the cathode surface increases leading to a decrease in the concentration of copper in the bulk solution. Hence, at high current density, the surface roughness observed at low average copper concentration is high compared to surface roughness at a high average copper concentration because for the same deposition rate the copper ions in low copper concentration will be depleted more than at high copper concentration in the bulk solution for the same plating time.

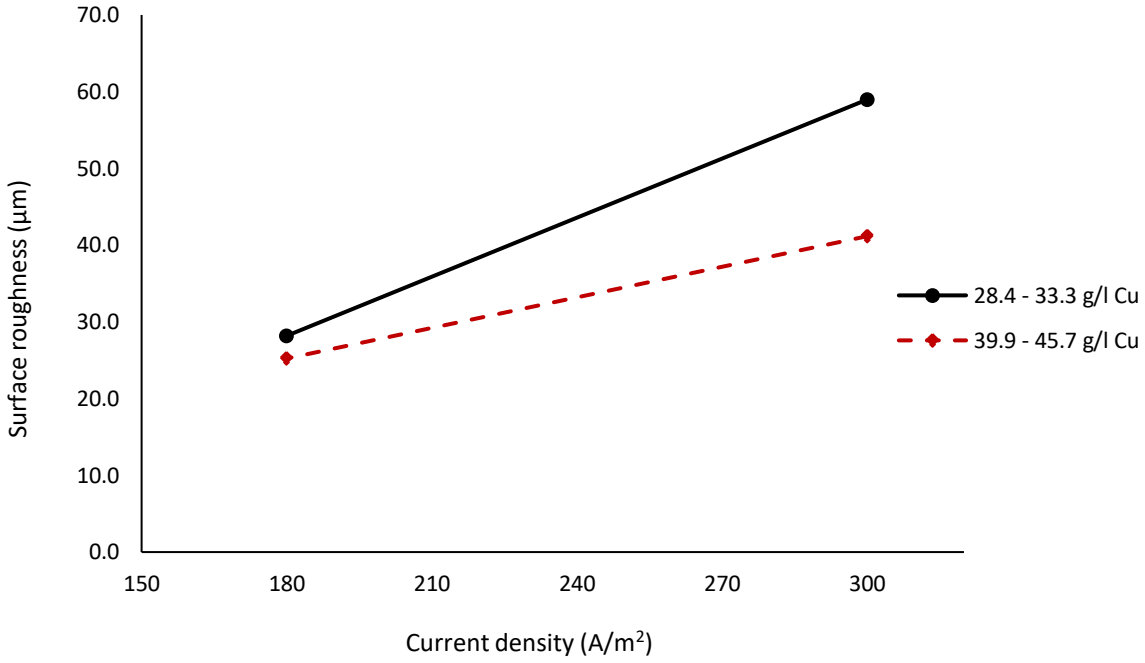

Figure 4.13: Current density/copper concentration interaction plot.

4.1.4.2. Effect of current density and sulphuric acid concentration on surface roughness

Figure 4.14 shows that increasing sulphuric acid concentration from 150 g/l to 180 g/l has no significant influence on the surface roughness. Even though the effect is insignificant it can be seen that increasing sulphuric acid concentration results in a slight increase in the surface roughness. This effect can be explained by faster guar degradation under high sulphuric acid conditions than at low sulphuric acid conditions (Stankte, 1999). An attempt was made to investigate guar degradation to its monomers (galactose and mannose) at various sulphuric acid concentrations from hydrolysis tests as discussed in Appendix D-Guar degradation evaluation. From the hydrolysis tests it was observed that partial guar degradation may potentially support the marginal effect of sulphuric acid on the surface roughness value of copper deposits achieved. However, further investigations must be conducted to confirm the theory. Alternatively, the effect of sulphuric acid on surface roughness can be clearly seen from its interactive effect with copper concentration shown by Figure 4.15.

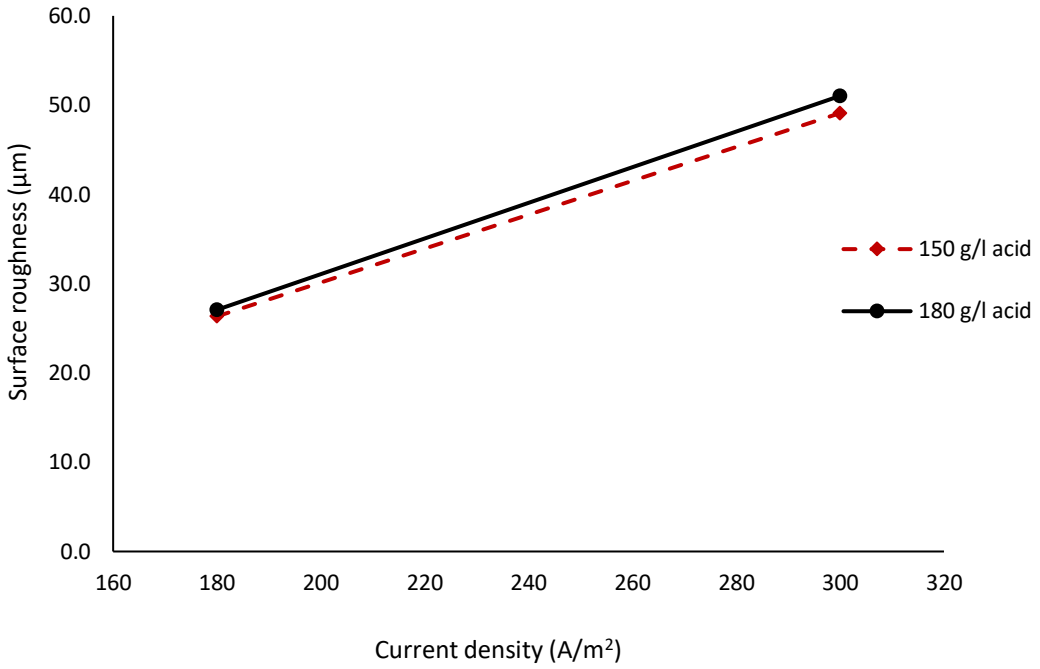

Figure 4.14: Current density/sulphuric acid concentration interaction plot.

4.1.4.3. Effect of copper and sulphuric acid concentration on surface roughness

Increasing the initial sulphuric acid concentration will lead to an increase in the mobility of H^+ ions over the cathode surface. Depending on the operating overpotential, the copper ions are more likely to be reduced and form metal copper than the hydrogen ions are to form hydrogen gas since copper has a higher electrode potential than hydrogen. However, even at sufficiently large overpotential where Cu^{2+} plating is dominate it might be possible for H^+ to be reduced marginally. At a higher average copper concentration, the surface roughness decreases as shown in Figure 4.15, and this can be attributed to a sufficient supply of copper ions on the cathode. However, if the mobility of copper ions is reduced (low average copper concentration) in the electrolyte the hydrogen ions tend to collect in the diffusion layer at the cathode and adsorb on the latter (Shreir and Smith, 1953). Hence, an increase in surface roughness observed since majority of sites suitable for crystal growth are covered instantaneously favouring the formation of nuclei and random orientation, and a reduction in crystal size at a low copper concentration. Furthermore, as the hydrogen ions collect in the diffusion layer at the cathode the concentration of hydrogen ions in the electrolyte decreases. According to Wang et al. (2021) when the concentration of H^+ decrease it will Lead to an increase in the pH of solution.

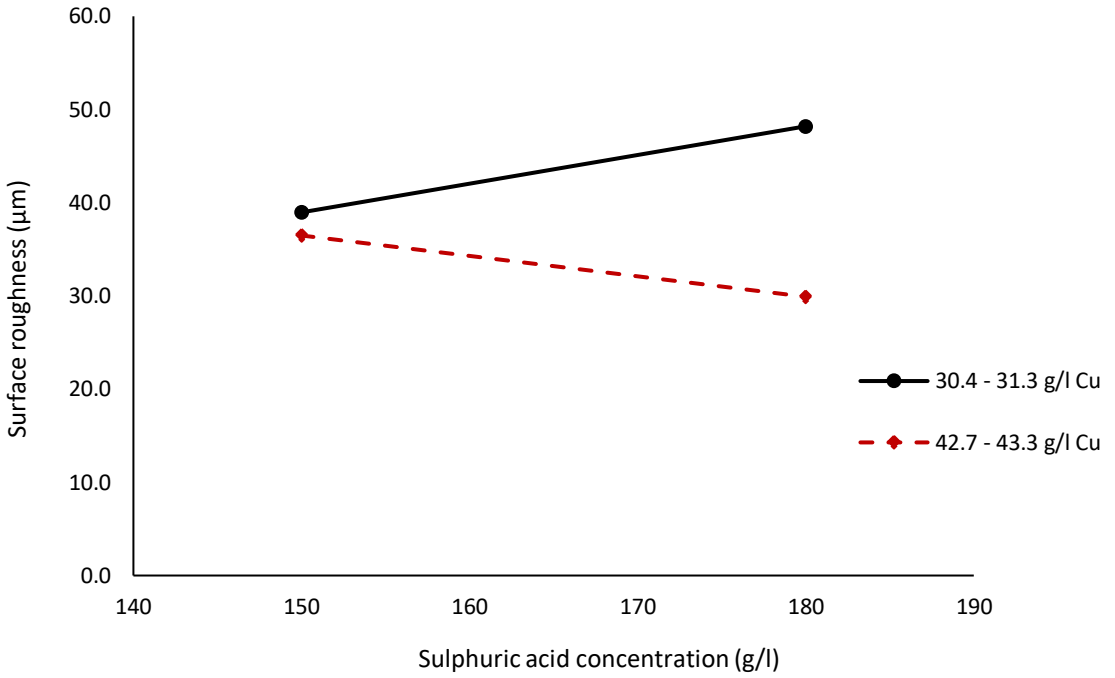

Figure 4.15: Sulphuric acid/copper concentration interaction plot.

4.1.4.4. Effect of current density and guar concentration on surface roughness

At a lower current density, increasing guar concentration decreases the surface roughness of copper deposit as it can be seen in Figure 4.16. This can be the expected trend since guar is dosed to control dendrites. However, Fabian et al. (2007) reported that increasing guar concentration increases surface roughness at lower current densities than about 300 A/m^2 and this does not correlate with the findings in this work. From Figure 4.16 it can also be observed that the surface roughness increases more steeply with increasing current density than with varying guar concentration. This observation can also be supported from the ANOVA results presented in Table 4.3 whereby the P-value of current density was 0.08 while for guar concentration it was 0.44. This observation correlates well with the findings of Shukla (2013) from a statistical analysis of copper deposit where it was observed that current density is the most influential parameter to affect the roughness of copper deposit than guar concentration.

At a higher current density, increasing guar concentration from 2 mg/l to 10 mg/l decreases the surface roughness following the trend observed at a low current density. Surprisingly, a further increase in guar concentration from 10 mg/l to 18 mg/l leads to a marginal increase in the surface roughness. However, this increase in surface roughness is lower when compared to 2 mg/l guar concentration. Therefore, it can be concluded that at increased guar concentrations (10 mg/l or 18 mg/l) the surface roughness will be lower compared to the surface roughness of copper deposits developed in addition of 2 mg/l guar concentration. It is recommended that future studies investigate the effect of increasing the guar concentrations higher than 18 mg/l on the surface roughness.

Furthermore, at higher current density the copper deposition is faster than the additive adsorption (Liu et al., 2005). This suggests that at high current density the guar molecules will desorb from the active sites at a faster rate. If guar desorb very fast it doesn't allow enough time for guar molecules to

inhibit the growth of dendrite on the copper cathode surface. As already discussed in Section 4.1.1, organic additives are believed to inhibit the copper electrodeposit to prevent further growth of dendrites on the copper cathode surface by adsorbing onto the active sites. Increasing guar concentration will allow sufficient larger molecules to adsorb on the active sites than low guar concentration. Thus, at high current density a higher surface roughness observed at low guar concentration than at high guar concentrations.

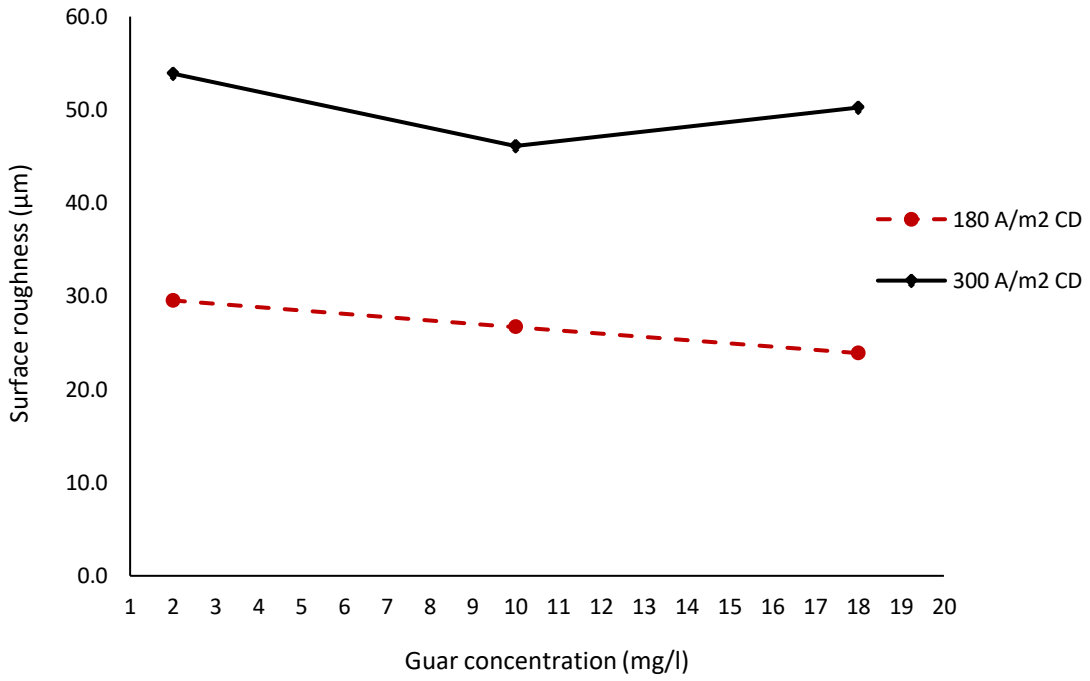

Figure 4.16: Current density/guar concentration interaction plot.

4.1.4.5. Effect of copper and guar concentration on surface roughness

At a lower average copper concentration, the surface roughness value is higher when compared to the surface roughness values at a higher average copper concentration as it can be seen in Figure 4.17. As already discussed in section 4.1.4.1, decreasing copper concentration in the bulk solution causes a decrease in diffusion limiting current. Consequently, this increases the ratio (i/i_L) which shifts the electrodeposition process at conditions where dendrite formation is highly possible along the x-axis from the Winand's diagram as shown in Figure 2.8. In order to inhibit the development and growth of dendrites, guar can be added in the electrolyte allowing a decrease in the surface roughness on the copper cathode surface during electrowinning.

At a lower average copper concentration, it can be observed that the roughness of copper deposit was not significantly affected by guar concentration over the range of concentrations investigated (2 mg/l to 18 mg/l). However, this marginal effect shows that the surface roughness of copper deposit decreases with an increase in guar concentration. Since the probability of formation of dendrite is high at low copper concentrations, these levels of guar concentration added were insufficient to completely eliminate the dendrite growth when compared to high copper concentration.

At a higher average copper concentration, the results show that increasing guar concentration from 2 mg/l significantly decreases the surface roughness than at low average copper concentration. According to Schleisinger et al. (2011) if there is a high copper concentration (40 g/l-50 g/l) in the electrolyte and steady recirculation of the electrolyte through the electrowinning cell it will ensure constant availability of Cu^{2+} ions on the cathode surface. This will allow a constant plating rate, which gives uniformity of crystals grain size in the cathode. The uniformity of the crystal grain size is assisted by maintaining consistent concentrations of smoothing additives in the electrolyte. At 2 mg/l it seems like guar was unable to adsorb effectively on all the high-active sites producing a plate which is rougher than the plate achieved at higher guar concentration. Therefore, to ensure a consistent adsorption of guar on the cathode surface its concentration can be increased.

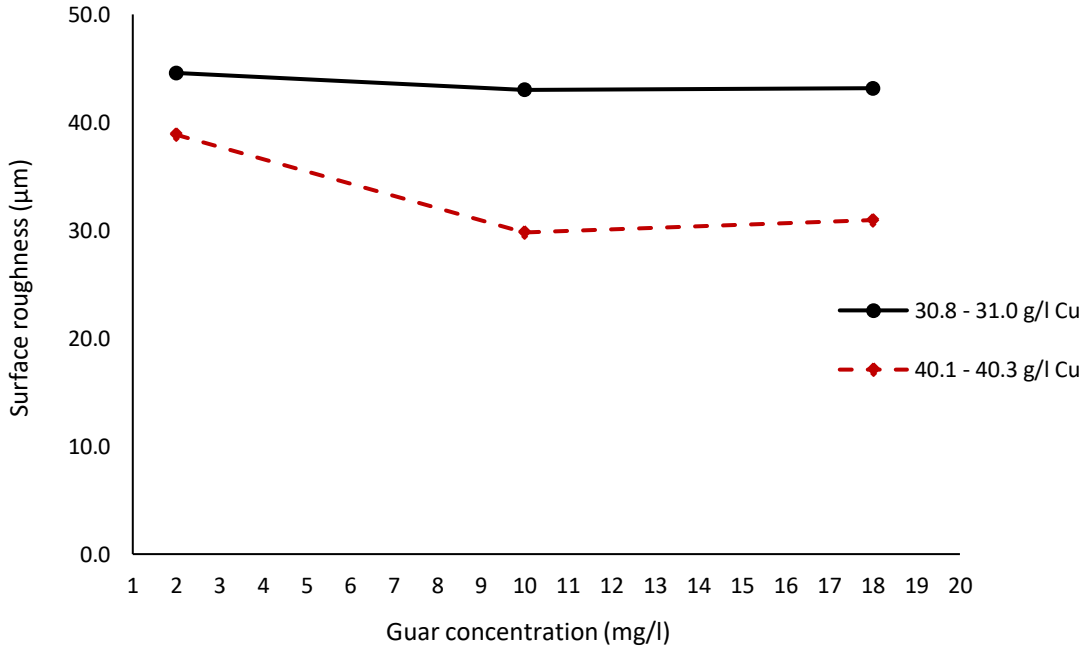

Figure 4.17: Copper concentration/guar concentration interaction plot.

4.1.4.6. Effect of sulphuric and guar concentration on surface roughness

Figure 4.18 shows that in the presence of 2 mg/l guar, increasing sulphuric acid results in a marginal increase in the surface roughness as already discussed in section 4.1.4.2. However, higher guar concentration in the electrolyte decreased the surface roughness of the copper deposit produced than at 2 mg/l guar concentration. Since guar is dosed to control dendrite formation on the copper deposit this can be the expected trend. But further investigations at higher levels of guar should be conducted to determine a more conclusive outcome of the effects on surface roughness.

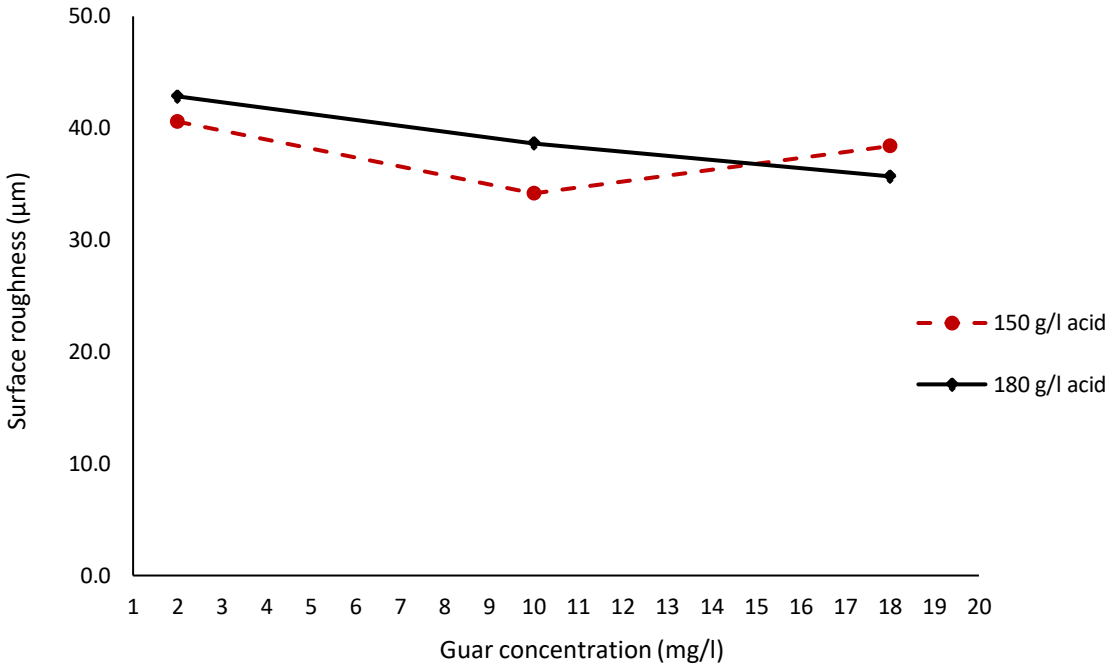

Figure 4.18: Sulphuric acid concentration/guar concentration interaction plot.

4.2. ELECTROWINNING TESTS: CURRENT EFFICIENCY

At the end of each electrowinning experiments the produced copper plates were weighed to determine the mass of each copper deposit to evaluate the electrowinning performance for each experiment by comparing their current efficiencies.

4.2.1. Current efficiency results

The total mass of copper deposited and the average rate of copper deposition for each plate are presented in Appendix C-Electrowinning supporting results. The differences in the amount of copper that was deposited on the plates varied slightly and is directly related to the difference in the current efficiency for the relative current applied to the cell. Figure 4.19 presents the current efficiency (CE) values obtained at various experimental conditions during the 24 hours of copper electrowinning. The CE values were calculated from the ratio between the actual and theoretical amount of copper plated as described in section 2.6.1. of this report. The theoretical amount of copper that was expected to plate assuming a 100% efficiency was only dependent on the current applied to the EW cell for each experiment since the plating time remained the same. Within the scope of ranges used for the operating parameters in this study, the electrowinning experiments yielded CE values that were very high (greater than 97.8%) compared to those achieved in industrial operations. Furthermore, the current efficiencies between repeats of the same experiments did not vary by more than 1% as it was previously reported in Table 4.1. These current efficiency values shows that majority of the current was utilized to electrowin copper with minimal losses. Depending on the operating overpotential there might be the possibility of marginal reduction of H^+ even though Cu^{2+} plating is dominate (as discussed in Section 4.1.4.3). Thus, the minimal losses of current efficiencies observed might be due to the marginal reduction of H^+ during the electrodeposition process.

For industrial operations, current efficiency ranges from 85 to 95% (Alfantazi and Valic, 2003; Robinson et al., 2013). The high CE values were expected since a pure electrolyte was used and the conditions in the EW cell were easily controlled. The pure electrolyte was made using reagent grade chemicals without impurities which may lead to parasitic reactions consuming current that would otherwise be used for the reduction reaction of copper ions to copper metal at the cathode surface during electrowinning. Secondly, the EW cell and experimental conditions were properly controlled and monitored.

Addition of guar does not significantly change the current efficiency during copper electrowinning as shown in Figure 4.19. However, it can be seen that the insignificant effect of guar on the current efficiency can vary depending on the level of its dosage and the various operating conditions of the dependent variables (copper concentration, sulphuric acid concentration and current density) during copper electrowinning. Even though the CE variation between the electrowinning experiments was little, higher current density generally increased the current efficiency compared to lower current density. This is the expected trend and correlates well with the findings from Panda and Das (2001) and Alfantazi and Valic (2003).

Even though current efficiency is widely used as a measure of the tankhouse proficiency in producing electrowon metal, it does not provide a direct measure of the produced metal quality (Alfantazi and Valic, 2003). These finding are well aligned with those of the current study. Looking at the current efficiency values from Figure 4.19 and the surface roughness values presented in Section 4.1.3 (Figure 4.11) as well as the physical appearance of the copper deposit, it can be seen that even though the experiments returned higher current efficiencies some of the plates had a less desirable surface roughness compared to the other plates depending on the conditions employed during experimentation. This shows that it is possible to have a good current efficiency but have a poor copper cathode deposit quality. The results of the current study also support that current efficiency cannot be used as the sole predictor of copper cathode quality. Hence, the surface roughness and chemical composition analysis of the copper deposit was also investigated. It is recommended to determine optimum operating conditions for each tankhouse.

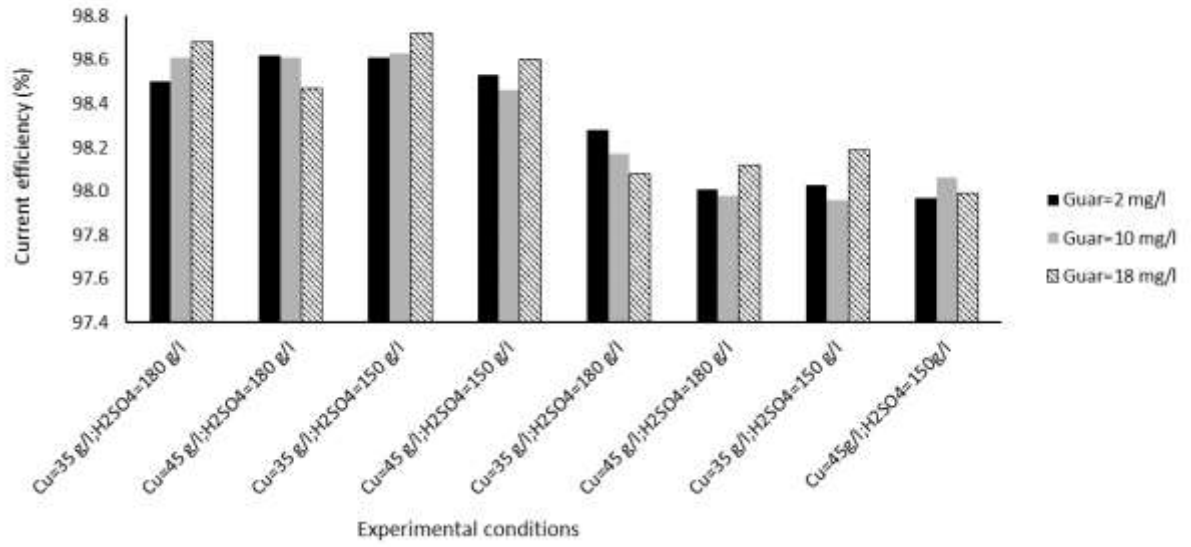

Figure 4.19: Calculated current efficiency values of copper deposited during 24 hours of electrowinning at various experimental conditions in the presence of guar.

4.2.2. Statistical analysis of operating parameters on current efficiency

As already discussed in Section 4.2.1, little variance was observed between the current efficiencies of the same experiments. Since little variation was observed for the same experiments, it is meaningful to compare the current efficiency of each experiment during copper electrowinning. It was observed that little variance in current efficiency was also observed when comparing each electrowinning scenario as shown in Figure 4.19. An analysis of variance was performed to determine the statistical significance of the individual and interactive parameters effects on current efficiency. Table 4.4 and Table 4.5 shows the ANOVA analysis of the individual and interactive effects of the operating parameters on current efficiency. It can be seen from Table 4.4 that statistically current density (P-value=0.00) and copper concentration (P-value=0.01) has a significant effect in current efficiency.

Table 4.4: Analysis of variance (ANOVA) for the current efficiency obtained for producing each copper deposit (main effects).

Parameters	Degrees of Freedom	P-value
Intercept	1	0.00
Current density (CD)	1	0.00
Sulphuric acid (SA)	1	0.37
Copper (C)	1	0.01
Guar (G)	2	0.38

However, Table 4.5 shows that the interactive terms had an insignificant effect on current efficiency (P-value>0.1), hence, the little variation observed between the current efficiencies. Since the P-value of guar concentration is 0.29 which is greater than 0.1 it implies that guar concentrations have an insignificant effect on current efficiency under the current operating conditions.

Table 4.5: Analysis of variance (ANOVA) for the current efficiency obtained for producing each copper deposit (interactive effects).

Parameters	Degrees of Freedom	P-value
Intercept	1	0.00
Current density (CD)	1	0.12
Sulphuric acid (SA)	1	0.43

Copper (C)	1	0.83
Guar (G)	2	0.29
CD*SA	1	0.34
CD*C	1	0.73
SA*C	1	0.95
CD*G	2	0.92
SA*G	2	0.26
C*G	2	0.66

The influence of individual and interactions of operating parameters on the current efficiency is discussed in more detail from the interaction plots in Figure 4.20-4.25.

4.2.2.1. Effect of current density and copper concentration on current efficiency

The current efficiency increases with an increase in current density at the operating temperature of 40°C as illustrated in Figure 4.20 and Figure 4.21. The effect of current density on the current efficiency follows the expected trends (Alfantazi and Valic, 2003; Su et al., 2017). The amount of current applied to the cell increases when operating the EW cell at high current density than operating at low current density. Current is a measurement of electrons flowing per second. Thus, if a high current applied to the cell more electrons are transferred from the anode to the cathode allowing more ions to be reduced and oxidised increasing the rate of electrodeposition in a direct proportion (Ayse Malis Aygar, 2009).

Figure 4.20 also shows the effect of copper concentration on the current efficiency during copper electrowinning. Increasing the average copper concentration at both low and high current density it can be observed that it results in a decrease in current efficiency. These findings contradict with the results reported by Moats and Khouraibchia (2009) and Owais (2009) where it was found that copper concentration has a positive effect on current efficiency because as copper concentration increases in the electrolyte the deposition rate of copper ions will improve. This will feed sufficient and constant amount of copper ion to the cathode surface. The increase in current efficiency with increasing the average copper concentration may be attributed to sufficient and constant amount of copper ions to the cathode surface increasing deposition rate or the plating rate of copper.

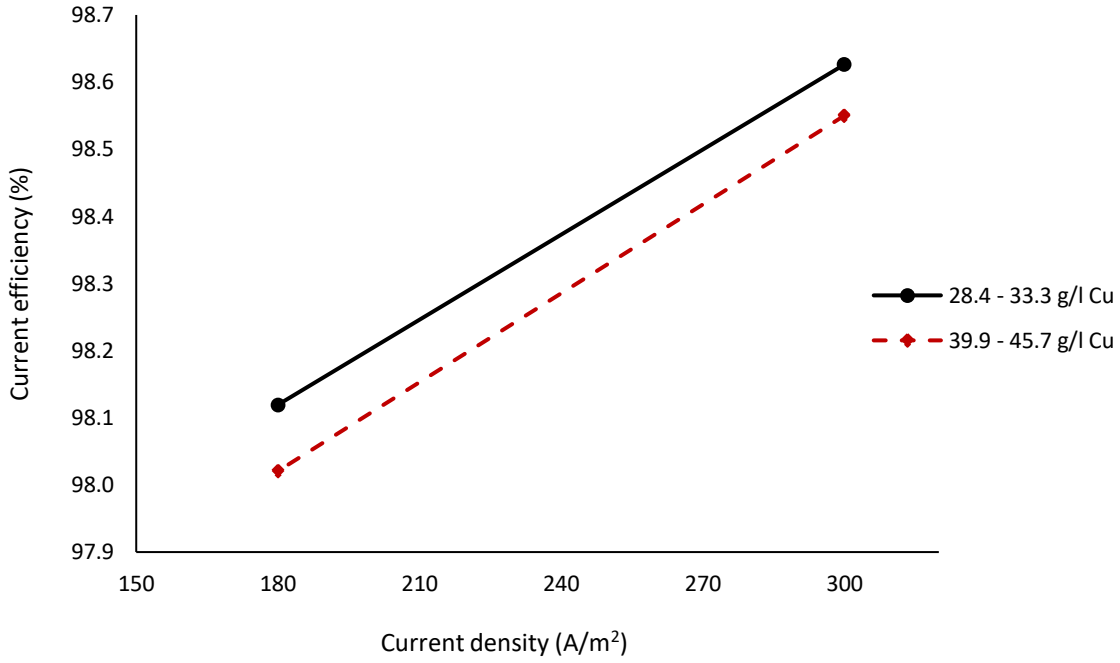

Figure 4.20: Current density/copper concentration interaction plot.

4.2.2.2. Effect of current density and sulphuric acid concentration on current efficiency

The interaction effect of current density and sulphuric acid concentration on current efficiency during copper electrowinning was studied at 150 g/l and 180 g/l at a temperature of 40°C. According to literature there are opposing effects of sulphuric acid on current efficiency which can be supported by the results presented in Figure 4.21. Within the range investigated, sulphuric acid concentration was found to have no significant influence on the current efficiency at low and high current density as shown Figure 4.21. However, at low current density it can be seen that current efficiency slightly increases with an increase in sulphuric acid. A similar outcome was observed by Moats and Khouraibchia (2009) where a slight increase in current efficiency was reported when the sulphuric acid concentration was varied from 160 g/l to 220 g/l. The effect of sulphuric acid concentration on the current efficiency can be clearly seen from its interactive effect with copper concentration shown in Figure 4.22.

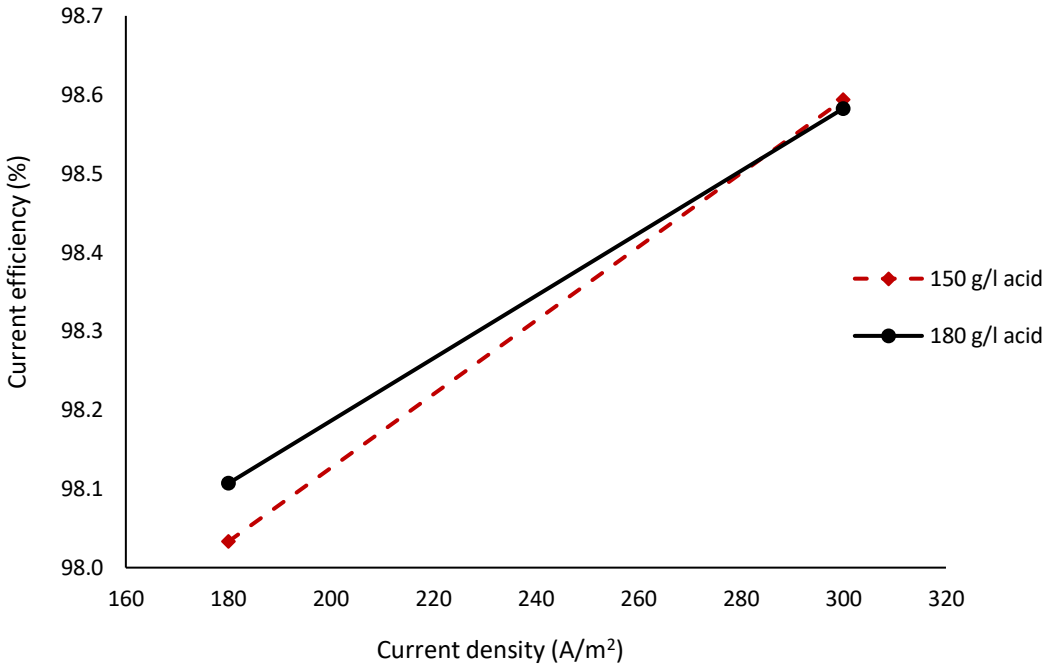

Figure 4.21: Current density/sulphuric acid concentration interaction plot.

4.2.2.3. Effect of copper and sulphuric acid concentration on current efficiency

Figure 4.22 shows the interaction effect of copper and sulphuric acid concentration on current efficiency during copper electrowinning. It can be observed from Figure 4.22 that varying sulphuric acid concentration within the range investigated also shows no significant effect on current efficiency at the low and high average copper concentration. Even though the effect is insignificant it can be seen that increasing sulphuric acid concentration slightly increases the current efficiency. Moats and Khouraibchia (2009) suggested that an increase in current efficiency with increasing sulphuric acid concentration may be attributed to the reaction presented by Equation 4.5 being controlled by the amount of dissolved oxygen. The solubility of oxygen decreases more in solutions containing high sulphuric acid concentration than low sulphuric acid concentration (Kaskiala, 2002). Thus, the decrease in oxygen solubility effectively opposes the effects on driving Equation 4.5 in the forward direction resulting in an increase in the current efficiency.

$$Cu^o + H_2SO_4 + \frac{1}{2}O_2 \rightarrow CuSO_4 + H_2O \qquad Equation\ 4.5$$

At high sulphuric acid concentration, the current efficiency decreases with an increase in the average copper concentration. This effect may be attributed to the main drawback of increasing sulphuric acid in the electrolyte which include the increase of viscosity and decrease of diffusion of ions to the cathode surface (Das and Krishna, 1996; Owais, 2009).

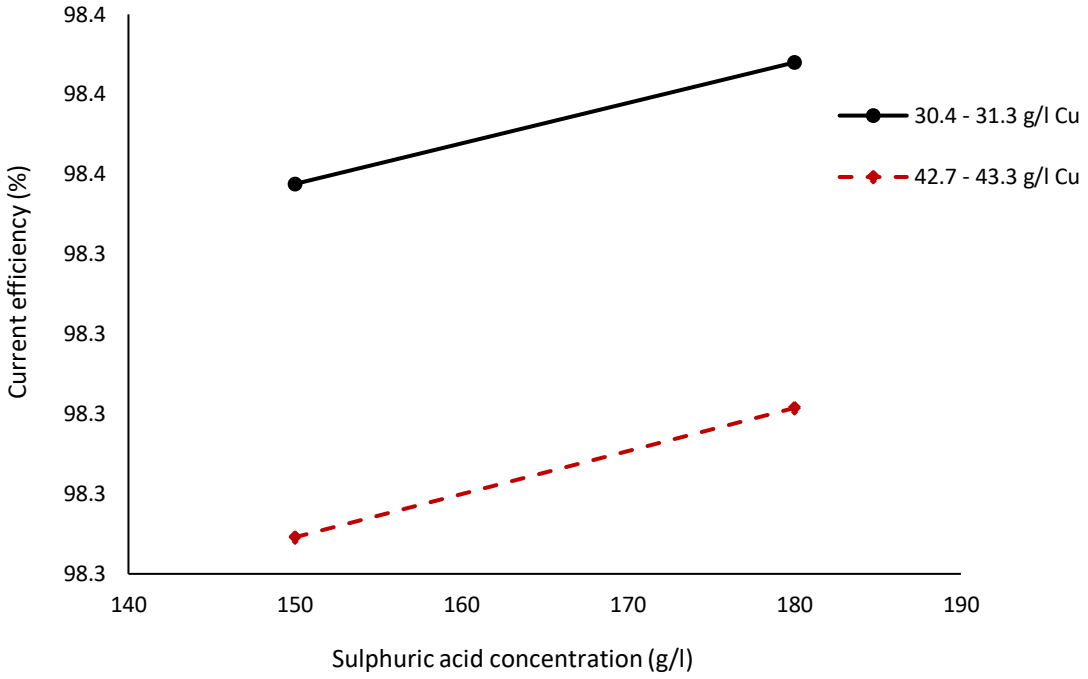

Figure 4.22: Copper/sulphuric acid concentration interaction plot.

4.2.2.4. Interaction effect of operating parameters and guar concentration on current efficiency

The interaction effect of the operating parameters with guar concentrations at various experimental conditions at temperature of 40°C is shown in Figure 4.23-4.25. These results indicated that for all the various experimental conditions the current efficiency slightly increases at a higher guar concentration (18 mg/l) than lower guar concentrations (2 mg/l and 10 mg/l). However, an opposite effect is observed in Figure 4.25 that presents the interaction effect of guar at various concentrations at higher sulphuric acid concentration. This interaction effect should be investigated further. Since the variance of current efficiency is very little as already discussed it can be concluded that under the current experimental conditions, all the various guar concentration in the electrolyte stabilize and maintain the current efficiency in the range of 98.04%-98.62%.

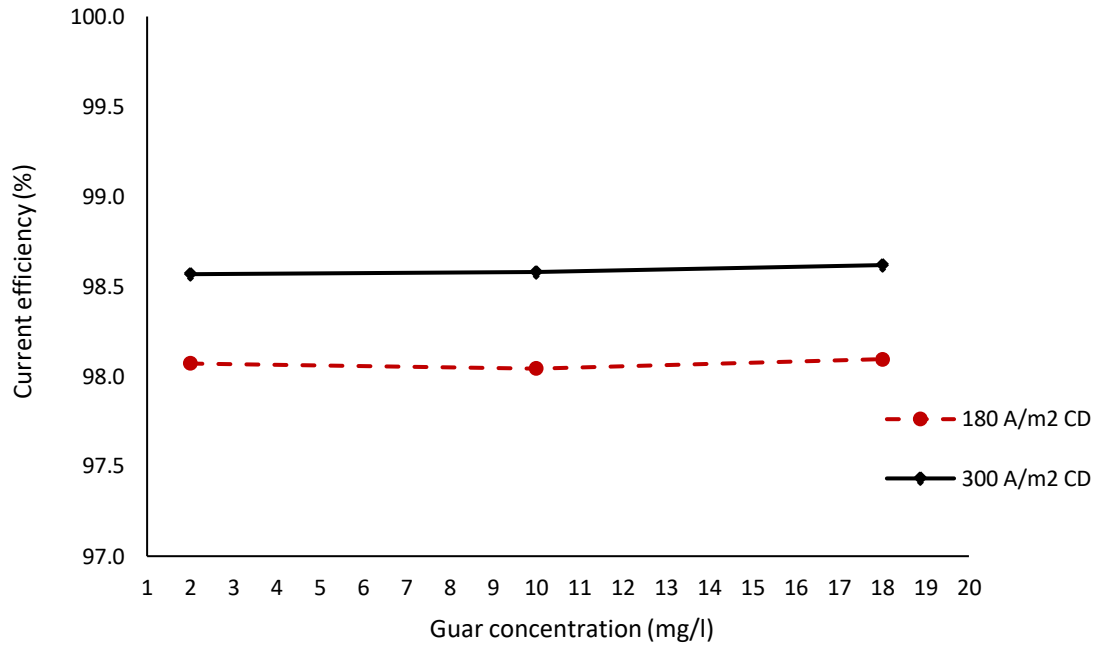

Figure 4.23: Current density/guar concentration interaction plot.

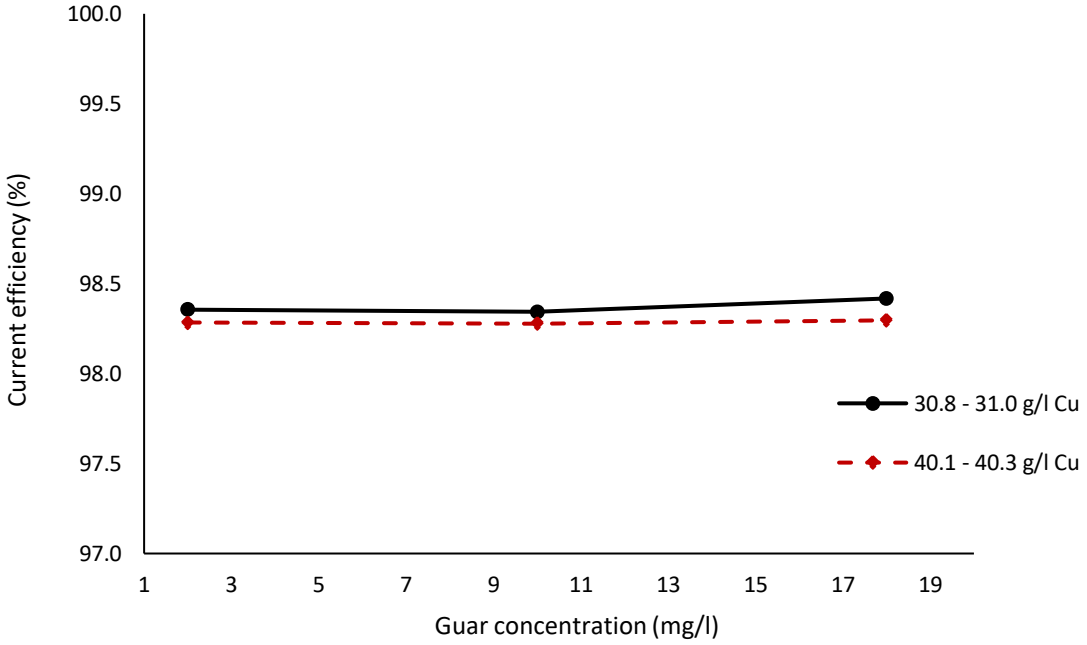

Figure 4.24: Copper/guar concentration interaction plot.

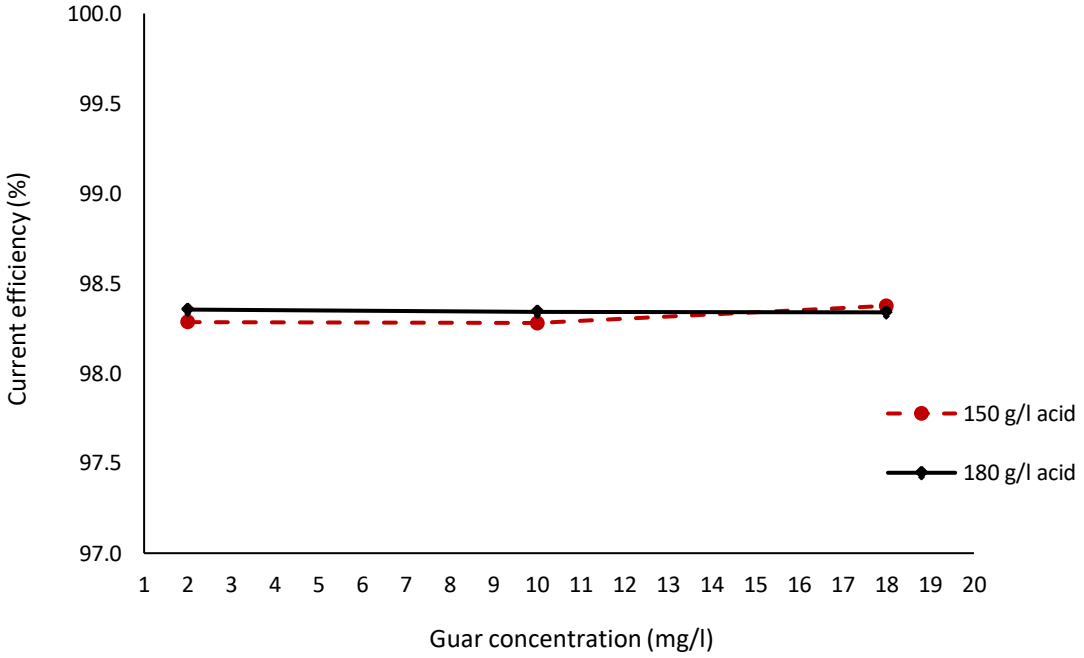

Figure 4.25: Sulphuric acid/guar concentration interaction plot.

4.3. ELECTROWINNING TESTS: COPPER DEPOSIT COMPOSITION

Identification of the composition of various impurities incorporated in the copper deposit achieved during copper electrowinning is important as impurities significantly affect the quality of copper electrodeposited. Sulphur, iron, and lead are the major impurities that are entrapped in the copper plate during copper electrowinning as already discussed in Section 2.6.2 of this report. For the current study, the copper deposits obtained after each electrowinning experiment in the presence of guar at various levels were analysed for sulphur only. Iron was not analysed since there was no iron added in the electrolyte for the current study, while lead was not analysed as negligible anode slimes are expected to be entrapped in the copper deposit over the 24-hour lab experiments compared to an industrial cell in which anodes have a service life of years. Using the ICP analysis technique, it was observed that the amount of copper in the various experiments was above the detection limit.

4.3.1. Sulphur results

The sulphur content observed in the cathode copper deposit samples after ICP analysis is presented in Figure 4.26. From the results presented in Figure 4.26 it can be seen that the amount of sulphur on each resultant copper plate achieved from the electrowinning experiments varies according to the experimental conditions. The source of sulphur content in copper deposits could be the sulphate ions from sulphuric acid or copper sulphate present in the bulk electrolyte. The adsorption mechanism of sulphur in the copper cathode is not well understood, however, according to Brown and Hope (1995) the anion adsorption in the copper cathode surface is dominated by SO_4^{2-} ions while a residual amount of HSO_4^- may interact weakly with the copper cathode surface. Previous studies also reported that the trapped impurities, such as SO_4^{2-} in copper deposited by electroplating can easily cause severe corrosion (Liu et al., 2005).

The sulphur content on the copper deposits was higher at most experimental conditions when compared to the target specified by the LME grade A specifications presented in Table 2.1. This may be associated to cathode porosity resulting in high entrainment of electrolyte (Kruyswijk, 2009). The findings from Fabian et al. (2007) provide evidence of a porous microstructure on the copper deposit in the presence of guar. Even though the entrapment of the fluid phase does not occur immediately when it collides with the solid as surface diffusion must be taken into consideration, if plating proceeds for a long time the surface roughness will increase (Fischer, 1945; Winand, 1992).

It is evident from Figure 4.26 that the level of guar concentration influences the sulphur content observed in each plate produced at various electrowinning experimental conditions. Increasing the guar concentration to 18 mg/l resulted in higher sulphur content in the copper deposits than at lower guar concentrations. This may be attributed to high sulphur in the form of sulphate ions present in the electrolyte being entrapped in the copper deposit along with guar as it is being adsorbed in the copper deposit. However, guar is partially consumed during the electrowinning process and its competitive adsorption effect also becomes weak due to the possible decomposition of molecule in the acidic environment. This implies that the use of a low-level guar causes a negligible impurity corporation in the copper cathode plate achieved during electrowinning (Lee and Chen, 2018). Furthermore, Coetzee (2018) observed a dissimilar polarization behaviour at low and high additive concentration suggesting that there are interactions between the organic additive and the copper in the system, and this interaction is enhanced at higher additive concentrations due to excessive additive. Therefore, more sulphate ion might be entrapped on the copper deposit along with guar as it interacts with copper at high guar concentrations than at low guar concentration.

According to Liu et al. (2005), the concentration of the various impurities is sensitive to the plating current density. This is evident from Figure 4.26 where it can be observed that the sulphur content on the copper deposit increases with a decrease in current density, i.e., the lower copper deposition rate. This observation is in agreement with the findings of Liu et al. (2005) where it was observed that the sulphur signals were high on electrodeposited Cu film for low current density. This phenomenon implies that the entrapment of sulphur into the copper deposits is not directly related to the electrochemical reduction at the cathode, but rather must be conducted by diffusion control. Sulphate ions adsorbed on the copper deposit may be entrapped to the cathodes along as guar adsorb effectively to the active sites of dendrite formation. The entrapment of sulphur increases with decreasing current density due to insufficient time for additive desorption (Liu et al., 2005). At high current density, the copper deposition is faster than the additive adsorption. Thus, low sulphur entrapment due to the lack of effective additive adsorption. According to Cheng et al. (2002), when the current density is low it can result in the production of porous copper electrodeposits with higher defect density, but the defects can be reduced by increasing the current density. This phenomenon again explains the reducing dependence of sulphur levels on increasing current density.

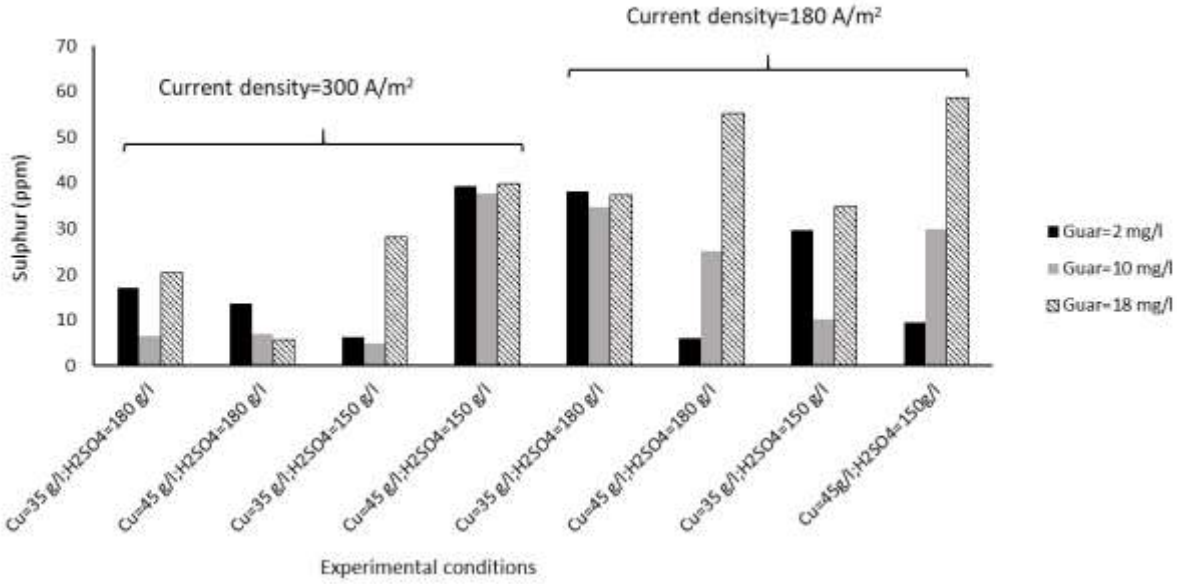

Figure 4.26: Sulphur content in the cathode copper samples.

4.3.2. Statistical analysis of operating parameters on copper deposit sulphur content

Table 4.6 shows the ANOVA analysis of the individual effects of operating parameters on sulphur content on the copper deposits produced during the 24 hours copper electrowinning experiments at various experimental conditions. It can be seen from Table 4.6 that only guar concentration had a significant influence on the sulphur content on the copper deposit.

Table 4.6: Analysis of variance (ANOVA) for the sulphur content on the copper deposits (main effects).

Parameters	Degrees of Freedom	P-value
Intercept	1	0.22
Current density (CD)	1	0.12
Sulphuric acid (SA)	1	0.40
Copper (C)	1	0.60
Guar (G)	2	0.05

When considering the interactive effects of the operating parameters on sulphur content as shown in Table 4.7 it can be seen as already discussed from the sulphur content values from Figure 4.26 that

the sulphur content in copper deposits is significantly influenced by current density (P-value=0.05), copper concentration (P-value=0.06), and sulphuric acid concentration (P-value=0.01), as well as the interactive term of SA*C (P-value=0.02) and CD*SA (P-value=0.01). Based on the probability values (P-values) obtained, it can be seen that sulphuric acid and the interaction term between CD*SA have more effect of the sulphur content on copper deposits than the other parameters. The interaction term involving sulphuric acid or copper concentration may be significant because sulphuric acid (S) and copper (C) contain sulphate ions which is a source of sulphur entrapped in copper deposits during the electrowinning process. However, the P-value for guar concentrations is more than 0.1 it is implying that guar concentration has an insignificant effect on the sulphur content entrapped in copper deposit produced during the copper electrowinning experiments.

Table 4.7: Analysis of variance (ANOVA) for the sulphur content on the copper deposits (interactive effects).

Parameters	Degrees of Freedom	P-value
Intercept	1	0.02
Current density (CD)	1	0.05
Sulphuric acid (SA)	1	0.01
Copper (C)	1	0.06
Guar (G)	2	0.59
CD*SA	1	0.01
CD*C	1	0.28
SA*C	1	0.02
CD*G	2	0.27
SA*G	2	0.46
C*G	2	0.20

5. CONCLUSIONS AND RECOMMENDATIONS

5.1. CONCLUSIONS

Uncontrolled dendrite growth on the copper cathode surface may cause short-circuits in the copper electrowinning cells. The purpose of the current study was to gain more understanding on the performance of guar at varying concentrations with other parameters to control localized growth (dendrites) in copper electrowinning and quantify relevant effects. This was achieved by addressing three objectives: the first objective to conduct bench-scale electrowinning experiments to investigate the interactive effects of guar with other operating parameters and their effect on the key performance indicators (copper cathode quality and current efficiency), the second objective to determine the quality of copper cathodes in terms of surface morphology by using 3D surface scanner, and the third objective to conduct acid digestion tests to investigate the quality of cathodes in terms of chemical composition to infer the grade of copper deposits produced at the various experimental conditions.

The conclusions made from the aforementioned tests are summarized in the following sections:

5.1.1. Deposit surface roughness

The 3D surface scanning tests on the copper cathodes produced during the bench-scale electrowinning experiments revealed both qualitative and quantitative analysis results which are necessary to draw accurate conclusions on the best experimental conditions in which guar can eliminate localized growth. According to the qualitative and quantitative analysis results presented in the results and discussion section; the following conclusions can be made:

The copper deposit that was achieved in the absence of guar in the electrolyte was rough and had dendrites. The addition of guar in the electrolyte generally improved the copper cathode deposits in terms of reducing localized growth or dendrite-like nodular growth compared to the copper deposits produced from the absence of guar in the electrolyte.

The S_a (mean surface height) values obtained in the presence of guar showed that the individual effects of initial copper concentration, current density, and sulphuric acid concentration on the surface roughness of copper cathode deposit is dependent on the various experimental conditions.

At high current density, the copper deposit achieved at high initial copper concentration (45 g/l), high sulphuric acid concentration (180 g/l) and high guar concentration (18 mg/l) had the lowest calculated S_a value of 30.95 µm and this experimental condition delivered the smoothest and arguably the brightest copper deposit with almost an absence of localized growth.

It was shown from the statistical analysis of the copper deposits that current density was the most influential parameter affecting the surface roughness of the copper deposit while guar concentration had a statistically insignificant effect on the surface roughness of copper deposits.

The interactive plots show that at a higher current density (300 A/m^2) the copper deposits delivered a rougher surface with the colour scale image analysis of the surface topography evidently revealing more positive deviations compared to copper deposits achieved at lower current density (180 A/m^2). The rough copper deposits were due to higher nucleation rates on the cathode surface promoting smaller crystals which lead to the formation of dendrites when higher growth rate of crystal grain normal to the electrode surface is favoured. At high current density, the rough copper deposits also

develop due to faster depletion of copper ions in the electrolyte leading to insufficient copper to the cathode surface during the electrodeposition process.

At higher current densities, increasing the initial copper concentration in the electrolyte reduced the surface roughness of copper deposits. Increasing copper concentration allows for sufficient supply of copper ions to the electrode.

At low and high current densities, increasing sulphuric acid concentration was found to insignificantly increase the surface roughness of copper deposits. The insignificant increase in surface roughness was mostly likely due to faster degradation of guar at higher sulphuric acid than at low sulphuric acid concentrations.

The interaction plot between copper concentration and sulphuric acid concentration suggests that at a high copper concentration, the surface roughness decreases with an increase in sulphuric acid concentration. The aforementioned trend was attributed to sufficient supply of copper ions to the cathode surface. It was also observed that lowering copper concentration resulted in an increase in the surface roughness, likely due to more hydrogen ions adsorbing to the cathode surface.

It was shown from the interaction plots between guar with copper concentration, current density as well as sulphuric acid concentration that the performance of guar to eliminate localized growth was more effective at high guar concentrations (10 mg/l or 18 mg/l) than at low guar concentration (2 mg/l) as expected.

5.1.2. Current efficiency

The current efficiencies of each electrowinning experiment in the presence of guar for various experimental conditions were calculated based on the mass of copper deposited in each run respectively and compared. The following conclusions can be made from these comparisons:

The CE values calculated for each electrowinning experiment conducted at varying experimental conditions in the presence of guar did not change with more than 1%. This indicates that the various operating conditions had little to no effect on the current efficiency in the presence of guar. Even though the CE variation was low between the electrowinning experiments, it was observed that the current efficiency slightly increases at high current density compared to low current density. This trend was attributed to an increase in the amount of current applied to the cell at high current density. This allows more electron transfer from the anode to the cathode allowing more ions to be reduced and oxidised increasing the rate of electrodeposition than at low current density.

From the statistical analysis of CE values, it was observed that current density had a significant effect on the current efficiency. However, all the other individual and interactive terms had an insignificant effect on the current efficiency.

Comparing the current efficiency values and the cathode morphology it was observed that it is possible to have a poor copper cathode morphology while the corresponding CE value calculated is high. Both the current efficiency and cathode quality must be considered during the copper electrowinning process.

5.1.3. Deposit composition

The third objective was to conduct acid digestion tests to determine the chemical composition of copper cathodes for the various experimental conditions. After acid digestions, the solutions of the copper cathodes were analysed for the composition of sulphur through ICP analysis. The following conclusions were drawn from the ICP analysis results:

The ICP analysis results obtained in this study indicated the presence of sulphur in each of the copper deposits produced during the copper electrowinning experiments at various experimental conditions. Sulphate ions from sulphuric acid or copper sulphate present in the bulk electrolyte may be the source of sulphur adsorbed or entrapped in the copper deposits.

Copper deposits achieved at most experimental conditions had a higher sulphur content compared to the target specified by the LME grade A specifications. This may be attributed to cathode porosity resulting in high entrainment of electrolyte.

Sulphur content in copper deposits increased at higher guar concentration (18 mg/l) than copper deposits achieved at lower guar concentrations. More sulphate ions were likely entrapped on the copper deposit along with excess guar as it interacts with copper as observed at high guar concentrations. The minimal contamination of sulphur at low concentrations when compared to high guar concentrations was also attributed to the possible decomposition of guar in acidic environments. This phenomenon should be investigated further.

The sulphur content on the copper deposit increased at lower current densities than at higher current densities. This was attributed to insufficient time for guar adsorption at low current density due to copper deposition being faster than guar adsorption at high current densities resulting in ineffective guar adsorption.

Statistical analysis of the sulphur content on each copper plate produced during the copper electrowinning experiments showed that current density, copper concentration, sulphuric acid concentration, and guar concentration significantly influenced the sulphur content in the copper deposits produced.

The interactive terms of CD*SA and SA*C from the statistical analysis also significantly affected the sulphur content in copper deposits.

5.2. RECOMMENDATIONS

A pure electrolyte without impurities was used in the current study to determine the performance of guar to produce a smooth, dense, and bright copper deposit. However, since the industrial electrolyte contain several impurities, it is recommended that future investigations must determine the effect of these impurities on current efficiency and cathode quality in the presence of guar.

The effect of guar on the copper deposit at various operating conditions can be investigated further by increasing guar concentration to determine the optimal range of guar dosage in copper electrowinning. Consequently, generating an electrowinning model for predicting the surface roughness on the copper deposit at optimal guar dosage in copper electrowinning.

Further recommendation in this research is to investigate the effect of the interaction of guar dosage with other operating parameters on the energy consumption during the copper electrowinning

experiments. Reporting the operating voltages for each experiment could also aid in determining the extent in which H^+ is reduced during the electrodeposition process compared to Cu^{2+} plating.

The growth type of copper deposits could not be classified by direct external observations from the visual analysis; thus, cross-section metallographic analysis of copper deposits could be done to determine the growth type of copper deposits as classified by the Winand's diagram at various electrowinning operating conditions in the presence of guar.

The surface roughness of copper deposits produced during electrowinning experiments were compared based on an assumption that the plating roughness is not dependent on the total plating duration (or deposit thickness) at the conditions investigated. Therefore, it is recommended that future investigations must conduct electrowinning experiments running at low current density experiments for a longer period or the high current density experiments for a shorter period.

It will also be worthwhile investigate the potential effects of forced convection past the plate in the current EW cell setup compared to the natural convection that occurs in the industrial electrowinning cells. The current electrowinning experiments assumed that the upward flow of the bulk electrolyte is not significant, however, its investigation might provide insight for mass transfer effects for both copper reduction and water oxidation.

6. REFERENCES

Abbey, C.E. 2019. Improving base metal electrowinning. *Published doctoral dissertation. Missouri University of Science and Technology*. .

Adamczak, S. & Zmarzły, P. 2019. Research of the influence of the 2D and 3D surface roughness parameters of bearing raceways on the vibration level. *Journal of Physics: Conference Series*. 1183(1).

Adcock, P.A., Quillinan, A., Clark, B., Newman, O.M.G. & Adeloju, S.B. 2004. Measurement of polarization parameters impacting on electrodeposit morphology. II: Conventional zinc electrowinning solutions. *Journal of Applied Electrochemistry*. 34(8):771–780.

Akbarzadeh, E. & Shakib, S.E. 2011. Comparison of effective parameters for copper powder production via electrorefining and electrowinning cells and improvement using DOE methods. *International Journal of Minerals, Metallurgy and Materials*. 18(6):731–740.

Alfantazi, A.M. & Valic, D. 2003. A study of copper electrowinning parameters using a statistically designed methodology. *Journal of Applied Electrochemistry*. 33(2):217–225.

Andersen, T.N., Pitt, C.H. & Livingston, L.S. 1983. Nodulation of electrodeposited copper due to suspended particulate. *Journal of Applied Electrochemistry*. 13(4):429–438.

Aqueveque, P.E., Wiechmann, E.P., Herrera, J. & Pino, E.J. 2015. Measurable variables in copper electrowinning and their relevance to predicting process performance. *IEEE Transactions on Industry Applications*. 51(3):2607–2614.

Aragón, J and Camus, J. 2011. Efecto de la concentracion de ion cloruro en la estructura de electrodepositos de cobre. *Revista Latinoamericana de Metalurgia y Materiales,*. 32(2):128-133.

Bard, A.J. & Faulkner, L.R. 2001. *Electrochemical methods: Fundamentals and Applications*. United States of America: John Wiley & Sons, Inc. 1-833.

Barton, J. L. & Bockris, J. O. 1962. The electrolytic growth of dendrites from ionic solutions. *Proc. R. Soc. Lond*. 485–505.

Beukes, N & Badenhorst, J. 2009. Copper electrowinning- theoretical and practical design. *Journal of the Southern African Institute of Mining and Metallurgy*. 213–240.

Bockris, J.O., Razumney, G.A., Bockris, J.O. & Razumney, G.A. 1967. Deposition and Dissolution Kinetics as a Function of the Initial Substrate. *Fundamental Aspects of electrocrystallization*. 57–66.

Brown, G.M. & Hope, G.A. 1995. SERS study of the adsorption of gelatin at a copper electrode in sulfuric acid solution. *Journal of Electroanalytical Chemistry*. 397(1–2):293–300.

Budevski, E., Staikov, G. & Lorenz, W.J. 1996. *Electrochemical phase formation and growth: An introduction to the initial stages of metal deposition*. John Wiley & Sons, Inc.

Budevski, E., Staikov, G. & Lorenz, W.J. 2000. Electrocrystallization Nucleation and growth phenomena. *Electrochimica Acta*. 45(15–16):2559–2574.

Castro, L.A. & Martins, A.H. 2009. Recovery of tin and copper by recycling of printed circuit boards from obsolete computers. *Brazilian Journal of Chemical Engineering*. 26(4):649–657.

Chang, J. 2009. Modeling of an electrochemical cell. University of Toronto. [Online], Available:

https://tspace.library.utoronto.ca/bitstream/1807/18247/6/ Chang_JinHyun _200911_MASc_Thesis.pdf [Accessed October 2020].

Chang, S.C., Shieh, J.M., Dai, B.T., Feng, M.S. & Li, Y.H. 2002. The Effect of Plating Current Densities on Self-Annealing Behaviors of Electroplated Copper Films. *Journal of The Electrochemical Society*. 149(9):G535.

Cifuentes, R., Bravo, R. & Schwarz, N. 2015. Effective Grain Modification in Copper Electrowinning with DXG-F7. Copper *Cobalt Africa, incorporating the 8th Southern African Base Metals Conference*. 389–396.

Coetzee, C., Tadie, M. & Dorfling, C. 2018. Characterizing the Role of Organic Additives in Copper Electrowinning. *Published Masters Thesis, Stellenbosch University*.

Collins, D.W. 2001. Additive monitoring and intereactions during copper electroprocessing. *4th International Conference COPPER 99-COBRE 99*. 461–477.

Cruz, D.P. 2019. A Method For Iron Determination During Copper Electrometallurgy And Its Application To The Calculation Of Current Efficiency. *Masters Thesis, The University of Texas*.

Cui, W. 2014. Effect and Interactions of Commercial Additives and Chloride Ion in Copper Electrowinning. *Masters Thesis, Missouri University of Science and Technology*.

Das, S.C. & Krishna, P.G. 1996. Effect of Fe(III) during copper electrowinning at higher current density. *International Journal of Mineral Processing*. 46(1–2):91–105.

Davenport, W.G., King, M., Schleisinger, M., Biswas, A.K. 2002. *Extractive metallurgy of copper: Fourth Edition*. Oxford: Pargamon. 399 Pages.

Dehghanpoor, M.H., Zivdar, M. & Torabi, M. 2016. Extraction of copper and gold from anode slime of Sarcheshmeh Copper Complex. *Journal of the Southern African Institute of Mining and Metallurgy*. 116(12):1153–1157.

Devos, O., Gabrielli, C., Beitone, L., Mace, C., Ostermann, E. & Perrot, H. 2007. Growth of electrolytic copper dendrites. III: Influence of the presence of copper sulphate. *Journal of Electroanalytical Chemistry*. 606(2):95–102.

Dini, J.W., Snyder, D.. 2011. Electrodeposition of copper. in *Modern Electroplatting: Fifth Edition.* M. Schlesinger, M., Paunovic (ed.). John Wiley & Sons, Inc. 33–78.

Doran, M.P. 2013. *Bioprocess Engineering Principles: Second Edition*.

Durai, L., Dhanasekaran, R., Ramasamy, P. 1987. Nucleation and Growth Kinetics of Electrocrystallization. *Academic Press, Inc.* 115(2).

Ehsani, A., Yazıcı, E.Y. & Deveci, H. 2016. The Effect of Temperature on the Electrowinning Of Copper. *8th International Metallurgy & Materials Congres*. 114(2968):521–523.

Fabian, C. 2005. Copper electrodeposition in the presence of guar or activated polyacrylamide. *Published doctoral dissertation. Queensland: James Cook University*. 1–75.

Fabian, C.P. 2003. Copper electrodeposition in the presence of guar.

Fabian, C.P., Ridd, M.J. & Sheehan, M.E. 2007. Assessment of activated polyacrylamide and guar as organic additives in copper electrodeposition. *Hydrometallurgy*. 86(1–2):44–55.

Fabian, C.P., Ridd, M.J., Sheehan, M.E. & Mandin, P. 2009. Modeling the Charge-Transfer Resistance to Determine the Role of Guar and Activated Polyacrylamide in Copper Electrodeposition. *Journal of The Electrochemical Society*. 156(10):D400.

Filzwieser, I. 2005. The analysis and mathematical modelling of the parameters influencing cathodic deposits in copper refining electrolysis.

Fischer, H. 1969. Electrocrystallization of Metals under Ideal and Real Conditions. *Journal of Chemical Information and Modeling*. 8(2).

Gabrielli, C., Moçotéguy, P., Perrot, H., Nieto-Sanz, D. & Zdunek, A. 2006. A model for copper deposition in the damascene process. *Electrochimica Acta*. 51(8–9):1462–1472.

Gadelmawla, E.S., Koura, M.M., Maksoud, T.M.A., Elewa, I.M. & Soliman, H.H. 2002. Roughness parameters. *Journal of Materials Processing Technology*. 123(1):133–145.

Gebbie, J. 2013. A theoretical study of crystal growth in nanoporous materials using the monte carlo method.

Güven, D.E. & Akinci, G. 2011. Comparison of acid digestion techniques to determine heavy metals in sediment and soil samples. *Gazi University Journal of Science*. 24(1):29–34.

Hasan, A.M.A. & Abdel-Raouf, M.E. 2018. Applications of guar gum and its derivatives in petroleum industry: A review. *Egyptian Journal of Petroleum*. 27(4):1043–1050.

Havlik, T., Orac, D., Petranikova, M., Miskufova, A., Kukurugya, F. & Takacova, Z. 2010. Leaching of copper and tin from used printed circuit boards after thermal treatment. *Journal of Hazardous Materials*. 183(1–3):866–873.

Hayes, P. 2003. Process Principles in Minerals and Materials Production. *Hayes Publishing*. 227–250.

Hibbert, D.. 1993. Introduction to electrochemistry. *Macmillan Physical Science Series*.

Hiskey, J.. 1999. “Principles and practical considerations of copper electrorefining and electrowinning” Copper Leaching, Solvent Extraction, and Electrowinning Technology. *Society for Mining, Metallurgy & Exploration Inc.* 169–186.

Hjerde, T., Kristiansen, T.S., Stokke, B.T., Smidsrod, O. & Christensen, B.E. 1994. Conformation dependent depolymerisation kinetics of polysaccharides studied by viscosity measurements. *Carbohydrate Polymers*. 24(4):265–275.

Hope, G.A. & Woods, R. 2004. Transient Adsorption of Sulfate Ions during Copper Electrodeposition. *Journal of The Electrochemical Society*. 151(9):C550.

Jacobs, J.C. & Groot, D.R. 2019. Improving cathode morphology at a copper electrowinning plant by optimizing Magnafloc 333 and chloride concentrations. *Journal of the Southern African Institute of Mining and Metallurgy*. 119(11):983–987.

Jansons, E., Lungevics, J. & Gross, K.A. 2016. Surface roughness measure that best correlates to ease of sliding. *Engineering for Rural Development*. 2016-Janua:687–695.

Kaskiala, T. 2002. Determination of oxygen solubility in aqueous sulphuric acid media. *Minerals Engineering*. 15(11):853–857.

Kersten, T.P., Przybilla, H.J., Lindstaedt, M., Tschirschwitz, F. & Misgaiski-Hass, M. 2016. Comparative geometrical investigations of hand-held scanning systems. *International Archives of the Photogrammetry, Remote Sensing and Spatial Information Sciences - ISPRS Archives*. 41:507–514.

Kruyswijk, L. 2009. Electrowinning of base metal refinery residue copper alloy for platinum group metal recovery. *Masters Thesis, Univeristy of Cape Town*. 221 pages.

Lancashire, H.T. 2017. A simulated comparison between profile and areal surface parameters: R_a as

an estimate of S_a . 1–9. [Online], Available: http://arxiv.org/abs/1708.02284. [Accessed July 2021].

Leahy, M.J. & Schwarz, M.P. 2010. Experimental validation of a computational fluid dynamics model of copper electrowinning. *Metallurgical and Materials Transactions B: Process Metallurgy and Materials Processing Science*. 41(6):1247–1260.

Lee, H. & Chen, C.M. 2018. Impurity effects in electroplated-copper solder joints. *Metals*. 8(6):4–6.

Liow, J.L., Frazer, A., He, Y., Eastwood, K. & Phan, E. 1992. Acid mist formation in the electrowinning of copper Abstract. *James Cook University Townsville 4811, Australia*. 1370–1380.

Liu, C.W., Wang, Y.L., Tsai, M.S., Feng, H.P., Chang, S.C. & Hwang, G.J. 2005. Effect of plating current density and annealing on impurities in electroplated Cu film. *Journal of Vacuum Science & Technology A: Vacuum, Surfaces, and Films*. 23(4):658–662.

llgar, E. & O'Keefe, T. 1997. Surface roughening of electrowon copper in the presence of chloride ions. *The Metals and Materials Society*. 51–62.

Lupo, C., Boulos, S. & Nyström, L. 2020. Influence of partial acid hydrolysis on size, dispersity, monosaccharide composition, and conformation of linearly-branched water-soluble polysaccharides. *Molecules*. 25(13).

Makipaa, E., Tanttu, J.T. & Virtanen, H. 1999. IR-based system for short-circuit detection during copper electrorefining process. *Machine Vision Applications in Industrial Inspection VII*. 2–9.

Mecucci, A. & Scott, K. 2002. Leaching and electrochemical recovery of copper, lead and tin from scrap printed circuit boards. *Journal of Chemical Technology and Biotechnology*. 77(4):449–457.

Mirza, A., Burr, M., Ellis, T., Evans, D., Kakengela, D., Webb, L., Gagnon, J., Leclercq, F., et al. 2016. Corrosion of lead anodes in base metals electrowinning. *Journal of the Southern African Institute of Mining and Metallurgy*. 116(6):533–538.

Moats, M. & Free, M. 2007. A bright future for copper electrowinning. *Jom*. 59(10):34–36.

Moats, M. & Khouraibchia, Y. 2009. Effective diffusivity of ferric ions and current efficiency in stagnant synthetic copper electrowinning solutions. *Minerals and Metallurgical Processing*. 26(4):179–186.

Moats, M.S. & Derrick, A. 2012. Investigation of nucleation and plating overpotentials during copper electrowinning using the galvanostatic staircase method. *Electrometallurgy*. 125–137.

Moats, M.S., Luyima, A. & Cui, W. 2016. Examination of copper electrowinning smoothing agents. Part I: A review. *Minerals and Metallurgical Processing*. 33(1):7–13.

Moongo, T.E. & Michael, S. 2021. A continuous quality improvement framework for electrowinning current efficiency. *Journal of the Southern African Institute of Mining and Metallurgy*. 121(1):21–28.

Msindo, Z.S. 2010. An Investigation of the Electrowinning of Copper With Dimensionally Stable Titanium Anodes and Conventional Lead Alloys Anodes. *Published Masters Thesis. University of the Witwatersrand.*

Mudgil, D., Barak, S. & Khatkar, B.S. 2014. Guar gum: Processing, properties and food applications - A Review. *Journal of Food Science and Technology*. 51(3):409–418.

Murray, A., Khakbaz, H., Pranowo, A., Aslin, N. & Kannan, M.B. 2016. Effects of process parameters on the adhesive strength of copper electrodeposits in a benchscale electrowinning cell.

Transactions of the Institutions of Mining and Metallurgy, Section C: Mineral Processing and Extractive Metallurgy. 125(1):10–16.

Najminoori, M., Mohebbi, A., Arabi, B.G. & Daneshpajouh, S. 2015. CFD simulation of an industrial copper electrowinning cell. *Hydrometallurgy*. 153:88–97.

Newman, J., Thomas-Alyea, E. 2004. Elecrochemical systems. *John Wiley & Sons, Inc.*

Ngandu, F. 2016. Investigating the Effects of Selenium and Thiourea Concentration on Copper Electrowinning . *Masters Thesis, Stellenbosch University*.

Nikoloski, A.N. & Nicol, M.J. 2008. *Effect of cobalt ions on the performance of lead anodes used for the electrowinning of copper - A literature review*. Vol. 29.

O'Keefe, T. 1984. Techniques for evaluating electrolytes for metal recovery. *Electroanal.Chem*. 131–146.

Oniciu, L. & Muresan, L. 1991. Some fundamental aspects of levelling and brightening in metal electrodeposition. *Journal of Applied Electrochemistry*. 21(7):565–574.

Owais, A. 2009. Effect of electrolyte characteristics on electrowinning of copper powder. *Journal of Applied Electrochemistry*. 39(9):1587–1595.

Panda, B. & Das, S.C. 2001. Electrowinning of copper from sulfate electrolyte in presence of sulfurous acid. *Hydrometallurgy*. 59(1):55–67.

Pasa, M.L. & Munford, A. 2006. Electrodeposition. *Encyclopedia of Chemical Processing, Taylor & Francis*. 821–832.

Pfalzgraff, C. 2009. Do's and Don'ts of Tankhouse Design and Operation. *Society for Mining, Metallurgy and Exploration*. 217–221.

Plessis, A. du, Sperling, P., Beerlink, A., Kruger, O., Tshabalala, L., Hoosain, S. & le Roux, S.G. 2018. Standard method for microCT-based additive manufacturing quality control 3: Surface roughness. *MethodsX*. 1111–1116.

Popov, K.I., Maksimović, M.D., Trnjančev, J.D. & Pavlović, M.G. 1981. Dendritic electrocrystallization and the mechanism of powder formation in the potentiostatic electrodeposition of metals. *Journal of Applied Electrochemistry*. 11(2):239–246.

Popov, K.I., Živković, P.M. & Nikolić, N.D. 2011. A mathematical model of the current density distribution in electrochemical cells. *Journal of the Serbian Chemical Society*. 76(6):805–822.

Pradhan, N., Krishna, P.G. & Das, S.C. 1996. Influence of chloride ion on electrocrystallization of copper. *Plating and Surface Finishing*. 83(3):56–63.

Ramanathan, T. & Ting, Y.P. 2015. Selection of wet digestion methods for metal quantification in hazardous solid wastes. *Journal of Environmental Chemical Engineering*. 3(3):1459–1467.

Rashidi, A.M. & Amadeh, A. 2008. The effect of current density on the grain size of electrodeposited nanocrystalline nickel coatings. *Surface and Coatings Technology*. 202(16):3772–3776.

Robinson, T.G., Sole, K.C., Sandoval, S., Moats, M., Siegmund, A. & Davenport, W.E. 2013. Copper electrowinning – 2013 world operating tankhouse data. *Copper-Cobre 2013 Conference*. 3–14.

Rossouw, W.A. 2015. Effect of pre-treatment on leaching of base metals from waste printed circuit boards. *Masters Thesis, Stellenbsch University. 144 pages*.

Schlesinger, M.E., King, M.J., Sole, K.C. & Davenport, W.G. 2011. *Extractive Metallurgy of Copper:*

Fifth Edition. Oxford: Elsevier.

Shakarji, R. Al, He, Y. & Gregory, S. 2011. Statistical analysis of the effect of operating parameters on acid mist generation in copper electrowinning. *Hydrometallurgy*. 106(1–2):113–118.

Shao, W., Pattanaik, G. & Zangari, G. 2007. Influence of Chloride Anions on the Mechanism of Copper Electrodeposition from Acidic Sulfate Electrolytes. *Journal of The Electrochemical Society*. 154(4):D201.

Sharma, P. & Gummagolmath, K.C. 2014. Reforming Guar Industry in India : Issues and Strategies Reforming Guar Industry in India.

Sharma, G., Sharma, S., Kumar, A., Al-Muhtaseb, A.H., Naushad, M., Ghfar, A.A., Mola, G.T. & Stadler, F.J. 2018. Guar gum and its composites as potential materials for diverse applications: A review. *Carbohydrate Polymers*. 199:534–545.

Shreir, B.Y.L.L. & Smith, J.W. 1953. Effects of addition agents on the cathode polarization potential during the electro-deposition of copper. *Metallurgy Dept., Battersea Polytechnic, London, S. W. 11*. 393–403.

Shukla, A. 2013. Modeling and measuring electrodeposition parameters near electrode surfaces to facilitate cell performance optimization. *Masters Thesis, University of Utah*. (434):1–32.

Sigley, J.L., Johnson, P.C., Beaudoin, S.P. 2003. Use of nonionic surfactant to reduce sulfuric acid mist in the copper electrowinning process. *Hydrometallurgy*. 70(1–3):1–8.

Stankte, P. 1999. Guar concentration measurement with the CollaMat system. in *Copper 99-Cobre 99*. 643–651.

Sui, X., Huang, Y., Han, T. & Zeng, X. 2017. Analysis on the influential factors of Cu^{2+} electro-deposition. *AIP Conference Proceedings*.

Sun, M. & O'Keefe, T. 1992. The effect of additives on the nucleation and growth of copper onto stainless steel cathodes. *Metallurgical Transactions B*. 23(5):591–599.

Thammana, M. 2016. A review on high performance liquid chromatography. *International Journal of Pharmaceutical Research*. 5(2):1–6.

Tucker, M., Tadie, M. & Dorfling, C. 2019. The Development of an Electrowinning Model to Predict Process Performance. *Masters Thesis, Stellenbosch University*. 166 pages.

Tuncuk, A., Stazi, V., Akcil, A., Yazici, E.Y. & Deveci, H. 2012. Aqueous metal recovery techniques from e-scrap: Hydrometallurgy in recycling. *Minerals Engineering*. 25(1):28–37.

Wang. Q, Ellis. P.R, Ross-Murphey. S.B. 2000. The stability of guar gum in an aqueous system under acidic conditions. *Medicina Clinica*. (14):129–134.

Wang, Y., Li, B., Xu, H. & Guo, J. 2021. Effect of Cd^{2+} on Electrodeposition of Copper in Cyclone Electrodeposition. *Metals*.

Werner, J.M. 2017. Modeling and Validation for Optimization of Electrowinning Performance. *Published doctoral dissertation. The University of Utah*.

Wiechmann, E.P., Vidal, G.A. & Pagliero, A.J. 2006. Current-source connection of electrolytic cell electrodes: An improvement for electrowinning and electrorefinery. *IEEE Transactions on Industry Applications*. 42(3):851–855.

Wiechmann, E.P., Morales, A.S. & Aqueveque, P. 2010. Improving productivity and energy efficiency

in copper electrowinning plants. *IEEE Transactions on Industry Applications*. 46(4):1264–1270.

Winand, R. 1992. Electrocrystallization- theory and applications. *Hydrometallurgy.* 29:567–598.

Winand, R. 1994. Electrodeposition of metals and alloys-new results and perspectives. *Electrochimica Acta*. 39(8–9):1091–1105.

Wranglén, G. 1960. Dendrites and growth layers in the electrocrystallization of metals. *Electrochimica Acta*. 2(1–3):130–143.

Wu, Y., Ding, W. & He, Q. 2017. Molecular characteristics of tara galactomannans: Effect of degradation with hydrogen peroxide. *International Journal of Food Properties*. 20(12):3014–3022.

7. APPENDICES

7.1. APPENDIX A – SAMPLE CALCULATIONS

Guar concentration

The calculations of guar concentration added into the electrolyte is based on a 2 mg/l, 10 mg/l and 18 mg/l final concentrations. A total of 400 mg guar is weighed and then added to 200 ml of de-ionized water (concentration of guar solution is 2 g/l) as shown by the calculation below:

$$Concentration\ of\ guar\ in\ prepared\ solution = \frac{400\ mg\ guar}{200\ ml\ de-ionized\ water}$$
$$= 2\ g/l$$

From the prepared guar stock solution, a final concentration of 2 mg/l is added into the electrolyte. A total of 15 ml was removed using a pipette from the guar prepared solution corresponding to 2 mg/l, and this sample contains 30 mg of gaur assuming a perfect distribution of organic additive in the prepared solution:

$$Amount\ of\ guar\ in\ 15ml\ sample\ solution = \frac{400\ mg}{200\ ml} \times 15\ ml$$
$$= 30\ \ mg$$

The concentration of guar in the electrolyte sample therefore translate to:

$$Guar\ concentration\ in\ electrolyte = \frac{0.030\ g\ guar}{15\ L\ electrolyte}$$
$$= 0.002\ g/l$$
$$= 2\ mg/l$$

Similar calculations were done for 10 mg/l and 18 mg/l final concentrations of guar whereby 75 ml and 135 ml of guar sample were removed from the prepared stock solution, respectively.

Electrolyte concentration

A design of experiments was used to determine the operating conditions for the electrowinning experiments hence the calculations of the amount of chemicals required in the electrolyte is based on a synthetic electrolyte which has low- and high-levels: 150 g/l and 180 g/l sulphuric acid, 35 g/l and 45 g/l initial copper concentration, and a chloride held constant at a concentration of 25 mg/l. The electrolyte was prepared in 4 L and 1 L volume bottles. De-ionized water was used to fill up the

electrolyte sample in either a 4 L or 1 L volume bottle. Table 7.1 presents the chemical densities at 25°C, and molecular weights sourced from literature.

Table 7.1: Relevant chemical densities at 25°C and their respective molecular weights.

Chemical element/molecule	Molecular weight (g/mol)	Density (kg/m³)
Cu	63.55	8960
$CuSO_4.5H_2O$	249.69	2286
H_2SO_4	98.08	1840
H_2O	18.02	1000
HCl	36.46	1490

To have a final concentration of 45 g/l of copper in a 1 L solution, 45 g of copper will be required. The total amount of copper sulphate pentahydrate needed was calculated to be 178.13 g to add 45 g of copper to the 1 L solution based on the following calculations:

$$n_{Cu} = \frac{m_{Cu}}{M_{Cu}}$$
$$= \frac{45}{63.546}$$
$$= 0.708\ mole$$

Based on the stoichiometric proportions of $CuSO_4.5H_2O$: 1 mole Cu = 1 mole SO_4 = 5 moles H_2O

Therefore: 0.70815 mole Cu = 0.708 mole SO_4 = 3.541 moles H_2O in $CuSO_4.5H_2O$

Moles translated into mass: 45 g Cu + 69.40 g SO_4 + 63.73 g H_2O = 178.13 g of $CuSO_4.5H_2O$ required.

The amount of sulphuric acid required in a 1 L electrolyte solution was calculated as follows:

$$Volume\ H_2SO_4\ required = \frac{Mass}{Density}$$
$$= \frac{150\ g}{1840\ kg/m^3}$$
$$= \frac{0.150\ kg}{1840\ kg/m^3}$$
$$= 0.0815\ L$$
$$= 81.52\ ml$$

To determine the amount of chloride, similar calculations to sulphuric acid were done. Table 7.2. shows all the required amounts of the chemicals for 4 L and 1 L volumes determined using similar calculations as above.

Table 7.2: Amount chemicals required to determine the operating concentration in electrowinning experiments.

Chemical	Concentration	Amount of chemical required in 4 L bottle	Amount of chemical required in 1 L bottle
Cu	35 g/l	554.19 g	138.55 g
	45 g/l	712.53 g	178.13 g
H_2SO_4	150 g/l	326.09 ml	81.52 ml
	180 g/l	391.30 ml	97.83 ml
Cl	25 mg/l	0.069 ml	0.017 ml

Faraday's law

As already discussed in Section 2.2.4, current density is the current applied in the electrochemical system per electrode surface area perpendicular to the flow of current (Newman and Thomas-Alyea, 2004). Hence, the electric current (I) applied in the system can be calculated from the current density (i) and surface area of the cathode (A) as shown in Equation 7.1.

$$I = \frac{i}{A} \qquad Equation\ 7.1$$

The unit of electric current is the ampere, which is equivalent to the charge carried in coulombs per second: 1 amp = 1 C/s. The charge of a single electron is e^-, where e is the fundamental unit of electric charge: 1 e = 1.60218×10^{-19} C. For chemical purposes, the charge carried by a mole of electrons is more commonly encountered. The charge carried by a mole of electrons is -1F, with the Faraday defined as the charge of a mole of fundamental charges:

$$1\ F = eN_A = 1.60218 \times 10^{-19}\ C\ (6.0221 \times 10^{23}\ mol^{-1}) = 96485\ C/mol$$

The Faraday establishes the equivalence of electric charge and chemical change in oxidation/reduction reactions. For the current study, the reduction of copper (Equation 2.1) at the cathode of an electrochemical cell will be considered. It can be seen from Equation 2.1 that the reduction of one mole of Cu^{2+} ions require 2 moles of electrons, with corresponding charge $Q = -2F$. If the current flowing through the electrochemical cell is constant, the charge carried through the cell can be calculated as shown in Equation 7.2.

$$Q = It \qquad Equation\ 7.2$$

Where: Q is the charge

I is current in amperes

t is the time the current is applied in the electrochemical cell in seconds.

Let the number of electrons transferred in the balanced electrochemical reaction be z. For copper, z is 2. Therefore, the number of moles of product, n, is given by dividing the total charge carried by zF as shown in Equation 7.3.

$$n = \frac{Q}{zF} \qquad Equation\ 7.3$$

This expression is called Faraday's Law of electrolysis and the concept of Faraday's law was discussed in Section 2.2.2 of this report. The theoretical mass of copper (m_{Cu}) plated during the electrowinning process can then be calculated using the atomic molar mass of copper (M_r) using Equation 7.4.

$$m_{Cu} = nM_r \qquad Equation\ 7.4$$

The lowest initial copper concentration that was investigated during the electrowinning experiments in the current study is 35 g/l. Hence, the theoretical residual copper concentration in the reservoir after the copper electrowinning experiments with initial copper concentration of 35 g/l was determined by using the Faraday's law and the parameter values presented in Table 7.3.

Table 7.3: Parameter values used to calculate the theoretical number of moles of copper plated.

Parameters	Units	Values
Cathode area	m^2	0.0318
Current density	A/m^2	300
Current	A	9.54
Initial Cu concentration in electrolyte	g/l	35
Mass Cu in feed electrolyte	g	525
Plating time	hrs	24
Total electrolyte volume	L	15

Total charge over plating period	C	824256
Faraday's constant	C/mol	96485
Copper electrons		2
Assumed current efficiency	%	100
Mol Cu plated	mol	4.27
Molecular weight Cu	g/mol	63.55
Mass of Cu plated	g	271.49
Mass Cu in reservoir after plating time	g	253.51
Residual Cu in reservoir after plating time	g/l	16.90

From Table 4.3, it can be seen that the calculated theoretical residual copper in the reservoir after plating for 24 hours is 16.90 g/l from an initial copper concentration of 35 g/l in the electrolyte used for the experimental work. Therefore, the difference in copper concentrations is given below:

$$\%\ Cu\ concentration = \frac{Residual\ Cu\ concentration}{Initail\ Cu\ concentration} \times 100$$

$$= \frac{16.90}{35} \times 100$$

$$= 48.3\%$$

Depending on the operating conditions (i.e., with the highest operating current density of 300 A/m^2), about 51.7% of the initial copper concentration in the electrolyte is plated in a 24-hour plating period.

7.2. APPENDIX B – EXPERIMENTAL PROCEDURE

Experimental design matrix for the bench-scale copper electrowinning experiments

Table 7.4: Experimental design of input (independent) parameter operating conditions for the bench-scale copper electrowinning experiments.

Experimental no:	Current density (A/m^2)	Sulphuric acid concentration (g/l)	Initial copper concentration (g/l)	Guar concentration (g/l)
Base case	300	150	35	0
1	300	180	35	2
2	300	180	35	10
3	300	180	35	18
4	300	180	45	2
5	300	180	45	10
6	300	180	45	18
7	300	150	35	2
8	300	150	35	10
9	300	150	35	18
10	180	150	35	2
11	180	150	35	10
12	180	150	35	18
13	180	150	45	2
14	180	150	45	10
15	180	150	45	18
16	180	180	45	2
17	180	180	45	10

18	180	180	45	18
19	300	150	45	2
20	300	150	45	10
21	300	150	45	18
22	180	180	35	2
23	180	180	35	10
24	180	180	35	10
11-repeat	180	150	35	10

Guar solution preparation procedure

A step-by-step procedure used for dissolving guar into a solution to be used as an additive in the electrowinning experiments is outlined as follows:

1. Fill an Erlenmeyer flask with 200 ml of de-ionized water.
2. Place the flask containing de-ionized water on the heater stirrer.
3. Switch on the heater stirrer and set it at a temperature of 40°C.
4. Wait for the de-ionized water to reach 40°C. Use a thermometer to measure and confirm the temperature.
5. Weigh 400mg of guar and add to the glass conical flask containing de-ionized water at 40°C. (Concentration in the flask is 2 mg/L).
6. Allow guar to unfold in solution for 2 hours.

Electrolyte preparation procedure

Preparation of 1 L solution:

1. Clean a 5 L sealable glass bottle.
2. Add 250 ml of de-ionized water into the clean bottle.
3. Add 81.52 ml or 97.83 ml of sulphuric acid to the bottle to get the required 150 g/l or 180 g/l sulphuric acid concentration respectively.
4. Weigh 138.55 g or 178.13 g of copper sulphate pentahydrate and add to the sulphuric acid/water mixture to get the required 35 g/l or 45 g/l initial copper concentration, respectively.
5. Add 0.017 ml of hydrochloric acid using a pipette.
6. Fill up the bottle with de-ionized water to the 1 L mark.
7. Stir the synthetic electrolyte solution until the copper sulphate crystals dissolve completely.

Preparation of 5 L solution:

1. Clean a 5 L sealable glass bottle.

2. Add 2 L of de-ionized water into the clean bottle.
3. Add 326.09 ml or 391.30 ml of sulphuric acid to the bottle to get the required 150 g/l or 180 g/l sulphuric acid concentration respectively.
4. Weigh 554.19 g or 712.53 g of copper sulphate pentahydrate and add to the sulphuric acid/water mixture to get the required 35 g/l or 45 g/l initial copper concentration, respectively.
5. Add 0.069ml of hydrochloric acid using a pipette.
6. Fill up the bottle with de-ionized water to the 4 L mark.
7. Stir the synthetic electrolyte solution until the copper sulphate crystals dissolve completely.

Detailed step-by-step electrowinning experimental procedure.

A detailed experimental methodology used for the execution of the electrowinning experiments conducted in a bench scale electrowinning cell is outlined as follows:

1. Pour sufficient water into the water bath.
2. Switch on the thermostat placed on the water bath and set it to a temperature which will maintain the operating temperature at 40° in the EW cell.
3. Place polystyrene balls in the water bath to prevent water from evaporating causing the thermostat to switch off automatically.
4. Prepare 15 L feed electrolyte by dissolving the required weighed mass of copper sulphate, measured sulphuric acid and chloride in de-ionized water.
5. Clean stainless-steel cathode by rinsing it with distilled water and acetone and let it dry.
6. Weigh and record the mass of the cathode blank.
7. Inert the cleaned cathode in the middle of the electrowinning cell and bolt the negative terminal wire of the power source to the cathode hanger bar.
8. Inert two anodes on each side of the cathode plate such that 25 mm distance between the anode and cathode is maintained. Bolt the positive wires from the power source to the anode hanger bars using lugs.
9. Pour 10 L of the prepared electrolyte into the stock solution and place it in the water bath.
10. Once the setpoint temperature is achieved in the water bath place the inlet and outlet pipes into the stock solution bottle.
11. Check if all the valves on the pipelines are closed.
12. Ensure that the extraction system is running.
13. Switch on the pump and set it to the desired pump speed (25%).
14. Allow the electrolyte to circulate through the electrowinning cell until steady state is achieved at the desired operating temperature.
15. Add the required amount of dissolved guar (organic additive) solution to the 10L stock solution bottle.
16. Add the remaining 5 L of the electrolyte into the stock solution bottle and allow circulation for atleast 15 minutes for system to reach steady state at the desired operating temperature.
17. Switch on the power supply and set it to a current which translate to the desired operating current density.
18. Allow electrowinning to take place for a duration of 24 hours.
19. After 24 hours of plating switch off the power supply.
20. Remove cathode from electrolyte, wash it with water and hang to air dry.
21. After drying weigh the mass of cathode plate and store for further analysis.
22. Remove the anodes from electrolyte.

23. Take 50 ml of spent electrolyte sample and store for ICP analysis.
24. Reduce the speed of pump to 0% and switch it off.
25. Open the valves individually to collect spent electrolyte into the waste bottle to be discarded.
26. Flush the electrowinning setup with water and allow to dry before initiating the proceeding experimental run.

Copper deposit acid digestion test conditions

The weight of copper sheets required for acid digestions tests and the amount of aqua regia required based on the weight of copper sheets to be dissolved is indicated in Table 7.5.

Table 7.5: The amount of aqua regia required for acid digestions tests based on the weight of copper plate to be dissolved for 24 hours.

		Copper plate side 1		Copper plate side 2	
Copper plate	**Square piece block no:**	**Mass (g)**	**Aqua regia (ml)**	**Mass (g)**	**Aqua regia (ml)**
1	Block 1	8.09	80.9	9.35	93.5
	Block 2	7.33	73.3	8.81	88.1
	Block 3	7.88	78.8	9.64	96.4
	Block 4	9.05	90.5	9.64	96.4
	Block 5	8.78	87.8	10.32	103.2
	Block 6	9.35	93.5	10.36	103.6
2	Block 1	8.95	89.5	9	90
	Block 2	8.88	88.8	7.47	74.7
	Block 3	8.91	89.1	8.02	80.2
	Block 4	12.08	120.8	10.25	102.5
	Block 5	10.92	109.2	8.83	88.3
	Block 6	10.18	101.8	8.28	82.8
3	Block 1	9.36	93.6	9.11	91.1
	Block 2	7.96	79.6	7.28	72.8
	Block 3	7.28	72.8	8.16	81.6

	Block 4	9.27	92.7	9.68	96.8
	Block 5	9.23	92.3	10.24	102.4
	Block 6	8.13	81.3	9.23	92.3
4	Block 1	11.05	110.5	8.54	85.4
	Block 2	8.34	83.4	8.42	84.2
	Block 3	8.68	86.8	8.3	83
	Block 4	12.07	120.7	10.72	107.2
	Block 5	9.97	99.7	9.8	98
	Block 6	9.59	95.9	8.92	89.2
5	Block 1	7.23	72.3	10.19	101.9
	Block 2	7.25	72.5	10.08	100.8
	Block 3	7.27	72.7	9.96	99.6
	Block 4	9.35	93.5	10.79	107.9
	Block 5	8.21	82.1	10.25	102.5
	Block 6	8.11	81.1	11.59	115.9
6	Block 1	7.52	75.2	10.07	100.7
	Block 2	8.21	82.1	9.56	95.6
	Block 3	8.11	81.1	10.57	105.7
	Block 4	8.41	84.1	12.36	123.6
	Block 5	8.24	82.4	11.19	111.9
	Block 6	8.07	80.7	11.38	113.8
7	Block 1	7.62	76.2	9.68	96.8
	Block 2	7.55	75.5	8.07	80.7
	Block 3	8.96	89.6	8.48	84.8
	Block 4	10.15	101.5	9.27	92.7
	Block 5	9.6	96	9.41	94.1

	Block 6	9.64	96.4	9.65	96.5
8	Block 1	8.71	87.1	8	80
	Block 2	9.68	96.8	7.69	76.9
	Block 3	9.11	91.1	7.53	75.3
	Block 4	9.53	95.3	8.91	89.1
	Block 5	9.95	99.5	8.57	85.7
	Block 6	9.74	97.4	8.74	87.4
9	Block 1	10.3	103	7.78	77.8
	Block 2	9.27	92.7	6.96	69.6
	Block 3	7.27	72.7	7.63	76.3
	Block 4	11.92	119.2	8.31	83.1
	Block 5	10.91	109.1	8.25	82.5
	Block 6	11.58	115.8	9.1	91
10	Block 1	5.2	52	6.24	62.4
	Block 2	4.87	48.7	5.92	59.2
	Block 3	4.68	46.8	6.24	62.4
	Block 4	6.58	65.8	6.9	69
	Block 5	6.98	69.8	7.08	70.8
	Block 6	5.73	57.3	6.8	68
11	Block 1	6.35	63.5	5.36	53.6
	Block 2	5.3	53	4.79	47.9
	Block 3	5.98	59.8	4.83	48.3
	Block 4	6.26	62.6	6.08	60.8
	Block 5	6.52	65.2	5.57	55.7
	Block 6	6.95	69.5	5.54	55.4
12	Block 1	5.7	57	6.53	65.3

	Block 2	5.09	50.9	6.23	62.3
	Block 3	4.98	49.8	6.64	66.4
	Block 4	6.41	64.1	7.28	72.8
	Block 5	5.63	56.3	7.03	70.3
	Block 6	5.62	56.2	6.84	68.4
13	Block 1	6.01	60.1	5.29	52.9
	Block 2	5.53	55.3	5	50
	Block 3	6.47	64.7	5.12	51.2
	Block 4	6.62	66.2	6.52	65.2
	Block 5	6.59	65.9	5.8	58
	Block 6	7.01	70.1	5.78	57.8
14	Block 1	6.13	61.3	5.24	52.4
	Block 2	5.85	58.5	5.05	50.5
	Block 3	6.27	62.7	5.14	51.4
	Block 4	7.28	72.8	5.15	52.4
	Block 5	6.87	68.7	5.10	51.0
	Block 6	7.08	70.8	5.19	51.9
15	Block 1	4.9	49	6.57	65.7
	Block 2	4.21	42.1	6.21	62.1
	Block 3	4.35	43.5	6.22	62.2
	Block 4	5.89	58.9	7.68	76.8
	Block 5	4.67	46.7	7.31	73.1
	Block 6	4.85	48.5	6.97	69.7
16	Block 1	9.09	90.9	2.74	27.4
	Block 2	8.2	82	2.37	23.7
	Block 3	8.01	80.1	2.43	24.3

	Block 4	10.2	102	3.78	37.8
	Block 5	9.24	92.4	3.52	35.2
	Block 6	8.72	87.2	3.66	36.6
17	Block 1	5.51	55.1	5.41	54.1
	Block 2	5.1	51	5.1	51
	Block 3	5.62	56.2	5.25	52.5
	Block 4	6.44	64.4	6.75	67.5
	Block 5	6.21	62.1	5.95	59.5
	Block 6	6.64	66.4	6.18	61.8
18	Block 1	4.73	47.3	7.69	76.9
	Block 2	4.52	45.2	7.45	74.5
	Block 3	4.75	47.5	7.35	73.5
	Block 4	4.96	49.6	7.95	79.5
	Block 5	4.5	45	7.99	79.9
	Block 6	4.54	45.4	7.73	77.3
19	Block 1	10.39	103.9	10.04	100.4
	Block 2	9.31	93.1	9.1	91
	Block 3	9.5	95	9.23	92.3
	Block 4	10.43	104.3	10.15	101.5
	Block 5	9.7	97	9.67	96.7
	Block 6	10.07	100.7	9.79	97.9
20	Block 1	10.24	102.4	9.7	97
	Block 2	9.42	94.2	9.13	91.3
	Block 3	9.15	91.5	9.04	90.4
	Block 4	9.67	96.7	11.67	116.7
	Block 5	9.84	98.4	10.54	105.4

	Block 6	8.95	89.5	10.1	101
21	Block 1	10.22	102.2	9.71	97.1
	Block 2	9.11	91.1	8.81	88.1
	Block 3	9.06	90.6	8.84	88.4
	Block 4	11.57	115.7	10.35	103.5
	Block 5	10.29	102.9	9.96	99.6
	Block 6	8.93	89.3	9.54	95.4
22	Block 1	6.03	60.3	5.74	57.4
	Block 2	5.27	52.7	5.21	52.1
	Block 3	5.37	53.7	5.58	55.8
	Block 4	6.5	65	6.31	63.1
	Block 5	5.95	59.5	5.91	59.1
	Block 6	6.3	63	6.38	63.8
23	Block 1	5.76	57.6	5.86	58.6
	Block 2	4.78	47.8	5.15	51.5
	Block 3	5.21	52.1	5.74	57.4
	Block 4	6.62	66.2	6.59	65.9
	Block 5	5.89	58.9	6.3	63
	Block 6	5.86	58.6	6.53	65.3
24	Block 1	5.74	57.4	6	60
	Block 2	4.78	47.8	5.19	51.9
	Block 3	4.87	48.7	5.1	51
	Block 4	6.67	66.7	6.58	65.8
	Block 5	5.89	58.9	6.5	65
	Block 6	5.77	57.7	6.39	63.9

Detailed step-by-step acid digestion procedure.

A detailed experimental methodology used for the performing the acid digestion tests is outlined as follows:

1. Weigh out the amount of copper sheet piece cut.
2. Measure out the amount of hydrochloric acid (HCl) and nitric acid (HNO_3) required based on the amount of copper sheet weighed. The ratio between the amount of copper deposit and aqua regia volume required is 1:10. Note: carefully add the nitric acid to the hydrochloric acid.
3. Pour the freshly mixed acids into a conical flask. The amount of liquid should never be more than 50% of the volume of the conical flask.
4. Slowly add the copper sheet pieces to the conical flask. Note: if boiling starts, stop addition of copper sheet immediately.
5. Add the magnetic stirrer into the conical flask to spin slowly and ensure adequate agitation.
6. Cover the conical flask with watch glass.
7. Set hot plate temperature to 55°C.
8. After leaving the solution for 24 hours, switch off the magnetic stirrer and hot plate.
9. Remove the flask from heat and allow cooling to ambient temperature.
10. Remove the magnetic stirrer bar.
11. Take sample of the leached solution for ICP analysis.

Preparation of the leached solution for ICP analysis

The solution of copper obtained after dissolving the copper deposit plate through acid digestion was diluted (21X) using the following step-by-step procedure to bring the concentration of sulphur and lead into a range of 0.5-100ppm which is the quantification range for sulphur when using the ICP technique:

1. Filter a sample of the homogenised solution using a 45 µm syringe filter into 50 ml Falcon tube for storage.
2. Using a pipette fill a 15 ml Falcon tube with 10ml distilled water.
3. Add 500 µl copper dissolved solution I into the Falcon tube using a pipette.
4. Place the lid on top of the Falcon tube and invert it several times to homogenise the solution.

7.3. APPENDIX C – ELECTROWINNING SUPPORTING RESULTS

Validation with literature

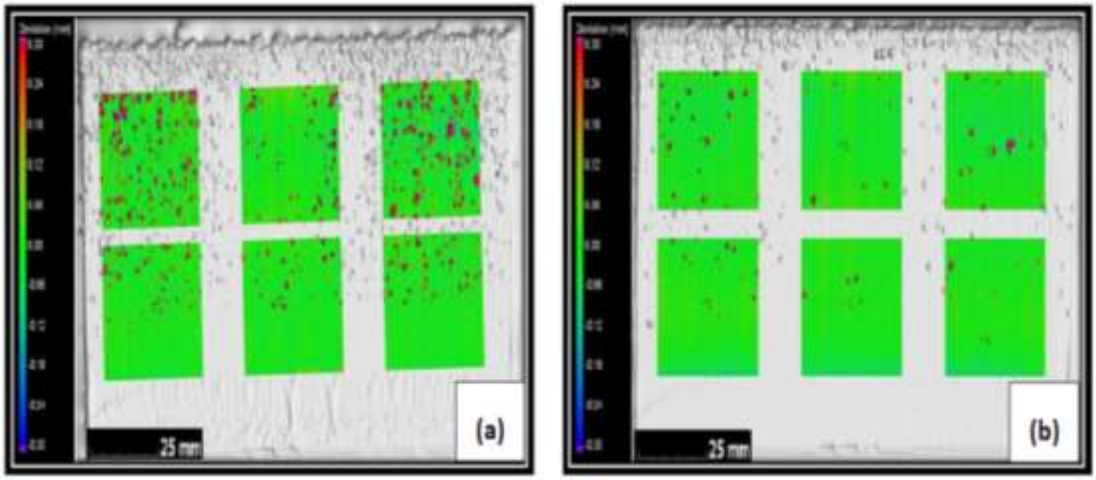

Figure 7.1: Surface topography analysis of copper plates obtained at 300 A/m^2 current density and 160 g/l sulphuric acid for 50 g/l initial copper concentration and 10 mg/l guar concentration where (a) base case scenario and (b) 2 mg/l guar concentration.

Figure 7.1 (a) shows that at a base case scenario more positive deviations were observed than when 2 mg/l guar concentration was dosed in the electrolyte as shown by Figure 7.1 (b). In the current study the same experimental procedure used to achieve Figure 7.1 (a) and Figure 7.1 (b) was used for validation. Figure 4.5 (a) and Figure 4.5 (b) provides similar results showing that for the base case scenario more positive deviations developed on the cathode deposit compared to deposit produced in the presence of 2 mg/l guar concentration in the electrolyte.

Validation experiments

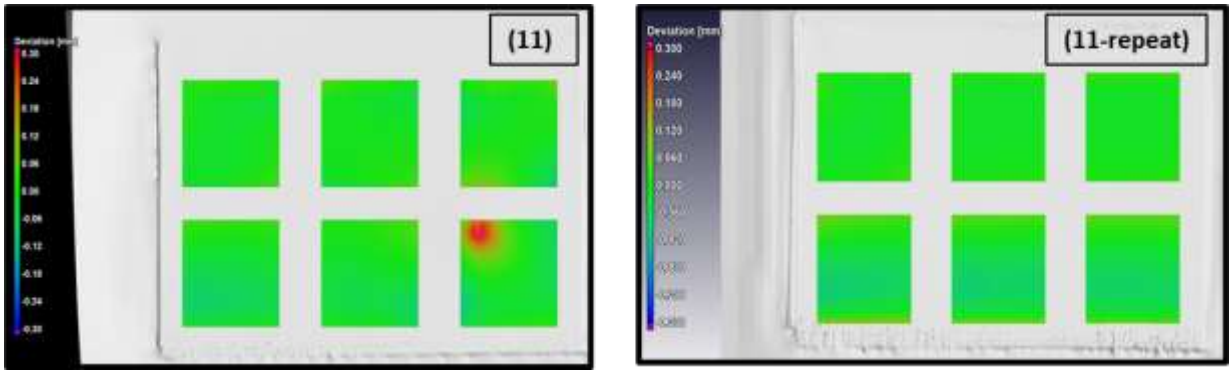

Figure 7.2: Surface topography analysis of copper plates obtained at 180 A/m^2 current density and 150 g/l sulphuric acid for 35 g/l initial copper concentration and 10 mg/l guar concentration where (a) is Experiment 11 and (b) is Experiment 11-repeat.

Comparing the colour scales for copper deposit achieved for experiment 11 and the reproducibility experiment (experiment 11-repeat) it can be seen that both deposits achieved a smooth deposit because there are no positive deviations. Positive provides evidence of localized growth on the copper deposit surface and undesirable during the copper electrowinning operation.

Surface topography analysis

The surface topography analysis of copper plates at a low current density (180 A/m^2) for various operating conditions is provided in Figure 7.3 and Figure 7.4.

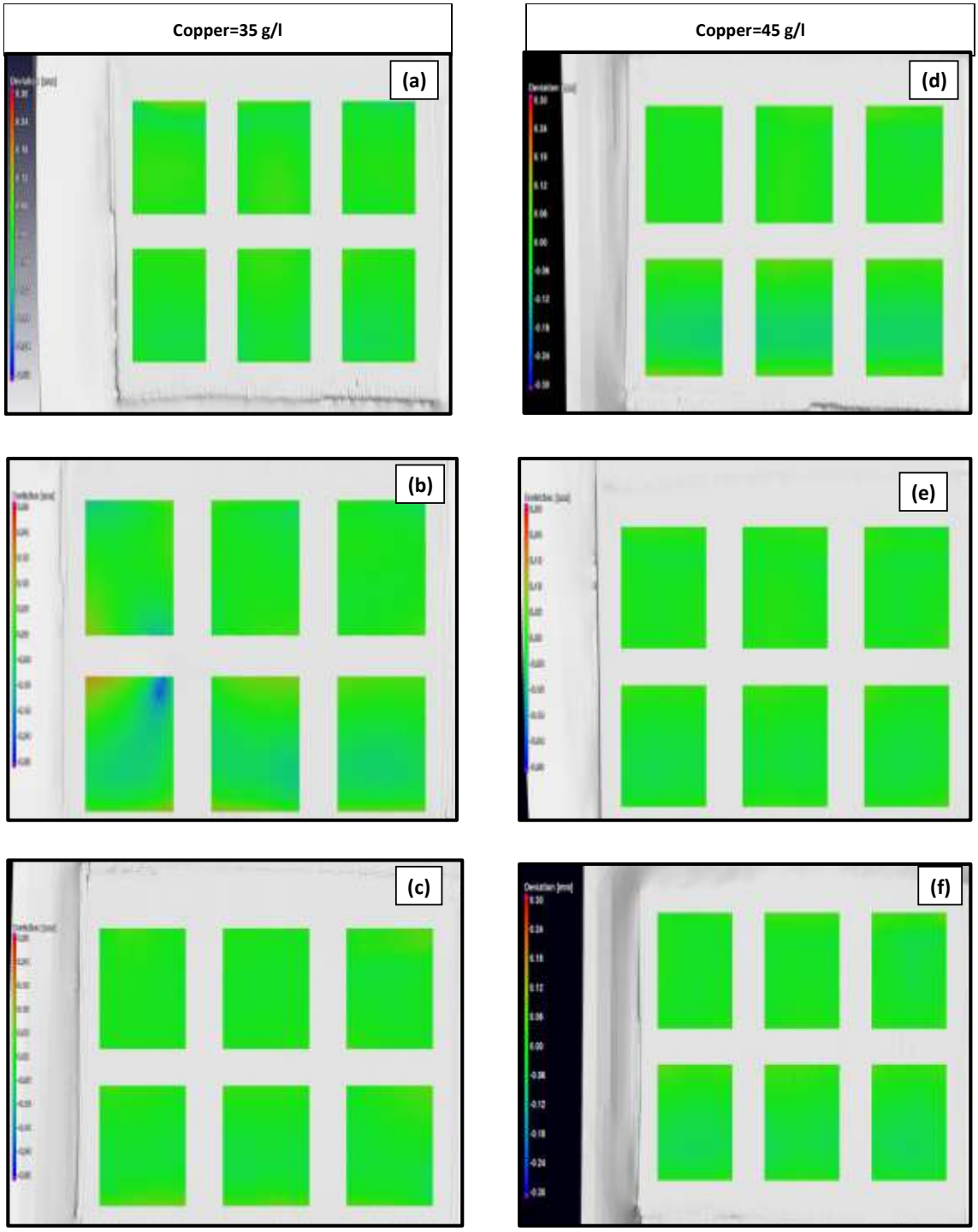

Figure 7.3: Surface topography analysis of copper plates obtained at 180 A/m^2 current density and 150 g/l sulphuric acid for 35 g/l initial copper concentration with guar concentration of (a) 2 mg/l, (b) 10 mg/l, (c) 10 mg/l) and for 45 g/l initial copper concentration with guar concentration of (d) 2 mg/l, (e) 10 mg/l, (f) 18 mg/l).

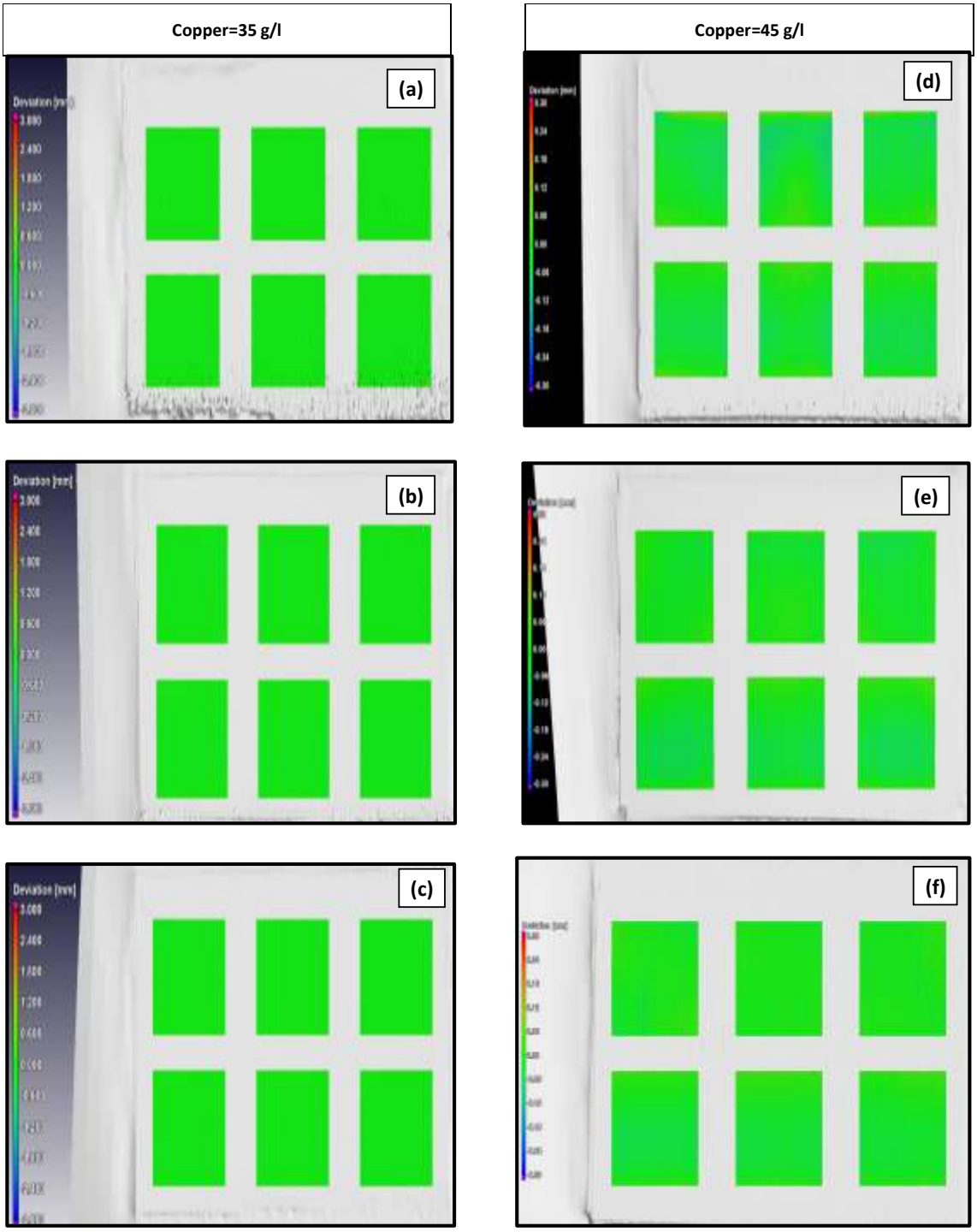

Figure 7.4: Surface topography analysis of copper plates obtained at 180 A/m^2 current density and 150 g/l sulphuric acid for 35 g/l initial copper concentration with guar concentration of (a) 2 mg/l, (b) 10 mg/l, (c) 10 mg/l) and for 45 g/l initial copper concentration with guar concentration of (d) 2 mg/l, (e) 10 mg/l, (f) 18 mg/l).

Surface area deviations

Figure 4.9 translate into Figure 7.5 when considering only the positive deviations from the normalized flattest part of the surface showing the effect of guar addition during copper electrowinning.

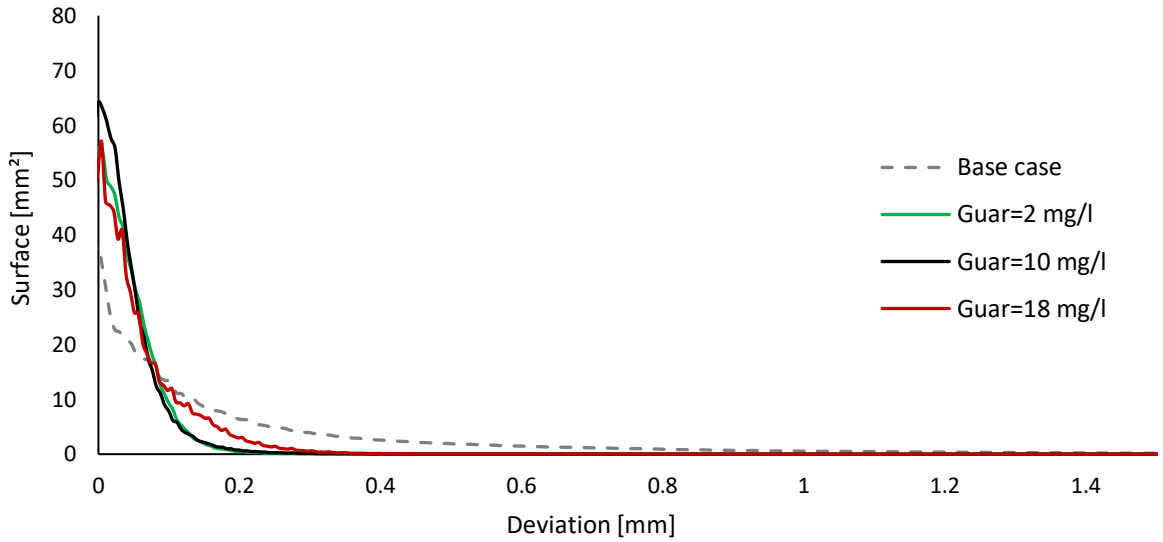

Figure 7.5: Average total surface elements (area) deviation from the flattest surface plane (normalized) for each plate achieved in the base case scenario, 2 mg/l, 10 mg/l and 18 mg/l guar electrolyte at 300 A/m^{2}with sulphuric acid and initial copper concentration of 150 g/l and 35 g/l, respectively.

Visually, the variance in the spread of surface elements (area) on the x-axis with increasing positive deviation from the flattest surface for the Base case scenario copper deposit compared to the other copper deposit achieved in the presence of guar can be clearly seen in Figure 7.5. It can be seen from Figure 7.5 that the Base case scenario has the highest total surface present at greater positive compared to the copper plates achieved in the presence of guar. This is comparable with the conclusions made in the qualitative analysis presented in Section 4.3.1 -4.3.1 of this report. However, it is important to evaluate the quantitative analysis of copper plates at various experimental conditions for varying guar dosages. For this reason, the S_a values, which encapsulates all these data in one numerical value, were calculated and plotted compared to each other in Figure 4.11.

The surface area deviation curve showing the effect of sulphuric acid during copper electrowinning is provided in Figure 7.6.

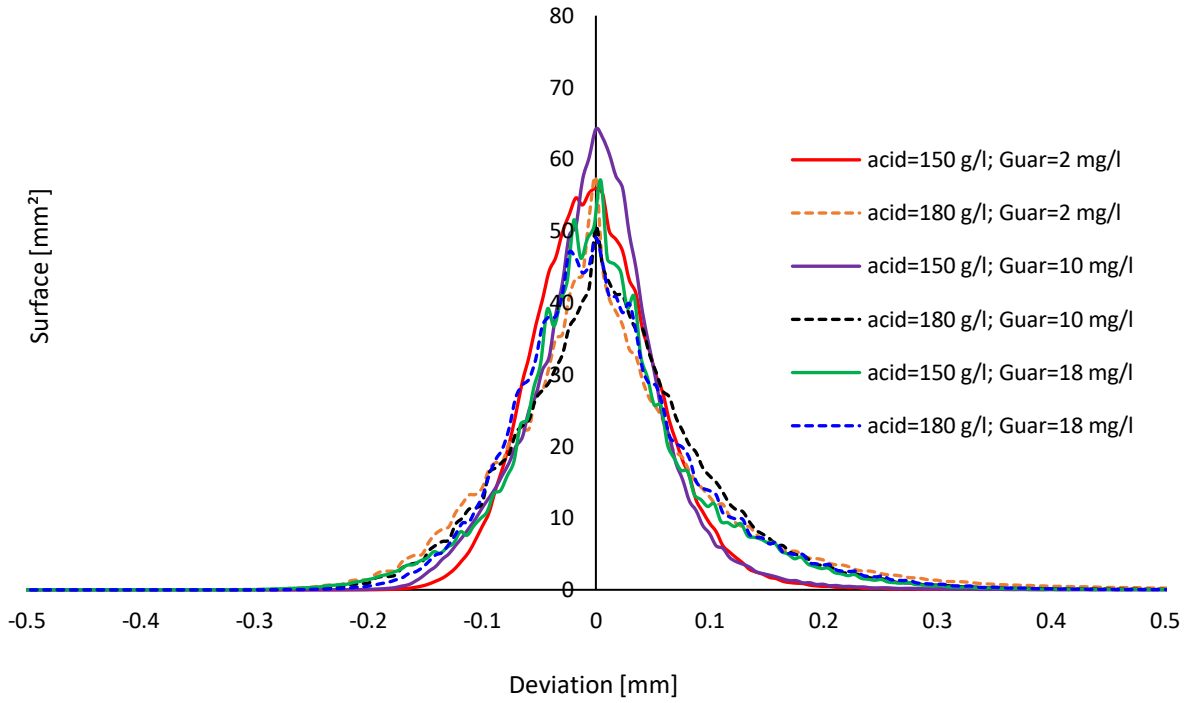

Figure 7.6: Average total surface elements (area) deviation from the flattest surface plane (normalized) for each plate achieved in the presence of guar electrolyte at 300 A/m^2 current density and 35 g/l initial copper concentration.

The surface area deviation curve showing the effect of copper during copper electrowinning is provided in Figure 7.7.

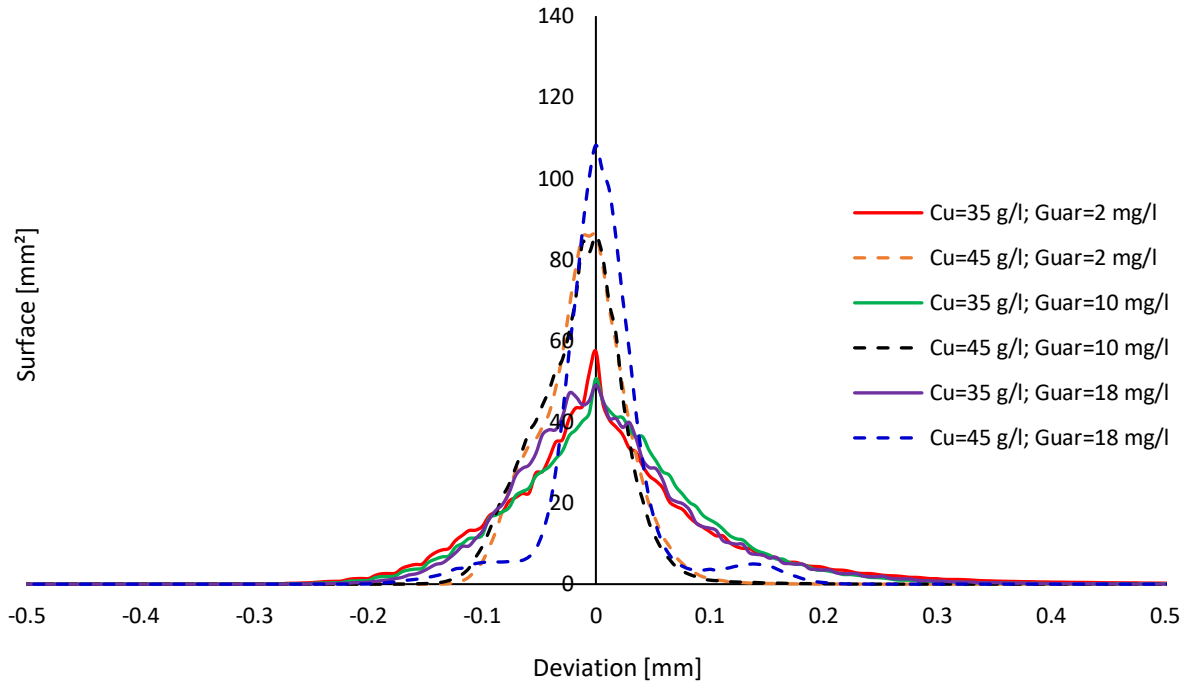

Figure 7.7: Average total surface elements (area) deviation from the flattest surface plane (normalized) for each plate achieved in the presence of guar electrolyte at 300 A/m^2 current density and 180 g/l sulphuric acid concentration.

Rate of copper deposition

Table 7.6: The amount and average rate copper deposited during 24 hours of electrowinning for all experimental conditions in the presence of various guar concentrations.

Experiment no:	Amount of copper deposit (g)	Rate of deposition (g/hour)
1	267.43	11.14
2	267.71	11.15
3	267.91	11.16
4	267.75	11.16
5	267.72	11.16
6	267.34	11.14
7	267.73	11.16
8	267.78	11.16
9	268.01	11.17

10	157.17	6.55
11	157.07	6.54
12	157.43	6.56
13	157.08	6.55
14	157.22	6.55
15	157.11	6.55
16	157.14	6.55
17	157.09	6.55
18	157.32	6.56
19	267.50	11.15
20	267.32	11.14
21	267.70	11.15
22	157.58	6.57
23	157.40	6.56
24	157.26	6.55

Feed and spent electrolyte copper concentration

Table 7.7: Feed and spent electrolyte concentration per sample with initial concentration of 35 g/l, determined by ICP analysis technique.

Experiment no:	Current density (A/m^2)	Feed electrolyte (g/l)	Spent electrolyte (g/l)
1	300	35	22.7
2	300	35	20.5
3	300	35	21.9
7	300	35	22.5
8	300	35	22.7
9	300	35	22.1
10	180	35	34.5

11	180	35	33.0
12	180	35	33.3
22	180	35	29.5
23	180	35	32.1
24	180	35	31.6

7.4. APPENDIX D - GUAR DEGRADATION EVALUATION

Aim

Develop an understanding on the extent of guar degradation to its monomers (galactose and mannose) under acidic conditions by conducting hydrolysis tests.

Materials

A commercial grade guar powder (Sendep Opt43) purchased from an industrial reagent manufacturing company (SENMIN) was used to carry out all the hydrolysis tests in the present study. The chemicals used for the hydrolysis tests are listed in Table 7.8.

Table 7.8: List of chemicals used in the hydrolysis tests.

Reagent name	Supplier	Grade	Molecular weight (g/mol)
98% Sulphuric acid (H2SO4)	Scienceworld	*AR	98.08
97% Sodium hydroxide (NaOH)	Scienceworld	*AR	40.00

*AR-Analytical Reagent

Experimental procedure

A water bath was filled with sufficient water and heated to a temperature of 30°C by switching on the thermostat. A test tube rack was constructed using stainless steel and placed on the water bath. For all the tests, 300 mg guar powder was weighed and added into the 10 ml glass test tubes. To ensure that the test tubes remain in a fixed position throughout the hydrolysis tests rubber O-ring seals were slipped onto the test tubes. Thereafter, the test tubes were inserted into the holes on the test tube rack as shown in Figure 7.8. The acid hydrolysis process was initiated by adding 3 ml of the desired sulphuric acid concentration (150 g/l, 180 g/l and 210 g/l) into the test tubes containing the guar powder. The samples were stirred manually and periodically within the desired hydrolysis time using a glass stir rod to ensure even acid to guar contact and uniform hydrolysis.

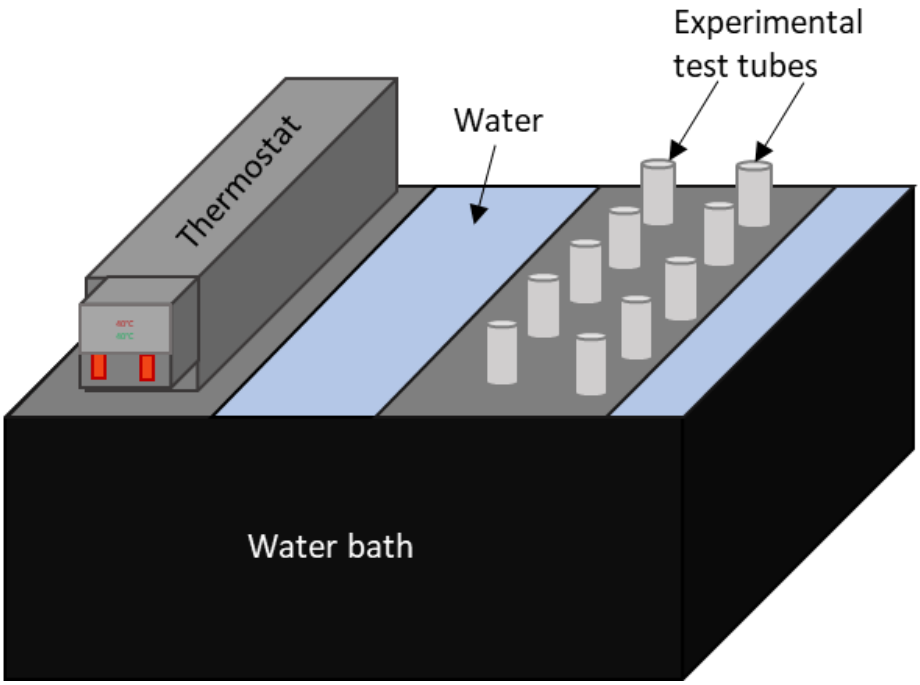

Figure 7.8: A schematic diagram of a setup constructed for conducting guar hydrolysis tests.

The test tubes containing the guar/acid mixture sample were removed from the water bath periodically after the desired hydrolysis time (2-4 days) allowed for each sample was complete. Each sample was then transferred int a 250 ml bottle and 84 ml of de-ionized water was added into to dilute the acid concentration. From the 250 ml, 10 ml of the hydrolysate was transferred into a 15 ml Falcon tube. The hydrolysate sample (aliquot) was then neutralized to prepare for HPLC analysis. Sodium hydroxide was used to neutralize the sample to a pH range between 4-6 and pH indicator papers were used to confirm the pH range required. Once the aliquot was neutralized, a 10 ml syringe filter was used to draw out a sample of the aliquot and thereafter passed through a 0.22 µm syringe filter into 1.5 ml labelled vial which was sealed afterwards. The sample was stored in a refrigerator at 7°C prior HPLC analysis.

HPLC analysis

The guar hydrolysed and neutralized samples stored at 7°C were filter sterilised using 0.22 µm Nylon syringe filters just before the High-Performance Liquid Chromatography (HPLC) analysis. HPLC is one of the types of chromatography analytical techniques used for the separation, identification, and quantification of each component in a mixture (Thammana, 2016). A schematic illustration of the HPLC system is shown in Figure 7.9.

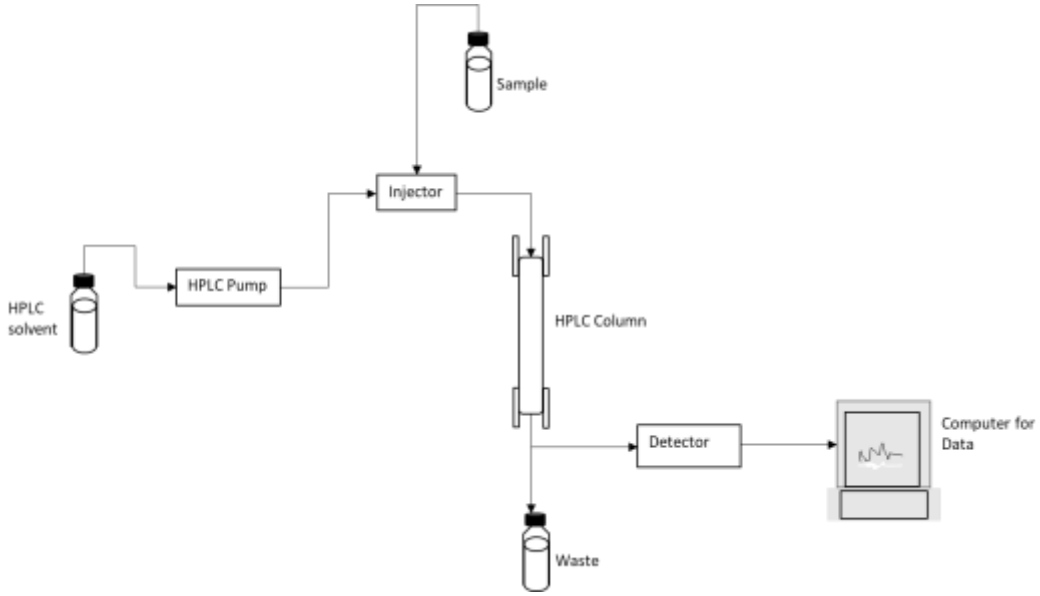

Figure 7.9: Schematic illustration of High-Performance Liquid Chromatography system.

Galactose and mannose were quantified from the samples using a Dionex 3000 HPLC system with a Waters XBridge Column (250×4.6 mm) with a Varian Evaporative Light Scattering Detection (ELSD) at a column temperature of 37°C. The column was eluted with Acetonitrile-Water with 10 mM Acetate as the mobile phase and eluted at a flowrate of 0.7 ml/min over a 100% - 75% acetonitrile gradient. The sample injection volume into the column was set at 10 µl. The injected sample to be separated is then transported through the column by the mobile phase at a run time of 45 minutes. The elution program that was applied to separate the monomer sugars in the guar hydrolysed samples for quantification using HPLC is shown in Table 7.9. The elution program is the timetable that controls the water and acetonitrile ratio over time, i.e., how fast the ratio changes over time. The instrument mixes water and acetonitrile ratios to allow for the sugars to release from the column at their respective solubilities. Thus, the sugars all “stick” to the column at the initial time 0 mins, 100% acetonitrile concentration, and as the water content increases the sugars “release” from the column (better solubility in water) and then elute towards the detector. The Varian ELSD was used to detect and identify the peaks of the analytes (mannose and galactose) in the sample. Thereafter, mannose and galactose quantification were performed by comparing peak areas to those of external calibration standards of mannose and galactose as shown in Figure 7.10.

Table 7.9: The mobile phase elution program.

Time (min)	Acetonitrile (%)
0	100
27	92
33	75
35	75

40	100
45	100

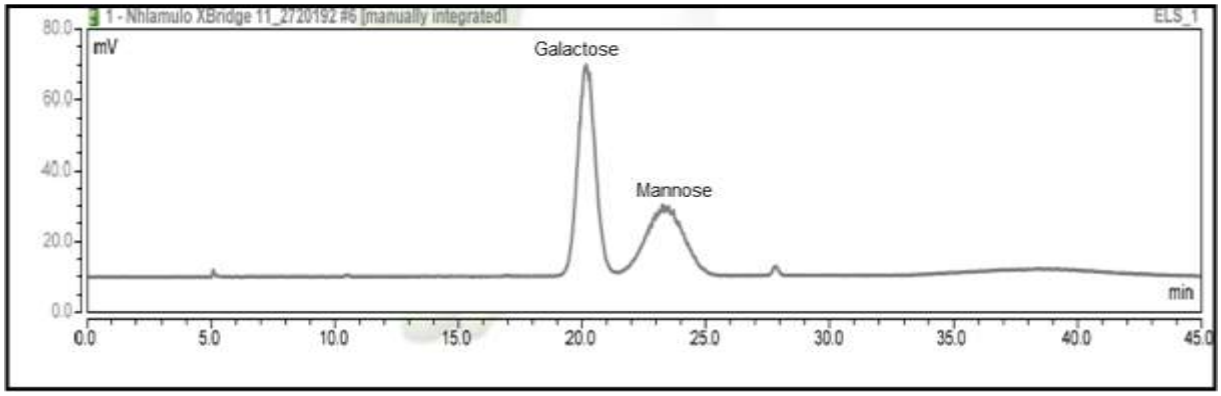

Figure 7.10: Chromatogram showing the galactose-mannose standards.

Results & discussion

Guar hydrolysis tests were conducted at 150 g/l, 180 g/l, and 210 g/l sulphuric acid concentrations for 2-4 days. Chromatograms obtained after each day for all the various concentrations showed that guar did not degrade to mannose and galactose compounds were not detected from the HPLC analysis as shown in Figure 7.11. At retention time 28-29 min a peak was observed which may show that there might be partial guar degradation taking place. However, this must be confirmed by further investigations. At 39 minutes retention time a very large peak is observed which might be guar appearing as a polymeric form with a decrease in molecular weight. However, the molecular weight of guar is still high to be detected and quantified using the HPLC analysis technique. A decrease in the molecular weight of guar is expected during hydrolysis with increasing acid concentration (Wang et al., 2000). Furthermore, the monosaccharide composition analysis after hydrolysis showed that for galactomannan the composition remained largely unaffected or the degradation products kept the structure molecule of galactomannan (Lupo et al., 2020; Yanbei et al., 2017). This provides evidence the in acidic conditions (i.e., copper electrowinning) guar does not degrades to its monomers (galactose and mannose) but instead it degrades to a smaller molecule with a decrease in molecular weight.

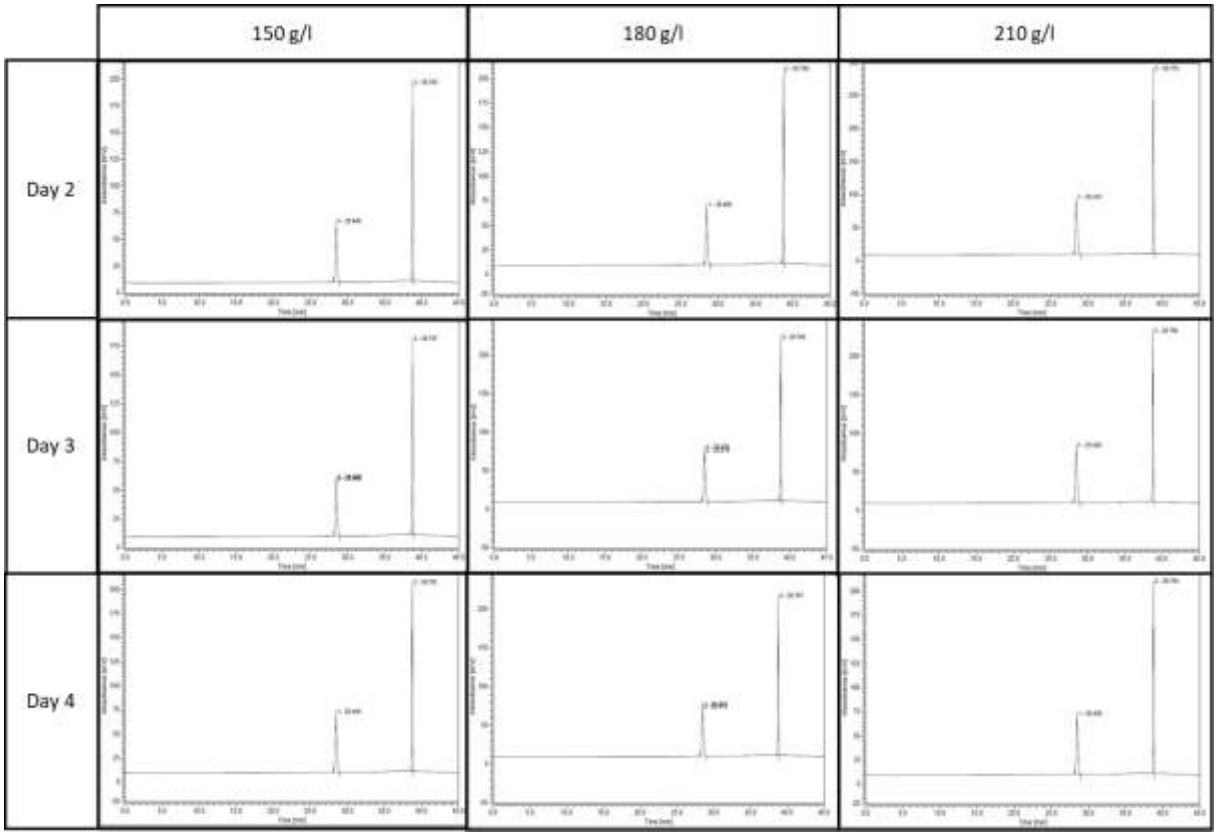

Figure 7.11: Chromatogram of guar hydrolysis at ambient pressure conducted with 3 ml of 150g/l H_2SO_4, 300 mg guar and 84 ml de-ionized water.

The decrease in molecular weight of guar will either deteriorate or improve the copper electrowinning performance. Even though the results were based of polyacrylamides it was observed that adsorption increased with a decrease in the polyacrylamide molecular weight (Coetzee, 2018). Therefore, when applying this theory to the molecular weight of guar it can be expected that as the molecular weight of guar decrease (smaller guar molecule) the adsorption on the surface will increase improving the surface roughness during copper electrowinning. The worst case of guar losing its activity at once during copper electrowinning is not going to happen. However, it is difficult to say when guar is going to deteriorate to its monomers since it is already degrading to a smaller molecule during hydrolysis.

Conclusion & recommendations

Both galactose and mannose were not detected from guar hydrolysis tests conducted with varying sulphuric acid concentrations.

Varying sulphuric acid concentration did not have a significant influence on the degradation of guar during the hydrolysis tests. Therefore, future hydrolysis tests should be investigated at higher temperature which are within the range of copper electrowinning operating temperatures in the industry to understand the extent in which guar degradation will be affected.

Hydrolysis time can also be extended equivalent to the number of days it takes to complete an electrowinning cycle in the industry.

In the industry guar degradation occurs in the electrolyte. It is proposed that in future investigations to determine a method that will allow for guar degradation rate to be determined from the electrolyte during the electrowinning experimental run.